THE SYNTHESIS AND CHARACTERIZATION OF NEW TRANSITION METAL COMPLEXES CONTAINING IMIDAZOLIDINE NITROXYL LIGAND

BY

HASTRY MUWOWO

A DISSERTATION SUBMITTED TO THE UNIVERSITY OF ZAMBIA IN PARTIAL FULFILMENT OF THE REQUIREMENTS OF THE DEGREE OF MASTER OF SCIENCE IN CHEMISTRY.

The University of Zambia

LUSAKA

1997

DECLARATION

I hereby declare that this dissertation or any part of it has not previously been submitted for a degree in this or any other University.

ABSTRACT

ML_3 coordination complexes where (M = V^{3+}, Cr^{3+}, Mn^{3+} and L = phenacetylidene -2, 2, 5, 5 - tetramethyl -3- imidazolidine -1- oxyl free radical ligand), have been synthesized.

Vanadium(III) complex was prepared by refluxing a mixture of Vanadium Pentoxide and the ligand in ethanol containing aqueous sodium hydroxide. Chromium(III) complex and Manganese(III) complex were prepared by refluxing the mixture of the aqueous metal salt with the ligand (LH) in ethanol.

The ML_3 metal chelates formed have been found to be soluble in most organic solvents such as carbon tetrachloride, chloroform, benzene, Ether, ethanol and are insoluble in water.

The complexes have been characterized by elemental analysis, Mass Spectroscopy (FAB), X-ray Flourescence Spectrometry, Fourier Transform Infra-red (FTIR) Spectroscopy, Electron Spin Resonance (ESR) and magnetic susceptibility measurements. Cyclic voltammetric studies were also carried out.

All the ML_3 complexes have been found to be paramagnetic, but unlike the known ML_2 complexes of the first row transition metals synthesized by Russian Scientists twenty years ago, these complexes have shown unique magnetic properties which reflect not only the spin properties of the electron, but also those associated with the orbital motion of the electron.

ACKNOWLEDGEMENTS

I wish to express my indebtedness to Professor E. M. R Kiremire for his painstaking Supervision and expert guidance throughout this research and also for countless helpful suggestions both before and during the writing of this dissertation. Furthermore I would like to thank Mrs Jain and Mr Richard Likumba for their assistance in drawing the graphs and diagrams appearing in this dissertation.

I wish to express my sincere appreciation and gratitude to Dr N. Boag of the University of Salford for the analytical, Magnetic, ESR and FAB data, Dr. Kelly Chibale of the University of Capetown, South Africa for the analytical and mass spectra data, Mr E Mukwanka of the University of Zambia for the polarographic measurements on the complexes, Dr. A. J. Van Reenen of the University of Stellenbosch South Africa for the FTIR spectra data of the complexes, and Mr Kasengela of the School of Mines University of Zambia for the X-ray flourescence analysis of the samples.

I acknowledge with gratitude the assistance of Mrs Justina H. Manyoma who typed the entire final manuscript with exceptional skill.

I gratefully acknowledge the assistance of the Ministry of Education and, in particular, the permanent Secretary, without whose understanding and continued administrative support I could not have been granted study leave to undertake this study, and not forgetting the Universities of Zambia, and Cape town and Directorate of Human Resource Development for the financial support.

Finally, I wish to express my appreciation to my Wife, Grace and my Son, Sangwani who not only encouraged me in this undertaking, but had to bear with my absence from home during the whole study period.

TABLE OF CONTENTS **PAGE**

CHAPTER I

CHAPTER II

CHAPTER III

TABLES AND FIGURES

TABLES:

FIGURES:

CHAPTER 1

INTRODUCTION:

The synthesis and characterization of coordination complexes of imidazoline and imidazolidine nitroxyl free radical ligands was initiated by Russian Scientists as early as 1975 [2]. As a follow up, this work demonstrates the synthesis of imidazolidine nitroxyl free radical complexes of Vanadium, Chromium and Manganese. The synthesized complexes were characterized by the well known published techniques, namely, Elemental Analysis, Infrared (IR), Mass Spectroscopy (FAB), magnetic susceptibility measurements, Electron Spin Resonance (ESR) spectroscopy, X-ray flourescence spectrometry and cyclic voltammetry [2, 3] in order to establish their physico - chemical properties.

1.0. VANADIUM, CHROMIUM AND MANGANESE CHEMISTRY

Vanadium, Chromium and Manganese belong to the first row d-block transition metal elements. The importance of transition metal chemistry for the development of technology in any country cannot be over-emphasized. After all, most transition elements are used as catalysts in many chemical reactions [4]. The chemistry of the transition metals named above is described below.

Vanadium has a configuration of $[Ar]4s^2\ 3d^3$. It is a fairly soft, ductile and white metal. It is stable in air but it is attacked by hydroflouric acid, nitric acid and readily combines

with carbon, nitrogen or oxygen, if heated. In nature, vanadium is quite abundant and constitutes about 0.02% of the earth's crust [4-6].

Chromium has a configuration of [Ar] $4s^1$ $3d^5$. It is a silverly white metal with a body-centred structure and is very reactive. It reacts with dilute hydrochloric acid and sulphuric acid, but the pure metal is insoluble in dilute nitric acid, and the concentrated acid renders the metal passive. It also reacts with sulphur, carbon, oxygen and nitrogen. In nature, chromium occurs in form of an ore called chrome, Fe Cr_2O_4.

On the other hand, manganese has a configuration of [Ar]$4s^2$ $3d^5$. It is a hard, brittle and grey metal and is highly reactive. It reacts with nitrogen and carbon. It also reacts with dilute acids and slowly decomposes water [4-6]. In nature, manganese is quite abundant and constitutes about 0.085% of the earth's crust [6]. The physical properties of the transition metals [5] described above are indicated in table 1.0 below.

TABLE 1.0: Some physical properties of Vanadium, Chromium and Manganese.

	Vanadium V	**Chromium Cr**	**Manganese Mn**
Atomic Number	23	24	25
Electronic structure	[Ar]$4s^2$ $3d^3$	[Ar] $4s^1$ $3d^5$	[Ar] $4s^2$ $3d^5$
Atomic radius (nm)	0.122	0.117	0.117
Ionic radius M^{3+} (nm)	0.074	0.069	0.066
Electronegativity	1.7	1.6	1.5
Density (g cm^{-3})	5.96	7.19	7.40
mp/°C	1,900	1,890	1,260
bp/°C	3,400	2,475	2,030
Some of the common oxidation states.	2, 3, 4, 5	2, 3, 6	1, 2, 3, 4, 5, 6, 7

From table 1.0, it is observed that moving across the first transition series from vanadium to manganese, an anormally in filling the 3d subshell occurs with chromium and this can be accounted for on the basis that a half - filled subshell represents a particularly stable state. Thus with chromium, one 4s electron is drawn into the 3d subshell to achieve this state. Besides, all the three elements exhibit the characteristic properties of metals i.e, bright luster, good conduction, high density, melting point and boiling point. The high melting and boiling points of the transition metals are related to their ability to use both 3d and 4s electrons for metallic bonding. A reduction in the melting and boiling points can be observed as the electrons pair up in the 3d subshell and become less available for metallic bonding [5].

VARIABILITY IN OXIDATION STATES OF VANADIUM, CHROMIUM AND MANGANESE.

The various oxidation states known for the transition metals such as those mentioned above are attributed to the unpaired inner **d** electrons which require little promotion energy for use as valency electrons. For example, vanadium exhibits a range of four oxidation states and has a tendency to form compounds in which all its oxidation states are represented, while chromium exhibits oxidation states (2, 3 and 6). The most stable oxidation state of the element is Cr^{3+} (d^3). The most characteristic of the oxidation state, Cr^{3+}, is the formation of a large number of relatively kinetically inert complexes.

It is largely because of this kinetic inertness that so many complex species [6] can be isolated as solids and that they persist for relatively long periods of time in solution even

under conditions where they are thermodynamically quite unstable. On the other hand, manganese exhibits a range of seven oxidation states and has a tendency to form compounds in which it is in a low oxidation state. Most manganese(III) salts are unstable and in solution either disproportionate or readily undergo hydrolysis. Table 2.0 below, shows some of the various transition metal complexes formed by vanadium, chromium and manganese in their various oxidation states [4-6 and 8] .

TABLE 2.0: Some transition metal complexes formed by Vanadium, Chromium and Manganese in their various oxidation states [8].

OXIDATION STATE	EXAMPLE OF TRANSITION METAL COMPLEXES FORMED		
	VANADIUM	CHROMIUM	MANGANESE
I	-	-	$Na_5[Mn(CN)_6]$
II	$[V(H_2O)_6]^{2+}$, $[V(CN)_6]^{4-}$	$Cr_2(CH_3COO)_4.2H_2O$ $K_4[Cr(CN)_6]$	$MnCO_3$
III	VCl_3, VF_6^{3-}, $V(CN)_3$	$CrCl_3(NMe_3)_2$ $Cr(acac)_3$	$Mn(CH_3COO)_3.2H_2O$ $Mn(acac)_3$
IV	$VO(acac)_2$ $V(NEt_2)_4$	$Cr(CH_2SiMe_3)_4$ $Cr(NEt_2)_4$	MnO_2 $K_2[MnO_3]$
V	V_2O_5, VF_6^- VF_5	-	-

*Abbreviations: acac = acetylacetonate ($CH_3COCH = \overset{\ominus}{C}OCH_3$),

Et = ethyl ($-CH_2CH_3$) and

Me = methyl ($-CH_3$)

MAGNETISM

Vanadium, Chromium and Manganese cations, like many transition metal cations and compounds posses unpaired electrons in the inner **3d** subshells and exhibit paramagnetism [7]. When the **3d** subshell is being filled, the added electrons enter the empty orbitals before any pairing takes place. The magnetic moment increases with the number of unpaired electrons and the observed magnetic moment gives a useful indication of the number of unpaired electrons present in the atom, molecule, or ion [5].

1.1.0. COORDINATION CHEMISTRY OF TRANSITION METALS

The transition-metal cations are small and highly charged and readily attract polar molecules or ions to form complexes particularly with cyanide, nitrite ions and ammonia molecules. A typical characteristic of these complexes is that the ligands bound to the metal ion are predominantly sigma donors with moderate to weak π - acceptor or π - donor tendencies [6].

Synthetic and structural determination studies of transition metal complexes containing imidazolidine nitroxyl free radical ligands are certainly important with respect to their physical and chemical properties and have been spurred by the progress on the theory of electronic, structural, thermodynamic, kinetic and redox properties of the complexes [6,9].

1.2.0. CHEMISTRY OF NITROXIDE FREE RADICAL LIGANDS

In the 1960s, interest in the chemistry of nitroxides heightened, owing to the expanding scope of their possible practical and theoretical applications. However, previous research has shown that interest in the chemistry of nitroxide free radical increased, largely because such nitroxides often exhibit a chemical inertness quite uncharacteristic of other free radicals. Of particular interest from a theoretical point of view have been the Electron Spin Resonance (ESR) studies of the magnetic interaction between two or more nitroxide groups in the same molecule. Perharps the most outstanding role played by nitroxide free radicals today is their use in the study of biological systems by Electron Spin Resonance technique [10,11].

Though, there is relatively adequate literature on the nitroxide free radicals especially in the Russian journals of inorganic chemistry, much of it is concentrated on their preparation, synthesis and characterization of metal complexes of the first row of the transition metals. Nitroxide free radicals are therefore, a new class of chemically stable and versatile free radicals. The methods of synthesizing these radicals and studies of their properties are covered in a number of reviews and monographs [10]. The fundamental chemical and physical properties of stable nitroxides have been studied by E.G.Rozantserv in the USSR and A. Rassat in France [47]. The advantages of the above nitroxides is that they contain an imine or imine-N-oxide (nitrone) group in a molecule which

nitroxides have been studied by E.G.Rozantserv in the USSR and A. Rassat in France [47]. The advantages of the above nitroxides is that they contain an imine or imine-N-oxide (nitrone) group in a molecule which dictates their stability in acidic media and extensive reactivity towards electrophilic and nucleophilic reagents. In addition, the presence in the molecule of an imidazolidine nitroxide free radical [1] of an additional nitrogen atom or an N-oxide group in combination with functional groups in position four of the heterocycle (see structure 1 below), allows complexation, chelation and cyclometallation without the participation of the radical centre. This makes it possible to characterize the complexes with the help of ESR methods [11, 15]. The imidazoline structure differs from the imidazolidine (1) in that it contains a double bond between C-4 and N-atom at position 3 of structure 1.

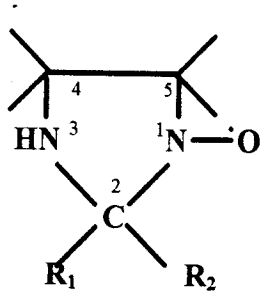

(1)

1.3.0. GENERAL COMMENTS REGARDING STABLE IMIDAZOLINE AND IMIDAZOLIDINE NITROXIDE FREE RADICAL LIGANDS.

The first imidazolidine derived nitroxide spin labels have been described by Keana et al [10]. The nitroxides were prepared by condensation of 2, 3-diamino-2, 5-dimethyl butane with a ketone (structure 2) followed by oxidation of the resulting imidazolidine with m-chloroperbenzoic acid (equ. 1).

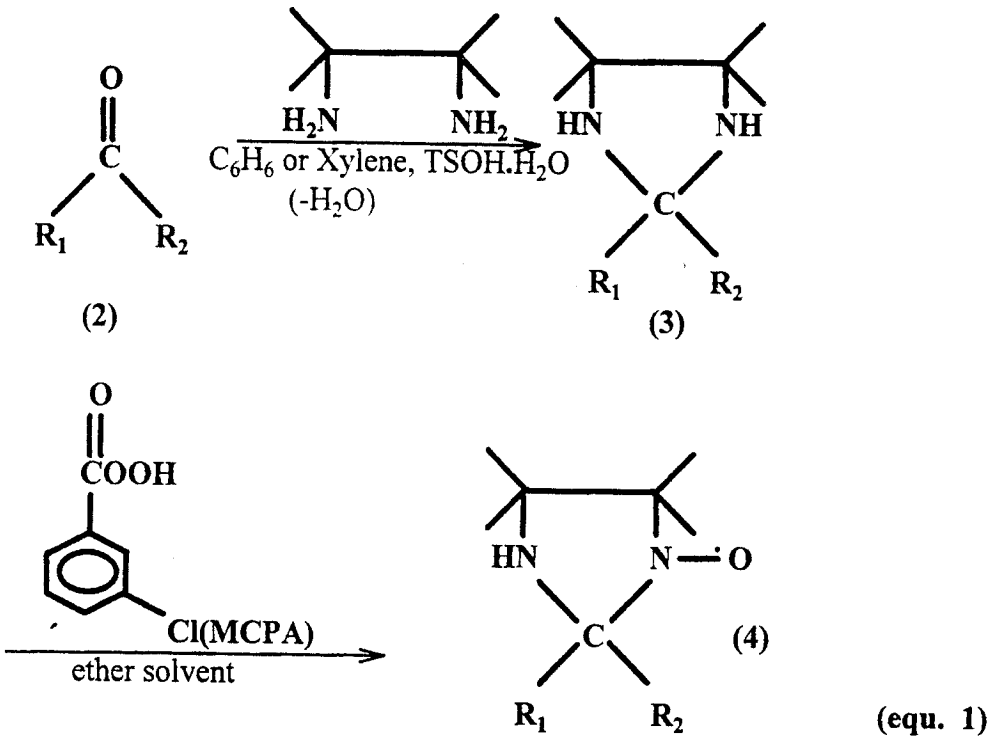

(equ. 1)

$TSOH.H_2O$ = Toluenesulfonic acid monohydrate.

MCPA = m - Chloroperbenzoic Acid.

Because of the rigid attachment of the nitroxide grouping to the parent molecule, this new series of labels show many advantages over other nitroxides studied. The remaining unreacted amino function (structure 4) additionally offers a site for the attachment of a second grouping to the nitroxide moiety via an alkylation or acylation.

STABILITY OF THE NITROXIDE GROUPING

In order for the nitroxide free radical to be useful in conventional spin - labelling studies, it must be reasonably stable. Fortunately, a large number of nitroxide free radicals are

chemically stable (i.e. the free radicals can be obtained in pure form, stored and handled in the laboratory with no more precaution than that observed when working with conventional compounds).

Nitroxides are considered to be derivatives of the 'stable' inorganic radical nitric oxide (NO) whose stability to dimerization can be attributed to its hybrid structure [5].

(5)

It has been represented by the structure with five bonding electrons : N• • • O: i,e with a σ - bond and a 3 - electron bond between the atoms. Such a structure is supported by the small dipole-moment, the bond length and the infra-red spectrum. The bond length (1.5Å) for (structure 5) is greater than the bond length for the triple bond of N ≡ O (1.06Å) and N_2 (1.06Å), and also greater than the bond length for the double bond present in N = O (1.18Å) and O_2 (1.21Å). The infrared vibration frequency (1806 cm^{-1}) is also intermediate between that of N_2 (2330 cm^{-1}) and that of O_2 (1556cm^{-1}) [12]. By analogy, nitroxides may be represented in three different ways as a resonance hybrid of forms (6) and (7) by a structure with a 3 - electron bond (8)

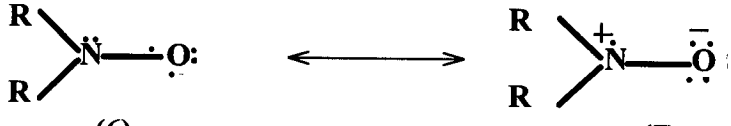

(6) **(7)**

are equivalent to structure (8),

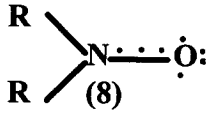

(8)

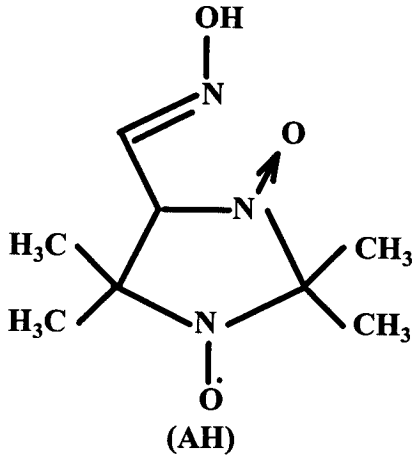

(AH)

The procedure for the synthesis of the complexes and the methods of characterization of the same are clearly described in the Russian journal of organic chemistry (Koordina tsionaya khimiya, vol. 1, No. 10, 1975 [17]). The complexes from the reaction between Cu(II), Ni(II) and Pd(II) ions and **A** were of the general formula MA_2, whereas the reaction between Co(III) ion and **A** formed the complex with a general formula, MA_3 [where M = Co(III)]. The bonding between **A** and the metal ions in these complexes was through the nitrogen atom of the oxime group and the oxygen atom of the nitrone group [1, 16, 17].

By 1983, V. I. Ovcharenko, S.V. Larionov, V. K. Mokhosoeva and L.B. Volodarskii [13] managed to synthesize compounds of Co(II), Ni(II), Cu(II) and Zn(II) ions with a stable radical 4(3′, 3′, 3′ - trifluoro- 2′ - oxopropylidene) - 2, 2, 5, 5 - tetramethyl - 3 - imidazolidine -1 - oxyl ligand (BH) and studied their physico chemical properties.

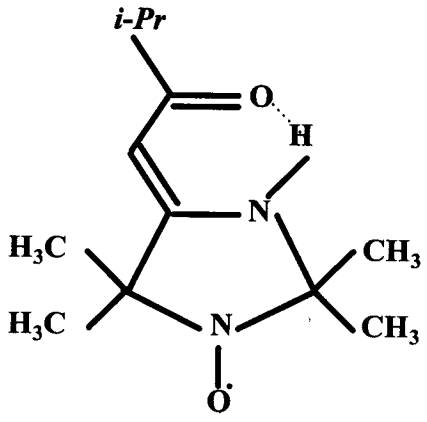

(CH)

The complexation of (C) with the metal ions resulted in the formation of complexes with a general formula MC_2 [M = Cu(II), Ni(II), Zn(II), Co(II) and Pd(II)]. It was noted that the metal ion in the complexes was coordinated to the oxygen atom of the carbonyl group and the nitrogen atom of the imine group of the ligand to give the chelate having the structure (P)[14] shown below.

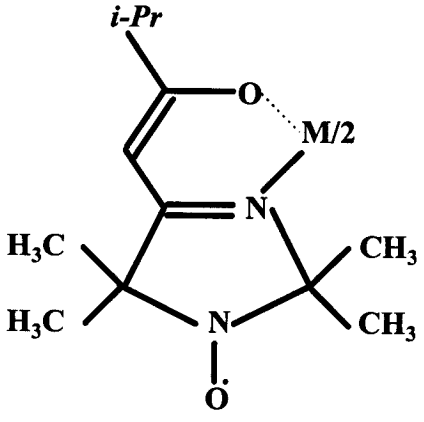

(P)

The complexes were synthesized according to the literature method [18] and were found to be volatile as well. For the purpose of expanding the list of volatile chelates with

stable nitroxide radicals in 1987, V. B. Durasov and other Scientists [3], synthesized and studied volatile chelates of Co(II), Ni(II), and Pd(II) with two new radicals, 4-(4-methyl-2-oxopentylidine)-2, 2, 5, 5, 5-tetramethyl -3-imidazolidine -1-oxyl ligand (DH) and 4-(3, 3-dimethyl -2-oxobutylidene)-2, 2, 5, 5-tetramethyl - 3- imidazolidine-1-oxyl ligand (EH) whose general structure is given below.

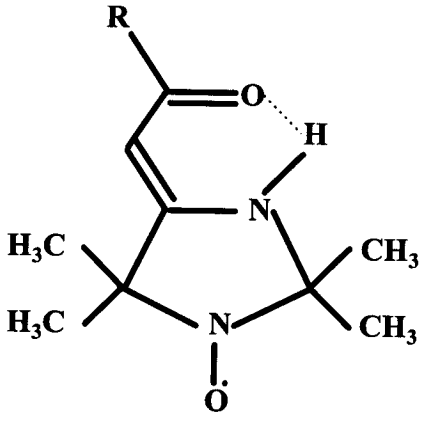

For DH, R = isobutyl [-CH_2 $CH(CH_3)_2$], and for EH, R =tert-butyl [-$C(CH_3)_3$] or t-C_4H_9. The choice of these two radicals as objects of investigation was governed by the earlier research which revealed that the presence of branched terminal hydrocarbon groups in the composition of the organic ligand has a favourable influence on the volatility of the chelates formed with these ligands [19].

The metal chelates of Co^{II}, Ni^{II}, Cu^{II}, Zn^{II} and Pd^{II} having the formulae MD_2 and ME_2 showed appreciable volatility [20] and the bonding between the metal ion and the ligand was realised through the oxygen atom of the carbonyl group and the nitrogen atom of the imine group of the ligand to give a chelate unit MO_2N_2.

1.4.2. METHODS OF CHARACTERIZATION OF TRANSITION METAL COMPLEXES CONTAINING IMIDAZOLINE AND IMIDAZOLIDINE NITROXIDE FREE RADICAL LIGANDS.

The literature available so far on coordination complexes of transition metals with imidazoline and imidazolidine nitroxide free radical ligands show that all the transition metal complexes that have been synthesized by S. V. Larionov and other Scientists [1-3] were characterized with the aid of electronic, IR, ESR and NMR spectroscopy, as well as magnetic susceptibility measurements. Each of these techniques was very vital to the successful determination of the structures of the synthesized complexes and properties. The details of each technique and how it was used have been described in many chemical journals and monographs [1-3, 11-14, 21-23].

COORDINATION OF 4-PHENACETYLIDENE -2, 2, 5, 5-TETRAMETHYL-3-IMIDAZOLIDINE -1-OXYL FREE RADICAL LIGAND (LH) TO TRANSITION METALS.

S. V. Larionov et al [2] have also synthesized the complexes of the transition metals with one of the sterically hindered paramagnetic enaminoketone [4-phenacetylidene-2, 2, 5, 5-tetramethyl -3- imidazolidine -1- oxyl free radical ligand (LH)].

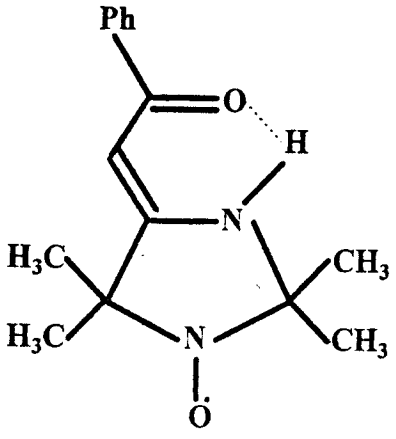

(LH)

The above imidazolidine free radical ligand (LH) possesses an ionizable nitrogen hydrogen. In the presennce of a base the hydrogen ion is removed and a chelating bidentate ligand, $L^{\ominus}$ is generated. The deprotonated ligand then binds to a metal central atom through the nitrogen atom of the imine group and the oxygen atom of the carbonyl group of the ligand, forming a six-membered ring. This is possible because the deprotonated free radical ligand can exist as any of the two tautomeric forms, **Y** and **Z**, increasing its stability.

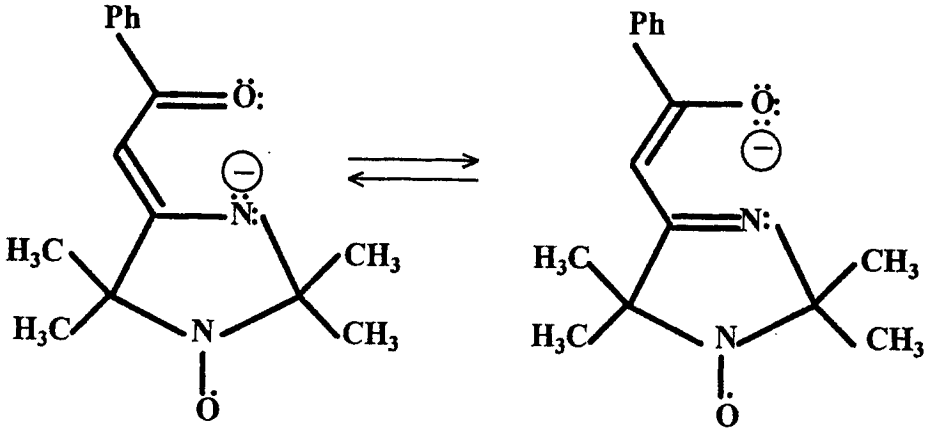

(Y) (Z)

Hence,complexation of the deprotonated ligand$L^{\ominus}$, with metal ions results in conversion of the form (**Y**) or (**Z**) into the chelate complexes with the structure (9).

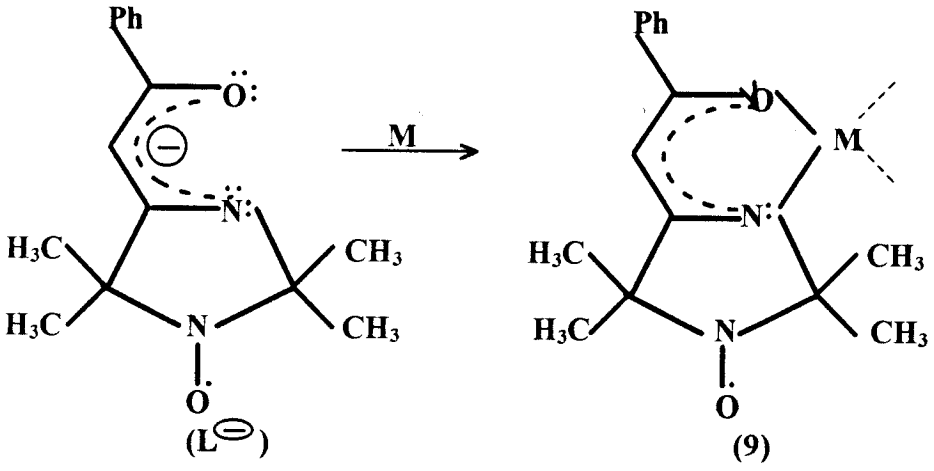

M = Central metal ion.

Therefore, the resonance factor and the ability to form chelating compounds by the above ligand enables it to generate highly stable complexes. Besides, the ligand has a unique characteristic of preserving its free radical entity (>N—$\dot{O}$) during its complexation. The retention of the (>N—$\dot{O}$) group influences the physical properties of its coordination complexes such as magnetic susceptibility, Electron Spin Resonance (ESR) and Nuclear Magnetic Resonance (NMR) properties.

Complexes with the composition ML_2, involving the metal ions Co(II), Ni(II), Cu(II), Zn(II) and Pd(II) with the ligand, have been synthesized and their physico-chemical properties studied [2]. The complexes were prepared by the reaction of aqueous salts of the above named metal ions with the ligand in a water-ethanol mixture and heated for about 30 - 60 minutes on a hot water-bath. The reaction mixture contained a base, whose

main function was to deprotonate the ligand (LH) to $L^{\ominus}$ before complexation with the metal ion.

All the complexes were found to be paramagnetic as indicated by their magnetic susceptibility measurements, and their ESR spectra data confirmed that the free radical entity (>N—O·) of the ligand is preserved during complexation. The complexes also showed appreciable volatility and the IR spectra results indicated that the deprotonated iminoenol form of LH was coordinated to the oxygen atom of the carbonyl group and the nitrogen atom of the imine group of the ligand, forming a chelate unit MO_2N_2.

SYNTHESIS OF NEW TRANSITION METAL COMPLEXES WITH 4-PHENACETYLIDENE-2, 2, 5, 5-TETRAMETHYL -3- IMIDAZOLIDINE-1-OXYL FREE RADICAL LIGAND.

The need to synthesize new complexes containing imidazolidine nitroxide free radical ligand was seen after thoroughly reviewing all the work that has been done by scientists in this area for the past twenty - years. In particular, it was noted that;

(i). Only a few transition metal elements of the first row of the periodic table have been used to synthesize complexes with stable imidazolidine nitroxide free radicals.

(ii). The few complexes of transition metals (only about five so far), i.e, complexes of Co(II), Ni(II), Cu(II), Zn(II) and Pd(II) ions with the above named ligand, that have been studied, showed interesting physical properties.

(iii). The ligand (4-phenacetylidene-2, 2, 5, 5- tetramethyl -3-imidazolidine-1-oxyl free radical) that has been used in the synthesis of the complexes is very stable,

it possible for the preparation of the complexes to be carried out under normal laboratory conditions [2].

The above observations prompted the search for new transition metal complexes containing 4-phenacetylidene-2, 2, 5, 5-tetramethyl-3-imidazolidine -1-oxyl free radical. Therefore, the overall objective of the present research work was to synthesise and characterize vanadium, chromium and manganese complexes containing 4-phenacetylidene -2,2,5,5-tetramethyl-3-imidazolidine-1-oxyl free radical ligand. Moreover, charaterization of metal Imidazolidine Nitroxide free radical complexes using voltammetric techniques is being reported for the first time.

CHAPTER II

2.0. EXPERIMENTAL SECTION.

2.1.0. GENERAL PROCEDURE.

All reactions were performed under normal laboratory conditions and ensured that all solvents were pure prior to their use (i.e. only distilled water and chemicals of analytical reagent were used). The following transition metal salts/compounds were used to synthesize the complexes; vanadium Pentoxide (V_2O_5), Chromium (III) acetate [$Cr(CH_3CO_2)_3$] and Manganese(III) acetylacetonate [$Mn(acac)_3$] (acac =CH_3 $COCH^{\ominus}COCH_3$).

All the complexes were prepared by the reaction of salts/compounds of transition metals with the ligand in a water-ethanol mixture under reflux for a suitable period of time. The reaction mixture had to contain an alkali where required, whose main function was to deprotonate the ligand (LH) to $L^{\ominus}$ before complexation with the metal ion Each complex was purified by recrystallization using a suitable solvent.

2.1.1. CHEMICALS AND SOLUTIONS.

4-Phenacetylidene-2, 2, 5, 5 -tetramethyl-3-imidazolidine-1-oxyl radical (LH) and ether were obtained from Aldrich and used without any further

purification. Chromium(III) acetate [Cr $(CH_3CO_2)_3$], vanadium pentoxide (V_2O_5), ethanol, sodium hydroxide (NaOH), chloroform, acetonitrile, tetra ethyl ammonium bromide (TEAB) and acetone were obtained from BDH chemical Ltd in England.

Manganese(III) acetylacetonate, was prepared in the laboratory according to the literature method [26]. All chemicals were of reagent grade.

2.2.0. A NEW APPROACH TO THE SYNTHESIS OF NEW TRANSITION METAL COMPLEXES OF VANADIUM, CHROMIUM AND MANGANESE CONTAINING IMIDAZOLIDINE NITROXYL FREE RADICAL LIGAND.

The synthesis of each of the complexes involves the preparation and isolation of the product. The isolated product, is then purified and its melting point and the percentage yield determined . The details of the synthesis procedure are described below.

2.2.1. SYNTHESIS OF THE VANADIUM (III) COMPLEX

The vanadium complex was prepared using the method described below. To a mixture of sodium hydroxide (0.4g, 0.01moles) and vanadium pentoxide (0.094g, 5.17×10^{-4} moles) in a $250cm^3$ round bottomed flask was added distilled water ($30cm^3$) and stirred until a yellow solution was obtained. To this solution was added a solution containing LH (0.4g, 1.54

x 10^{-3} moles) dissolved in ethanol ($20cm^3$). The mixture was then refluxed for about six-hours during which period, the solution changed from yellow to light yellow. The solution was then put in a $250cm^3$ beaker and evaporated to about half of its original volume. During the evaporation process a white precipitate formed in the light yellow solution and thus was separated after cooling the solution to room temperature.

The filtrate obtained was further cooled by leaving it in the fridge for one night. This led to the formation of yellow crystals which were separated by filtration using a sintered cruscible and washed with ether. The crystals were further purified by recrystallization from ethanol and dried under the suction pump. The melting point of the pure crystals as determined by the Gallen Kamp melting point apparatus was in the range of 184-186.5°C. The yield of the yellow product was 52%, and that of the white solid was 0.112g. The melting point of the white solid was very high and it gave an ESR signal in solid state only and this is shown in fig. 14(d) on page 70

2.2.2. SYNTHESIS OF THE CHROMIUM(III) COMPLEX

Attempts to prepare chromium(III) complex by the methods used by Larionov et al [2] were unsuccessful. Hence a modification was done by refluxing the mixture instead of merely heating on a water bath as it was in this case. A solution containing LH (0.30g, 1.157 x 10^{-3} moles)

dissolved in ethanol ($20cm^3$) was added to another solution prepared by dissolving chromium(III) acetate (0.095g, 3.84×10^{-4} moles) in distilled water ($10cm^3$). The mixture was put in a $250cm^3$ round bottomed flask and refluxed until the colour of the solution mixture changed from green to pale yellow. This took about six-hours of refluxing time. Then, the solution was removed from the flask and put into a $250cm^3$ beaker, and concentrated by evaporating off the solvent to about half of its original volume. The remaining solution was left for a period of twenty-four hours in a refridgerator to cool. After this period, it was found that greenish/yellow crystals had formed at the bottom of the yellow solution in the beaker. The crystals were separated by filtration and washed with two small portions of ether. Further purification of the crystals was done by recrystallizing the product from acetone and left it to dry under the suction pump for about half an hour. The recrystallized yellow product had a melting temperature range of 182-188°C, and the percentage yield was about 74%

2.2.3. SYNTHESIS OF MANGANESE(III) COMPLEX

Details of the synthesis of manganese(III) complex are as that applied to the synthesis of the chromium(III) complex above. The ligand (LH) (0.40g, 1.54 x 10^{-3} moles) was dissolved in ethanol (40cm^3) and the solution was added to another solution containing freshly prepared manganese(III) acetylacetonate (0.187g, 5.14 x10^{-4} moles) dissolved in ethanol (40cm^3). The mixture was put into a 250cm^3 round bottomed flask and refluxed until the colour of the solution changed from dark to brownish-yellow. The period of refluxing was about nine hours.

The solution was removed from the flask and put into a 250cm^3 beaker, and vaporised off to about one-fifth of the original volume on a hot water-bath. The solution that remained was left overnight to cool in a refridgerator. The brownish-yellow crystals that were formed were filtered, washed with ether and recrystallized from acetone. The recrystallised product had a melting temperature range of 178-181°C and gave a yield of 43%.

2.2.4. REACTION OF BIS (ACETYLACETONATO) OXOVANADIUM(IV) WITH 4-PHENACETYLIDENE - 2, 2, 5, 5 - TETRAMETHYL -3-IMIDAZOLIDINE-1-OXYL FREE RADICAL LIGAND.

The oxovanadium complex was prepared by refluxing a mixture of Bis(acetylacetonato)oxovanadium(IV), $VO(acac)_2$ and 4 -phenacetylidene-2, 2, 5, 5-tetramethyl-3-imidazolidine-1-oxyl free radical ligand (LH) in ethanol ($60cm^3$). Bis(acetylacetonato) oxovanadium(IV) was prepared in the laboratory according to the literature method [26],

The detailed procedure for the synthesis of the above complex is described below:

A solution containing LH (0.40g, 1.54×10^{-3} moles) dissolved in ethanol ($40cm^3$) was added to another solution prepared by dissolving bis(acetylacetonato) oxovanadium(IV) (0.14g, 5.13×10^{-4} moles) in ethanol ($20cm^3$). The pale green mixture was put in a $250cm^3$ round bottomed flask and refluxed until the colour of the solution mixture changed from pale-green to yellow. This took about nine hours of refluxing time. Then, the solution was removed from the flask and put into a $250cm^3$ beaker, and concentrated by evaporating off the solvent to about half of its original volume on a water-bath. The remaining solution was cooled by leaving it in the refridgerator at a temperature of 0^0C for one night. Upon cooling the yellow solution turned deep red and some yellowish crystals formed at the bottomed of the beaker. The crystals were separated by filtration and washed with ethanol. Further purification of the yellow crystals was done by

recrystallizing the product from acetone and drying it under the suction pump. The red filtrate collected, was left to evaporate to dryness at room temperature and a red sticky solid was collected at the bottom of the beaker. The recrystallized yellow crystals had a melting temperature range 175-179.6°C and the yield was 0.194g. (36.4%). The yellow product was found to be soluble in acetone, chloroform, ether and insoluble in water and ethanol.

The oily-sticky red product was kept for sometime to allow it to dry completely. The two products have not yet been characterized. However, arrangements are being made for them to be analysed.

The complexes for vanadium, chromium and manganese synthesized above were characterized by elemental analysis, infra-red (IR), X-ray flourescence, magnetic susceptibility measurements, Electron Spin Resonance (ESR) and Mass Spectroscopy, as well as cyclic voltammetry in order to establish their structures, general formulae and physico-chemical properties. Each of these methods has been described in detail under results and discussion in the next chapter.

CHAPTER III

3.0. RESULTS AND DISCUSSION

The complexes of vanadium, chromium and manganese containing 4-phenacetylidene-2, 2, 5, 5-tetramethyl-3-imidazolidine -1-oxyl free radical ligand (LH), were successfully prepared by the methods described in the experimental section of the dissertation.

In order to determine the formulae, structure and properties of the synthesized complexes, the compounds were subjected to elemental analysis, IR, ESR, X-ray flourescence and mass spectroscopy (FAB), as well as magnetic susceptibility measurements and cyclic voltammetric studies. The results of analysis of the above mentioned techniques are given and discussed below:

3.1.0. ELEMENTAL ANALYSIS RESULTS OF COMPLEXES OF VANADIUM, CHROMIUM AND MANGANESE CONTAINING 4-PHENACETYLIDENE -2, 2, 5, 5-TETRAMETHYL-3-IMIDAZOLAIDINE-1- OXYL FREE RADICAL LIGAND (LH).

The results obtained from elemental analysis of the complexes were compared with the calculated values for an expected formula of the complexes of ML_3. The experimentally determined elemental analysis and calculated results, including some characteristics of the synthesized complexes are listed in table 3.0. below:

TABLE 3.0: Elemental analysis data and some characteristics of Vanadium, Chromium and Manganese complexes.

COMPOUND	COLOUR	Tm, ^{O}K	FOUND/CALCULATED		
			C %	H %	N %
VL_3	Yellow	457-459	66.22/65.38	7.32/6.34	10.20/10.17
CrL_3	Light-yellow	455-461	68.88/65.30	7.46/6.53	10.77/10.12
MnL_3	Brown-yellow	451-454	68.70/65.06	7.26/6.51	10.32/10.12

The elemental data obtained from the elemental analysis is in agreement with the theoretically calculated values for each complex when their general formula was assumed to be ML_3 (table 3.0). This confirms that the synthesized complexes must have been of the composition ML_3, since the data does not agree with the ML_2 structure.

However, the found and calculated values for %C in complexes of CrL_3 and MnL_3 do not agree very well. The slight discrepancies between the experimentally determined element content and the theoretically calculated ones observed, indicate the possibility of having had some impurities in the complexes. It is also possible that some unusual reactions could have occured during the analysis due to the presence of the free radical entity ($\rangle N\!-\!\dot{O}$), which could have contaminated the complexes.

3.2.0. DETERMINATION OF VANADIUM, CHROMIUM AND MANGANESE ELEMENTS IN THE ML_3 COMPLEXES BY X-RAY FLOURESCENCE SPECTROSCOPY.

The aim of X-ray flourescence analysis is the qualitative detection of elements in samples having atomic numbers greater than 8. The phenomena used is the photoelectric absorption, whereby atoms of the sample will become excited and send out their characteristics radiation to all sides. Therefore the choice of the tube's target material should be done carefully in order to produce an X-ray spectrum favourable to excite the atoms of the required element in the sample. This implies that the sample acts as a radiation source, whose spectrum will be dependant on the element present in the sample [29].

The qualitative determination of vanadium, chromium and manganese elements in the synthesized complexes was done by X-ray flourescence using the following procedure. Standard samples of Vanadium, Chromium and Manganese of known concentrations were prepared according to the literature method [21]. Each of the standards was then slowly scanned over a 2Θ region using the x-ray flourescence spectrometer which registered the counts on a paper graph recorder, giving a 2Θ versus intensity plot (where 2Θ is the angle between the incident X-ray and the diffracted beam). A peak characteristic of vanadium, chromium and manganese appeared on each graph in a specific 2Θ range of values for each standard [21]. The above procedure was repeated using a sample of the synthesized complexes. Each sample of the metal complex, was slowly scanned over the same range of 2Θ

values as for its standard and a peak appeared on a paper graph recorder giving a 2Θ versus intensity plot. The peaks for each metal complex and its standard metal sample were recorded on the same graph paper.

The results for vanadium, chromium and manganese complexes and their respective standards are shown in figures 1, 2 and 3.

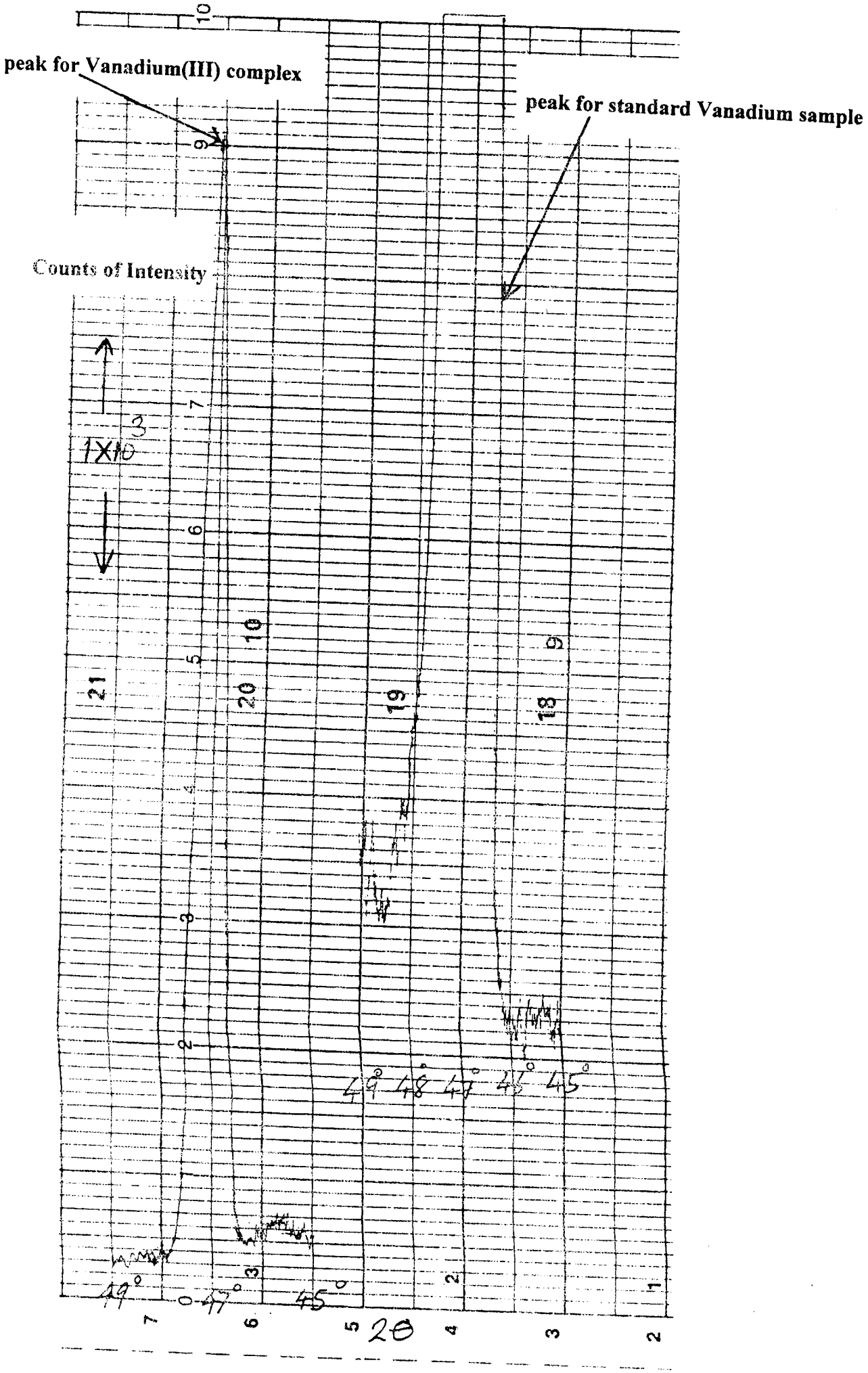

10. X-ray Flouresccence spectra of VL_3 complex and its standard sample.

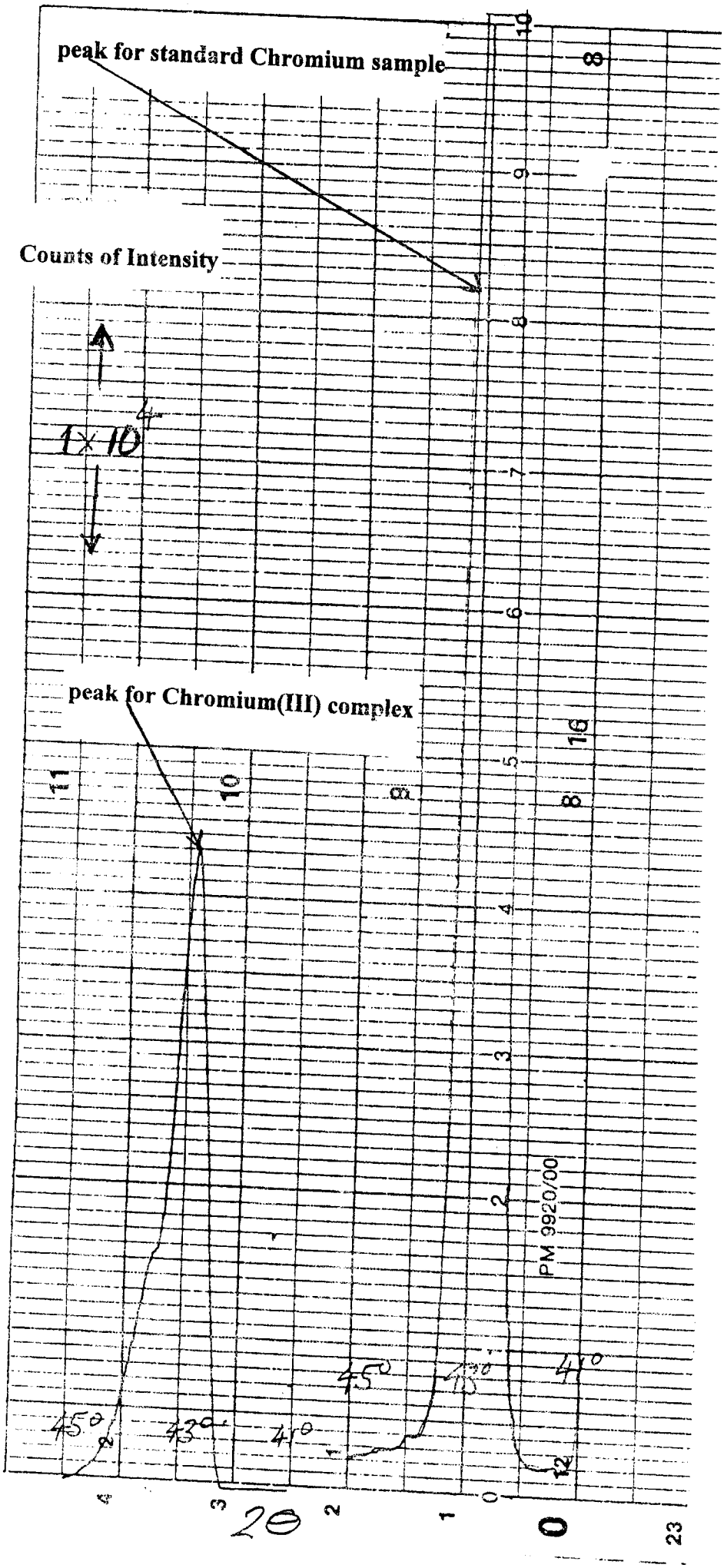

2.0. The X-rays Flourescence spectra of CrL_3 complex and its stan

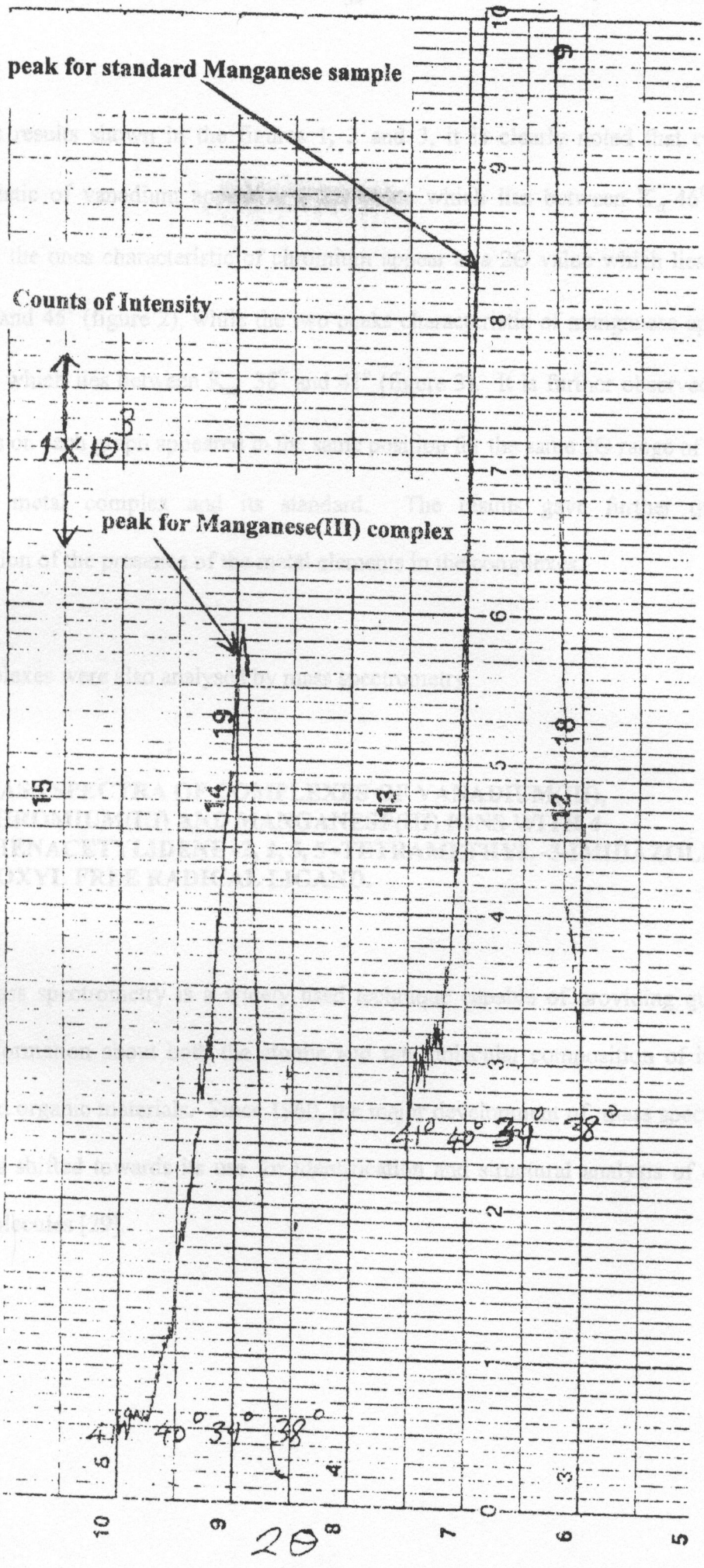

3.0. The X-ray Flourescence spectra of MnL complex and its standard

From the results shown in the figures 1, 2 and 3, it is clearly noted that two peaks characteristic of vanadium appear at a 2Θ value which lies between K_α-46° and 49° (figure1), the ones characteristic of chromium appear at a 2Θ value which lies between K_α - 41° and 45° (figure 2), while the two peaks characteristic of manganese appear at a 2Θ value which lies between K_α . 38° and 41° (figure 3). It is further observed that the two peaks on each graph appeared in the same position for the same 2Θ range of scanning for each metal complex and its standard. The results gave further qualitative confirmation of the presence of the metal elements in the complexes.

The complexes were also analysed by mass spectrometry.

3.2.1. MASS SPECTRA OF COMPLEXES OF VANADIUM(III), CHROMIUM(III) AND MANGANESE(III) IONS WITH 4-PHENACETYLIDENE -2, 2, 5, 5 -TETRAMETHYL -3-IMIDAZOLIDINE -1-OXYL FREE RADICAL LIGAND.

Mass spectrometry is a widely used technique capable of providing qualitative information about both the atomic and the molecular composition of inorganic and organic materials. Since 1960, the major development of mass spectrometry has shifted towards its use for identification and structural analysis of complex molecules [29].

A more recently developed method for producing ions for mass spectra is by fast atom bombardment (FAB). This technique is rapidly assuming a major role in the production of ions for mass spectroscopic studies of high molecular weight biologically active species. In fast atom bombardment spectrometry, samples in condensed form (often in a glycerol matrix) are ionised by bombardment with fast moving xenon or argon atoms at a relatively high pressure. The speeding ions undergo an electron exchange reaction with the lower energy atoms in which charge neutralization occurs without substancial loss of kinetic energy [29].

Fast atom bombardment of organic or biochemical complexes usually produces significant amounts of the parent ion (as ion fragments) even for high-molecular weight and thermally unstable samples [29]. This method has been found to be more efficient than the Electron Impact source (EI). The metal complexes containing LH mentioned above were analysed by fast atom bombardment technique (FAB). In order to facilitate the interpretation of the mass spectra of the complexes, the mass spectra of the ligand (LH) and the known Zinc(II) complex, ZnL_2 were also recorded. The mass spectra of prominent peaks for LH, ZnL_2 and the synthesized complexes are presented in table 4.0 below.

TABLE 4.0: Mass spectra peaks recorded for LH, ZnL_2 and the synthesized complexes.

COMPOUND	Characteristic Peaks in increasing order of (m/e) values	Deduced Molecular Mass
LH	*28, 41, 51, 59, 68 77, 82, 91, 105, 110, 124, 131, 146,* 158 172, 186, 196, 201, 214, 245,260	*259*
ZnL_2	28, 42, 56, 68, 77, 82, 91, 105, 110, 124, 129, 143, 158, 172, 186, 199, 214, 229, 239, 252, 260, 268, 276, 291, 296, 307, 333, 349, 414, 419, 430, 448, 462, 478, 504, 518, 534, 549, 568	581
VL_3	146, 172, 188, 214, 229, 245, 260, 282, 335, 367, 396, 435, 488, 516, 520, 581, 626, 649, 673, 710, 745, 778, 825	826
CrL_3	146, 172, 188, 214, 229, 245, 261, 283, 303, 335, 367, 396, 412, 431, 470, 500, 518, 543, 558, 608, 656, 710, 745, 778, 825.	827
MnL_3	131, 158, 172, 188, 214, 229, 245, 261, 283, 298, 323, 351, 380, 396, 436, 486, 518, 543, 653, 710 777, 825	829

From the mass spectra peaks listed in Table 4.0, for LH, ZnL_2 and the three synthesized complexes, the following observations could be made:

(i). Certain peaks are found to be common to the ligand, ZnL_2 and all the three complexes. These peaks appear at positions of (m/e) 172, 214 and 260 in the mass spectrum of each compound.

(ii). Some peaks appear in both the mass spectrum of the ligand and the ZnL_2 complex and these involve peaks at positions with (m/e) 28, 77, 82, 91, 105, 124, 158, 172, 186, 214 and 260.

(iii). Other peaks observed were common to all the three synthesized complexes and these occur at the positions in the mass spectrum of each complex with (m/e) 172, 188, 214, 229, 245, 260, 283, 396, 710, 778 and 825.

There are other peaks appearing at different positions in the mass spectra and these are unique to each compound. The common peaks observed in the mass spectra of LH and all the complexes indicate the presence of the ligand in the synthesized complexes.

The peaks listed in table 4.0 were extracted from the mass spectra (FAB) charts recorded for the compounds. The mass spectra results of the pure ligand and all the synthesized complexes are shown in figures 4, 5(page38), 6, 7(page39), and 8(page 40).

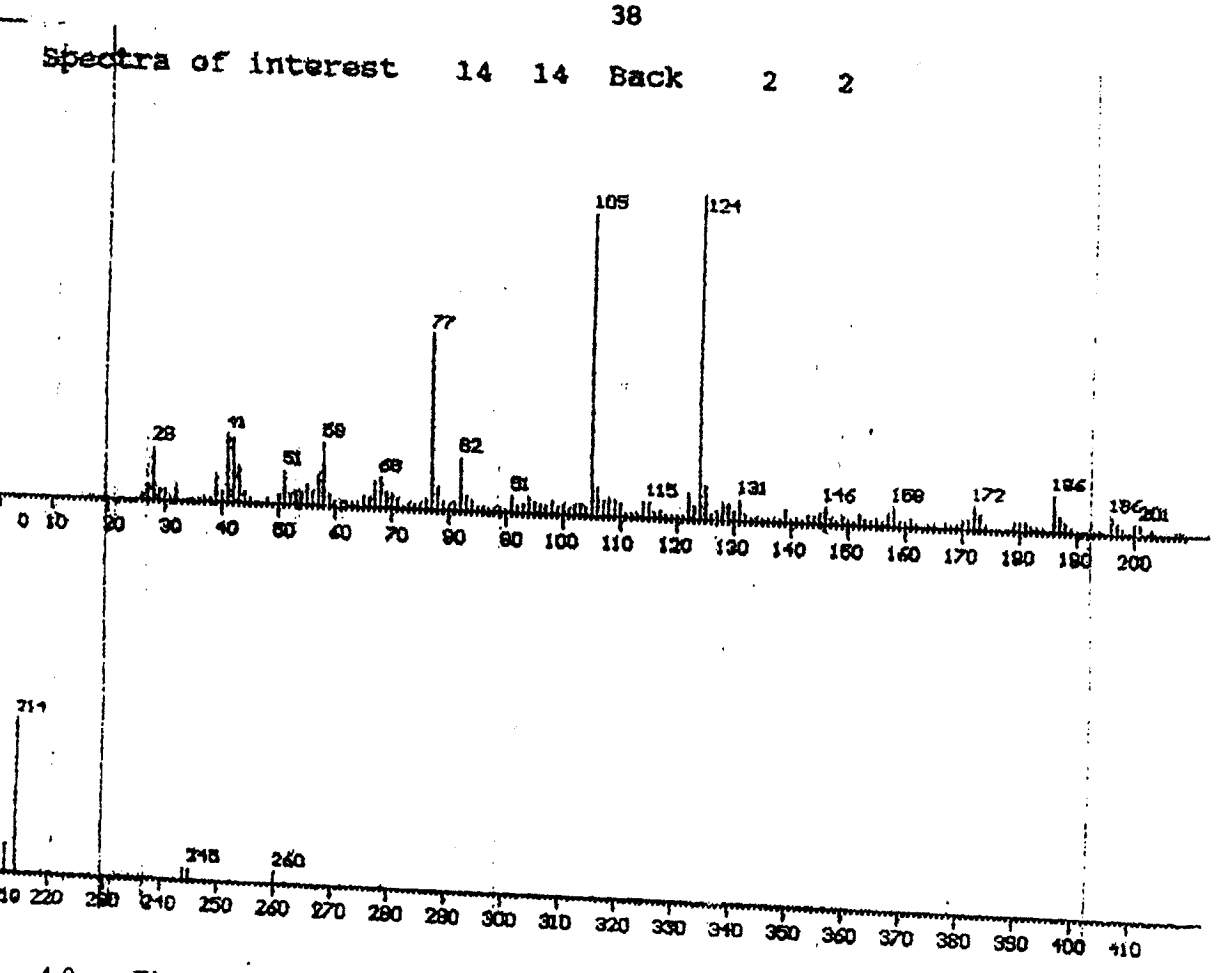

4.0. Electron impact mass spectrum of the pure Ligand (LH).

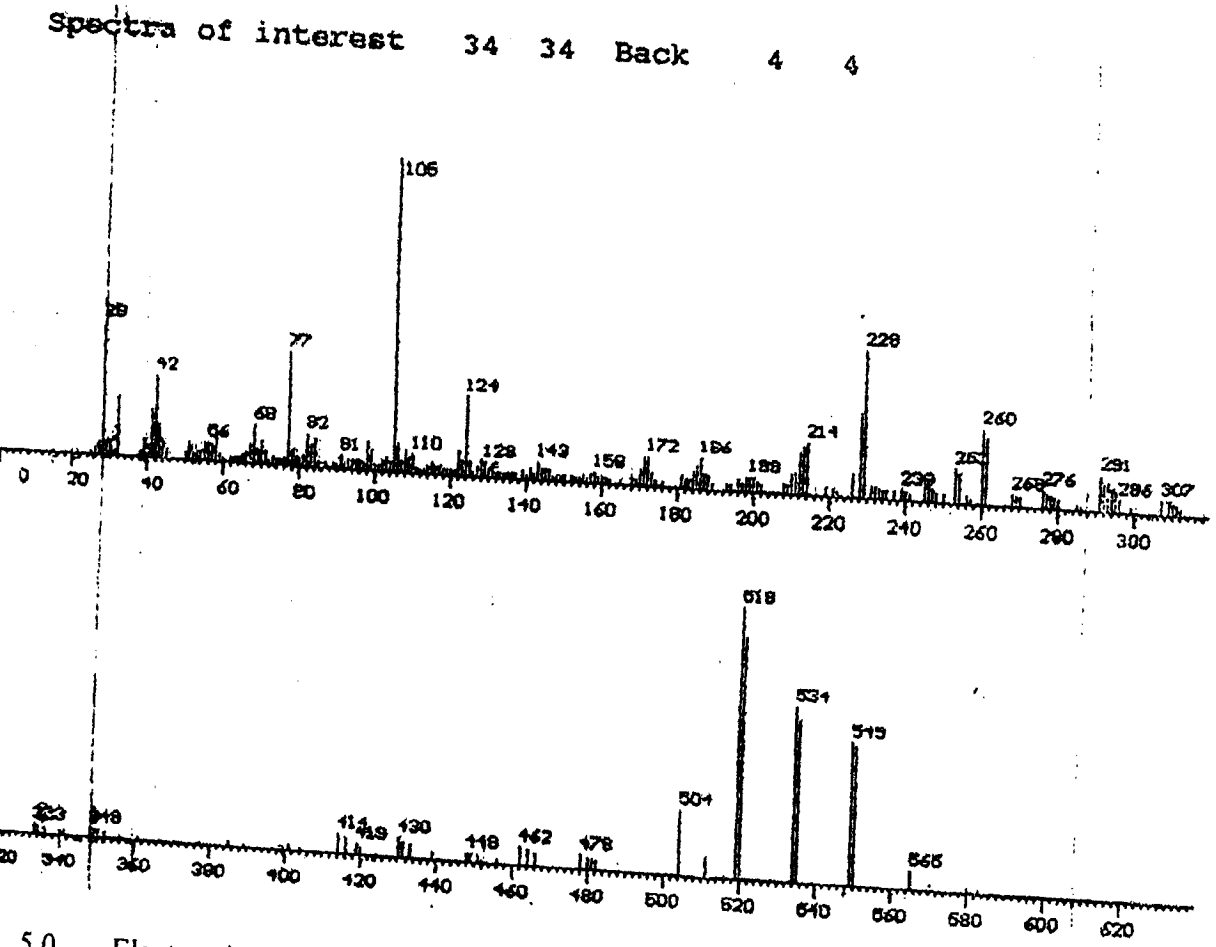

5.0. Electron impact mass spectrum of ZnL_2 complex.

fab1399 Scan 1 (Av 27-32 Acq) 100%=29287 mv 28 Feb 97 14:12
LRP +FAB Boag ZAMS +FAB in mNBA

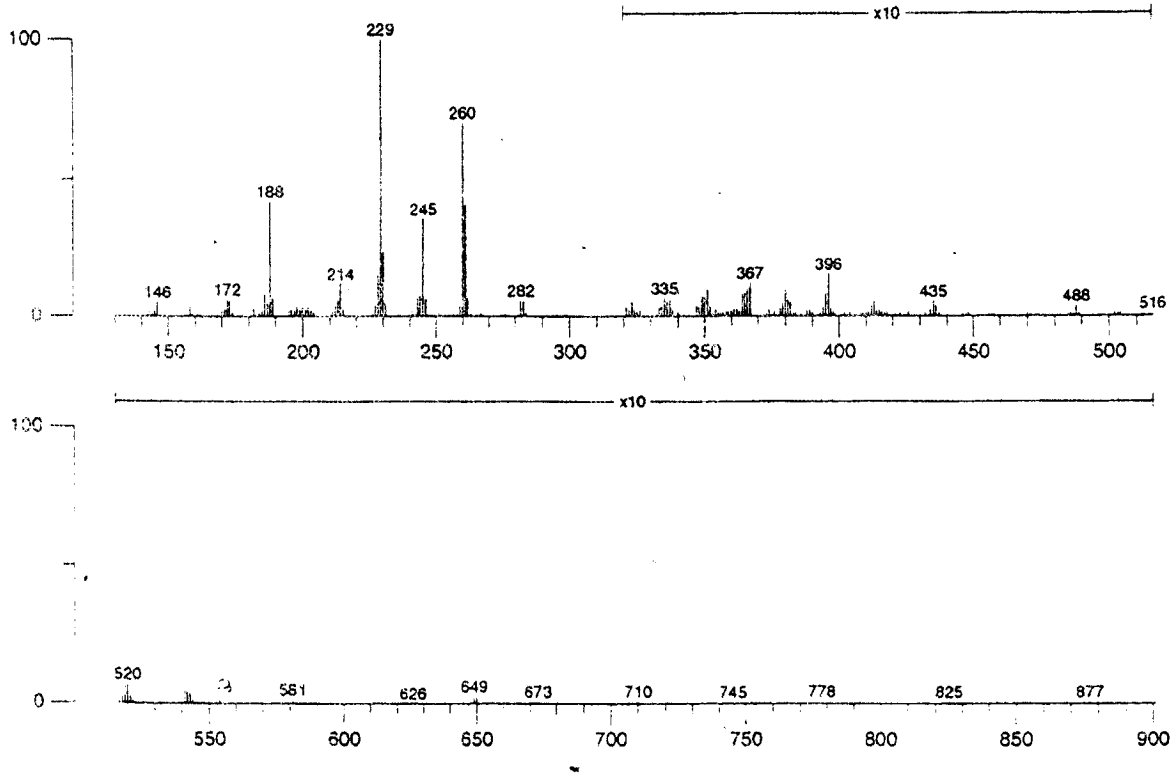

6.0. Fast Atomic bombardment mass spectrum of VL_3 complex.

fab1399 Scan 2 (Av 44-50 Acq) 100%=13075 mv 28 Feb 97 14:12
LRP +FAB Boag ZAMC +FAB in mNBA

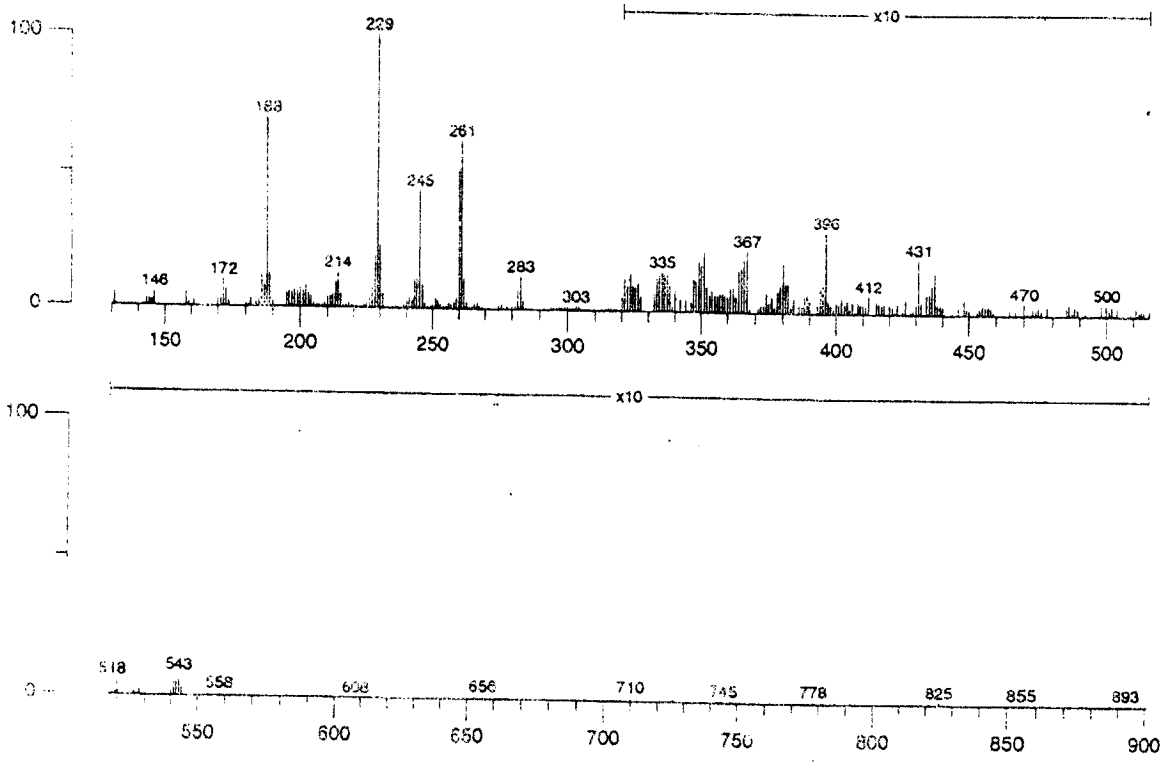

7.0. Fast Atomic bombardment mass spectrum of CrL_3.

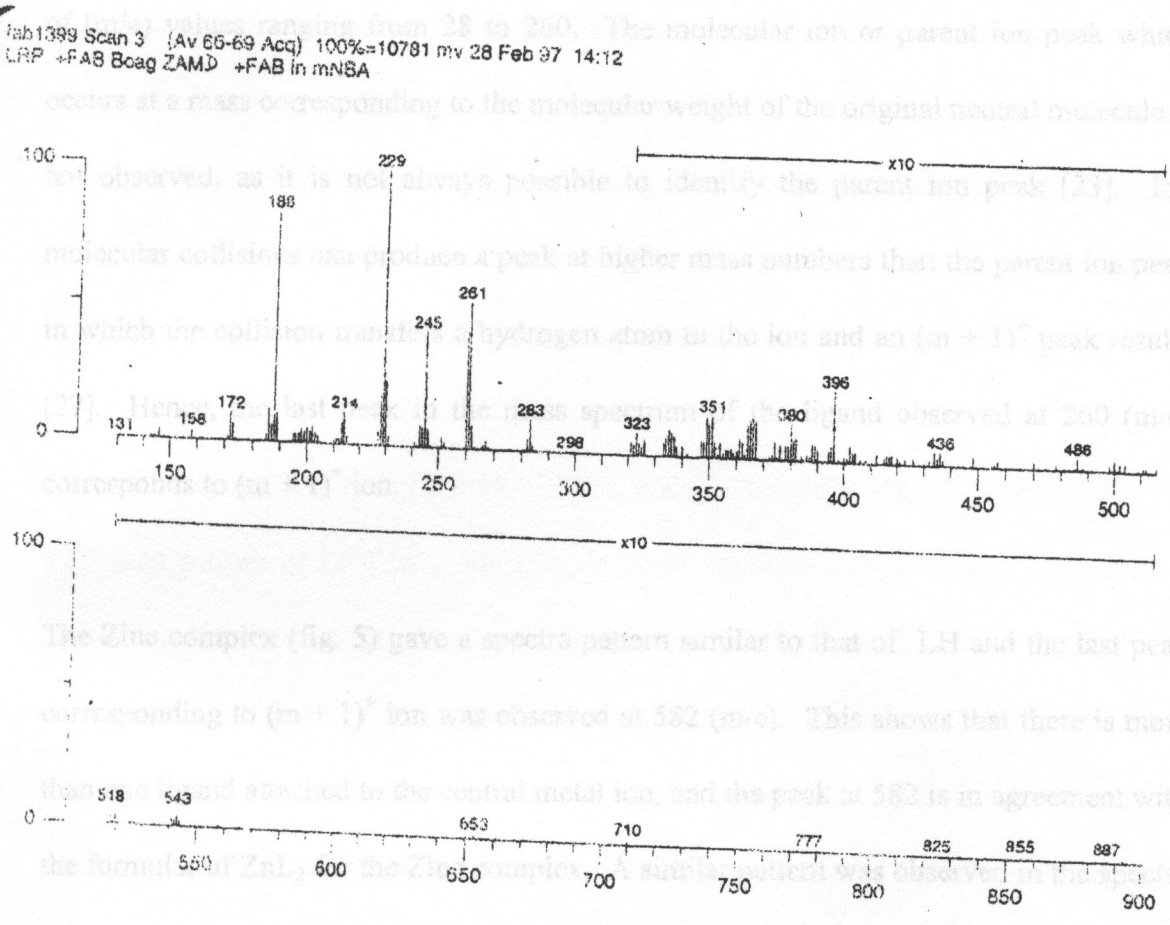

8.0. Fast Atomic bombardment mass spectrum of MnL_3.

The mass spectrum of the pure ligand, shown in figure 4, shows peaks in increasing order of (m/e) values ranging from 28 to 260. The molecular ion or parent ion peak which occurs at a mass corresponding to the molecular weight of the original neutral molecule is not observed, as it is not always possible to identify the parent ion peak [23]. Ion molecular collisions can produce a peak at higher mass numbers than the parent ion peak in which the collision transfers a hydrogen atom to the ion and an $(m + 1)^+$ peak results [27]. Hence, the last peak in the mass spectrum of the ligand observed at 260 (m/e) corresponds to $(m + 1)^+$ ion.

The Zinc complex (fig. 5) gave a spectra pattern similar to that of LH and the last peak corresponding to $(m + 1)^+$ ion was observed at 582 (m/e). This shows that there is more than one ligand attached to the central metal ion, and the peak at 582 is in agreement with the formular of ZnL_2 for the Zinc complex. A similar pattern was observed in the spectra of vanadium, chromium and manganese complexes. A parent ion peak corresponding to the original molecular weight of the neutral vanadium complex was observed at 825 (m/e) and the peaks observed at (m/e) 827 and 829 for the chromium and manganese complexes respectively, correspond to $(m +1)^+$ peaks. Besides the molecular masses of 826, 827,and 829 for vanadium, chromium and manganeses complexes deduced from FAB (table 4) mass spectra are consistent with VL_3, CrL_3 and MnL_3 formulations respectively.

THE BASE PEAKS

A base peak is the largest peak in a mass spectrum and such peaks were observed in the mass spectra of the synthesized ML_3 complexes. It is noted that in each of the mass spectra of the ML_3 complexes shown in figures 6.0 - 8.0, the base peak occurs at a mass of 229, which corresponds to the ion formed by the loss of two methyl ($-CH_3$) groups from $[LH]^+$ fragment remaining from the fragmentation of the ML_3 complexes.

FRAGMENTATION PATTERNS OF LH, ZnL_2 AND THE ML_3 COMPLEXES.

The mass spectra of LH, ZnL_2 and complexes of vanadium, chromium and manganese containing LH show sufficient intensive lines of molecular ions as shown in figure 4, 5, 6, 7 and 8. Analysis of the high resolution spectra of the ligand and all the above mentioned complexes, have shown that they undergo a somewhat more complicated fragmentation pattern [11]. Consequently, the radical ions formed initially are in a highly excited state and can undergo rearrangement or collision to give ions of higher masses than expected [27] as observed in the mass spectrum for the synthesized ML_3 complexes. The behaviour of these compounds upon fast atom bombardment (FAB) is a function of the ligand radical sites [23]. The mass spectra of all the above compounds studied displayed molecular ions as shown in table 5 below.

TABLE 5.0: Molecular ions responsible for the observed peaks in the mass spectra of LH, ZnL_2 and VL_3, CrL_3 and MnL_3 compounds.

FRAGMENTATION PATTERNS

ION	LH	ZnL_2	VL_3	CrL_3	MnL_3
$[M^+]$	-	581	826	827	829
$[M-15+2H]^+$	-	568	-	-	-
$[M-30-2H]^+$	-	549	-	-	-
$[M-45-2H]^+$	-	534	-	-	-
$[M-45-3H]^+$	-	-	778	-	-
$[M-45-4H]^+$	-	-	-	778	-
$[M-45-7H]^+$	-	-	-	-	777
$[M-60-3H]^+$	-	518	-	-	-
$[M-75-2H]^+$	-	504	-	-	-
$[M-75-6H]^+$	-	-	745	-	-
$[M-75-7H]^+$	-	-	-	745	-
$[M-C_6H_5CO+2H]^+$	-	478	-	-	-
$[M-C_6H_5CO-15]^+$	-	-	-	-	710
$[M-C_6H_5CO-15+1H]^+$	-	462	-	-	-
$[M-C_6H_5CO-15+3H]^+$	-	-	-	710	-
$[M-C_6H_5CO-15+4H]^+$	-	-	710	-	-
$[M-C_6H_5CO-30+2H]^+$	-	448	-	-	-
$[M-C_6H_5CO-45-H]^+$	-	430	-	-	-
$[M-C_6H_5CO-45-3H]^+$	-	-	673	-	-
$[M-C_6H_5CO-60+3H]^+$	-	419	-	-	-
$[M-C_6H_5CO-60-2H]^+$	-	414	-	-	-
$[M-C_6H_5CO-60-6H]^+$	-	-	-	656	-
$[M-C_6H_5CO-75+3H]^+$	-	-	649	-	-

ION	LH	ZnL_2	VL_3	CrL_3	MnL_3
$[M-C_6H_5CO-90-5H]^+$	-	-	626	-	-
$[M-C_6H_5CO-MnOH]^+$	-	-	-	-	653
$[M-2C_6H_5CO-9H]^+$	-	-	-	608	-
$[M-2C_6H_5CO-15-7H]^+$ -		-	349	-	-
$[M-2C_6H_5CO-30-5H]^+$ -		-	-	581	-
$[M-2C_6H_5CO-30-8H]^+$ -		-	333	-	-
$[M-L-15-H]^+$	-	307	-	-	-
$[M-L-15+ 4H]^+$	-	-	-	558	-
$[M-L-30+H]^+$	-	-	-	-	543
$[M-L-30+3H]^+$	-	296	-	-	-
$[M-L-30+4H]^+$	-	-	-	543	-
$[M-L-30-2H]^+$	-	291	-	-	-
$[M-L-45-2H]^+$	-	276	-	-	-
$[M-L-45-3H]^+$	-	-	520	-	-
$[M-L-45-6H]^+$	-	-	-	518	-
$[M-L-45-7H]^+$	-	-	516	-	-
$[M-L-60+5H]^+$	-	268	-	-	-
$[M-L-60+6H]^+$	-	-	-	-	518
$[M-L-60-3H]^+$	-	260	-	-	-
$[M-L-75+4H]^+$	-	252	-	-	-
$[M-L-75-5H]^+$	-	-	488	-	-
$[M-L-90+4H]^+$	-	-	-	-	486
$[M-L-CrOH]^+$	-	-	-	500	-
$[M-L-90-9H]^+$	-	-	-	470	-

ION	LH	ZnL_2	VL_3	CrL_3	MnL_3
$[M-L-ZnOH-2H]^+$	-	239	-	-	-
$[M-L-C_6H_5CO-30+2H]^+$	-	-	435	-	-
$[M-L-C_6H_5CO-VOH+H]^+$	-	-	396	-	-
$[M-L-C_6H_5CO-30-H]^+$	-	-	-	-	436
$[M-L-C_6H_5CO-30-3H]^+$	-	-	-	431	-
$[M-L-C_6H_5CO-45-7H]^+$	-	-	-	412	-
$[M-L-C_6H_5CO-60-8H]^+$	-	-	-	396	-
$[M-L-C_6H_5CO-75+4H]^+$	-	-	-	-	396
$[M-L-C_6H_5CO-90+3H]^+$	-	-	-	-	380
$[M-L-C_6H_5CO-90-6H]^+$	-	-	367	-	-
$[M-L-C_6H_5CO-90-7H]^+$	-	-	-	367	-
$[M-L-2C_6H_5CO-15+4H]^+$	-	-	-	-	351
$[M-L-2C_6H_5CO-15-8H]^+$	-	-	335	-	-
$[M-L-2C_6H_5CO-15-9H]^+$	-	-	-	335	-
$[M-L-2C_6H_5CO-30-9H]^+$	-	-	-	-	323
$[M-2L-8H]^+$	-	-	-	303	-
$[M-2L-15-H]^+$	-	-	-	-	298
$[M-2L-30+2H]^+$	-	-	282	283	-
$[M-2L-30-H]^+$	-	-	-	-	283
$[M-2L-45-5H]^+$	-	-	260	261	-
$[M-2L-45-8H]^+$	-	-	-	-	261
$[M-2L-60-5H]^+$	-	-	245	-	-
$[M-2L-60-6H]^+$	-	-	-	245	-
$[M-2L-60-9H]^+$	-	-	-	-	245
$[HL-15+H]^+$	245	-	-	-	-

ION	LH	ZnL_2	VL_3	CrL_3	MnL_3
$[HL-30]^+$	-	229	229	229	-
$[HL-45]^+$	214	214	214	214	214
$[HL-60]^+$	-	119	-	-	-
$[HL-75+4H]^+$ 188		-	- 188	188	
$[HL-75+2H]^+$ -		186	186 -	-	
$[HL-90+3H]^+$ 172		172	172 172	172	
$[HL-C_6H_5CO+4H]^+$	158	158	-	-	158
$[HL-C_6H_5CO+8H]^+$	146	-	146	146	-
$[HL-15-C_6H_5CO-8H]^+$	131	-	-	-	131
$[HL-30-C_6H_5CO]^+$	124	124	-	-	-
$[C_6H_5CO]^+$	105	105	-	-	-
$[C_6H_5]^+$	77	77	-	-	-
$[CO]^+$	28	28	-	-	-

The fragmentation pattern of the complexes and the ligand were used to explain the molecular ions responsible for the observed peaks, rather than using the actual ion's structure or formula responsible, because these are very unstable species and often times yied no actual molecular ion peaks, but instead fragmentation peaks [11,23, and 27].

The fragmentation pattern for LH, ZnL_2, VL_3, CrL_3 and MnL_3 compounds shown in (table 5) is very essential in that it helps one to explain the source of the peaks observed in the

spectrum of each compound. For the above compounds, the decomposition of the ions for each compound occured by the stages described below:

(a). Decomposition of the ions of LH. For the ligand(LH), the peaks in the range of (m/e) 245 to 28 are due to losses by a molecular ion $[LH]^+$ of fragments shown in table 5 under the columns of ION and LH.

(b). Decomposition of the ions of ZnL_2. The peaks in the range of (m/e) 568 to 28 for the Zinc complex are due to losses of a molecular ion $[M^+]$ of fragments shown in table 5 under the columns, ION and ZnL_2. The decomposition of the ions for this complex clearly shows the loss of two ligands with peaks appearing at (m/e) 307 and 229. The loss of central metal ion from the molecular ion also occured giving a peak at (m/e) 239. The information that can be gathered from the fragmentation pattern of the zinc complex is in agreement with the assumed formula of ZnL_2.

(c). Decomposition of the ions of vanadium complex. The peaks in the range of (m/e) 778 to 146 for this complex are due to the decomposition from the molecular ion $[M^+]$ of fragments shown in table 5 under the columns, ION and VL_3. The fragments lost from the molecular ion $[M^+]$, also involves the loss of three ligands, with the loss of the first ligand giving a peak at (m/e) 520, the second ligand gave a peak at (m/e) 282 and the last one, gave a peak at (m/e) 229. The fragmentation also involved the loss of the central metal ion, giving a peak at (m/e) 396. Therefore, this information further confirms the earlier assumption that the vanadium complex synthesized has the formular VL_3.

(d). Decomposition of the ions of chromium complex. The peaks in the range of (m/e) 778 to 146 for the complex are due to the losses from the molecular ion [M^+] of fragments shown in table 5 under the columns, ION and CrL_3. Here, again, it was observed that fragmentation involved the loss of three ligands with peaks appearing at (m/e) 558, 303 and 229, in this order. The metal central ion was also lost during fragmentation giving a peak at (m/e) 500. The above information is in agreement with the synthesized chromium complex having the formula, CrL_3.

(e). Decomposition of the ions of manganese complex. Like for the above compounds, the peaks in the range of (m/e) 777 to 131 for the manganese complex are as a result of the losses from the molecular ion [M^+] of fragments shown in table 5 under the columns, ION and MnL_3. There was a loss of three ligands and the central metal ion for this complex as well. The first, second and third ligands were lost, giving peaks at (m/e) 543, 298 and 214 respectively. On the other hand, the complex lost the central metal ion, giving a peak at (m/e) 653. Hence, with the above information obtained from the fragmentation pattern of the manganese complex, one can confidently say that the complex has the composition, MnL_3.

Table 5 shows that the mass spectra for vanadium(III) complex, chromium(III) complex and manganese(III) complex hardly differ relative to the set of peaks formed, indicating similarity in their fragmentation. It has been proposed that the unpaired electron of the

ligand is lost upon ionization of the metal complexes with free radicals and that the major factor determining fragmentation of such complexes is the localization of the positive charge and radical site in M^{+} in the ligands [23].

The appearance of peaks in each of the mass spectra of the ML_3 complexes at (m/e) 520, 282 and 229 for the VL_3, (m/e) 558, 303 and 229 for CrL_3 and (m/e) 543, 298 and 214 for MnL_3, is a clear indication that the initial fragmentation of the coordination compounds of metals with bidentate ligands is accomplished in such a way that only one ligand takes part in the decomposition, while the second and the third remain unchanged until the first ligand is completely cleared. Cases of the concurrent participation of two or three ligands in the initial fragmentation steps without the complete cleavage of one of the ligands are rare [28].

3.2.2. INFRA-RED SPECTRA RESULTS FOR ML_3 COMPLEXES, (M = V^{3+}, Cr^{3+} AND Mn^{3+}).

The infra-red spectrum of a compound is characteristic of that compound and may be used for identification, just as melting point, refractive index and boiling point.

To identify the synthesized ML_3 complexes, the infra-red spectra of each complex was taken. In order to facilitate the interpretation of the data obtained, the infra-red spectra data for the pure ligand (LH) (see page 16) was also recorded. The Fourier Transform Infra-red (FTIR) spectra data for the uncoordinated free radical ligand (LH) was then

compared with those obtained for each of the ML_3 complexes. The wave numbers (cm^{-1}) of some characteristic absorption bands in the FTIR spectra for LH and each of the ML_3 complexes are given in table 6 below.

Table 6.0 : Wave numbers (cm^{-1}) of some characteristeristic absorption bands in the FTIR spectra for LH and the ML_3 complexes.

LH: *638m, 662m, 673m, 697s, 738m, 1014m, 1030m, 1063m, 1180s, 1214ms,* 1252m, 1296s, 1310s, 1322v.s, 1366m, 1380m, 1436m, 1451s, 1495m, 1538s, 1550s, 1587s, 1628s, 2858m, 2930m, 2978m, 3020m, 3059m, 3225m.br., 3465m.br.

VL_3: 622m, 661m, 675m, 700m, 756v.s, 806s, 882m, 900m, 1025m, 1059m, 1194m, 1317m, 1378m, 1456m, 1506m, 1520m, 1540s, 1558v.s, 1651m, 1698m, 2360v.s, 2872w, 2938m, 2980m.

CrL_3: 696w, 794m, 806m, 882m, 952m, 1025m, 1059m, 1194m, 1317m, 1374m, 1456m, 1506m, 1521m, 1540s, 1558v.s, 1617m, 1651m, 1698w, 2360s, 2872w, 2930m, 2980m.

MnL_3: 806m, 882m, 951m, 1025m, 1059m, 1194m, 1317m, 1374m, 1456m, 1506m, 1520m, 1541s, 1558s, 1651m, 2358.6m, 2872w, 2931m, 2981m.

Symbols: m = medium intensity of a peak

s = strong intensity of a peak

w = weak intensity of a peak

v.s = very strong intensity of a peak

The absence of the band at 1628cm From the FTIR spectra data given above, it can be noted that the spectra data of the ML_3 complexes differ from that of LH, mainly in two ways. For example, in the FTIR data for LH above, an intense band at 1628 cm^{-1} is observed, which corresponds to ν(C =O) group and the bands between 3225 - 3465 cm^{-1}, corresponds to ν(N—H) group, broadened on account of intramolecular H-bonding which is characteristic of the uncoordinated free radical ligand (LH) given on page 16. The band occuring at 1436cm^{-1} in the FTIR data of LH can be assigned to ν(>N— O) stretching vibrations, which is found at 1440± 4cm^{-1} in imidazolidine nitroxides [24]. The above information is in agreement with the structure of LH given on page 16.

The absence of the band at 1628cm^{-1} and the bands between 3225 - 3465 cm^{-1} in the FTIR spectra data of the ML_3 complexes, indicate that the free radical ligands (LH), have become deprotonated and are coordinated to the central metal ion, forming complexes with the structure (T) shown below.

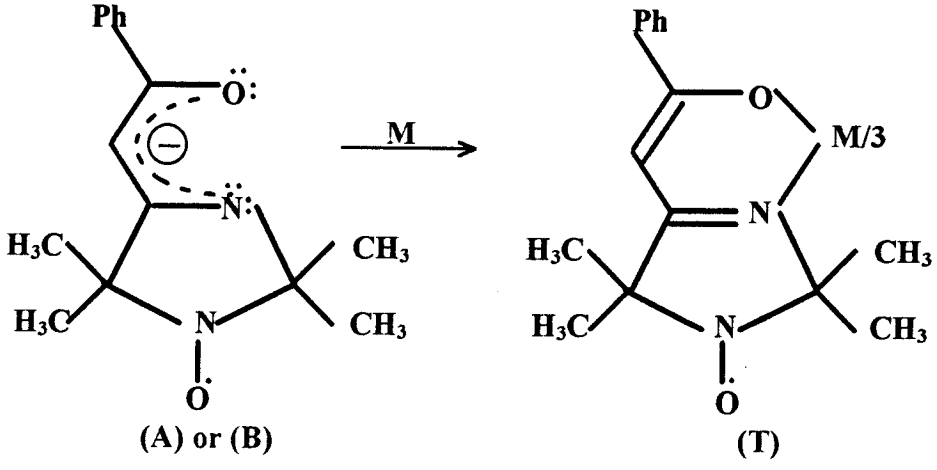

Where (M = V^{3+}, Cr^{3+} and Mn^{3+}).

Furthermore, it should be noted that the bands present in the FTIR spectra of the ML_3 complexes which are important for the characterization of the complexes are described below.

The bands between 1050 - 1317 cm^{-1} in the FTIR spectra of the ML_3 complexes may be assigned to ν (C — O) stretching vibration. The bands in the range 1500 - 1600cm^{-1} can be assigned to the conjugated system of C =C and C=N bonds, which is in agreement with structure **(T)** representing the ML_3 complexes.

The band occuring at 1456cm^{-1} in the spectra of the ML_3 complexes may be assigned to ν (>N— O) stretching vibration [24] which is attached to each ligand and is preserved during complexation. The other peaks present in the spectra of the ML_3 complexes occuring in the regions between 1000 - 700cm^{-1} and 2858 - 3200cm^{-1} could be due to 5 -adjacent hydrogen atoms on the aromatic ring of the phenyl group attached to the ligand (i.e. mono substituted) and the C - H vibrations in the methyl groups present in the structure **(T)**, respectively. The strong peak at 2360cm^{-1} appearing in each FTIR spectra of the ML_3 complexes is likely due to the presence of an impurity in each sample. The FTIR spectra of each of the ML_3 complexes and the ligand LH are given in figure 9, 10, 11 and 12 on pages 53, 54 and 55.

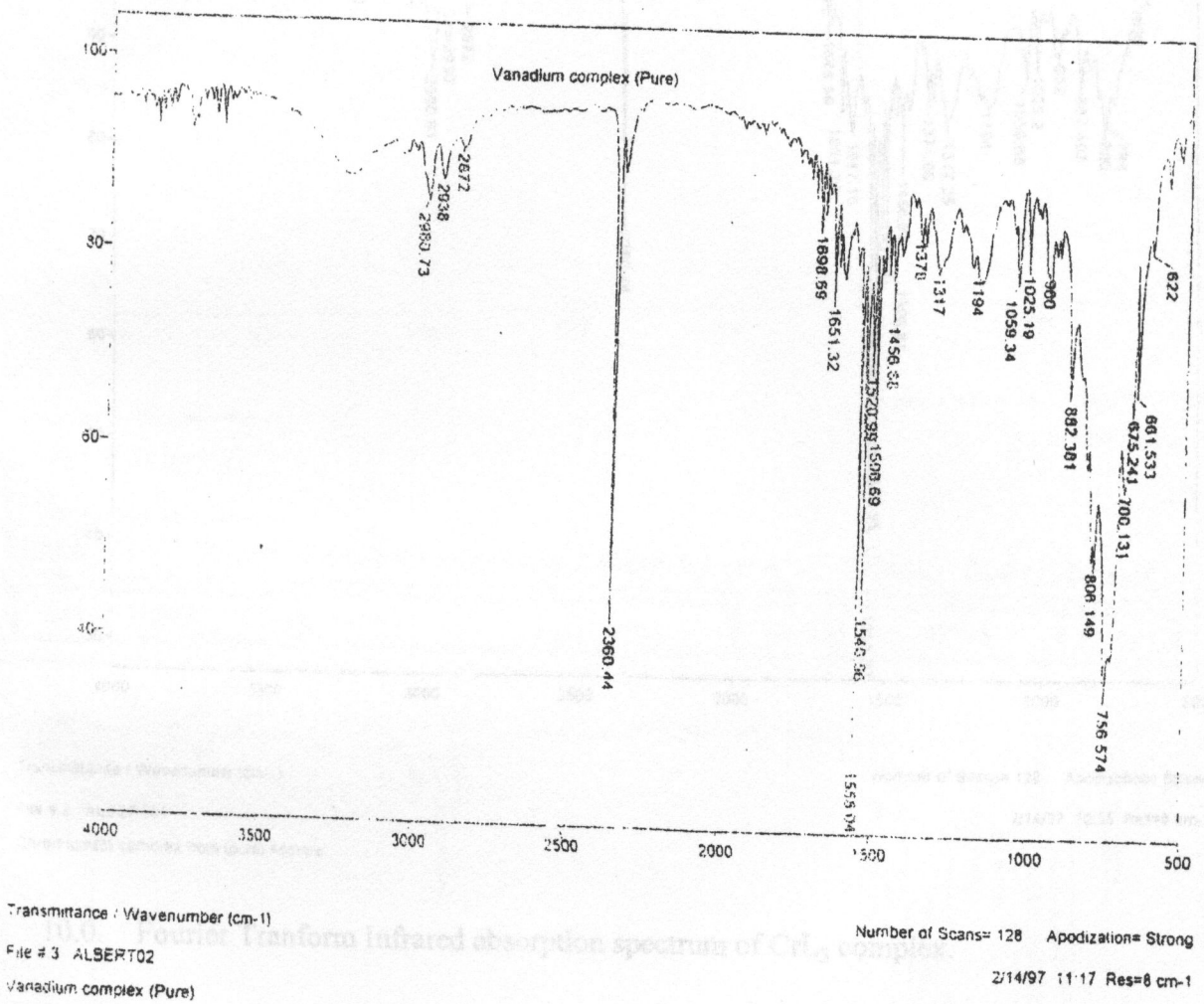

9.0. Fourier Transform Infrared absorption spectrum of VL_3 complex.

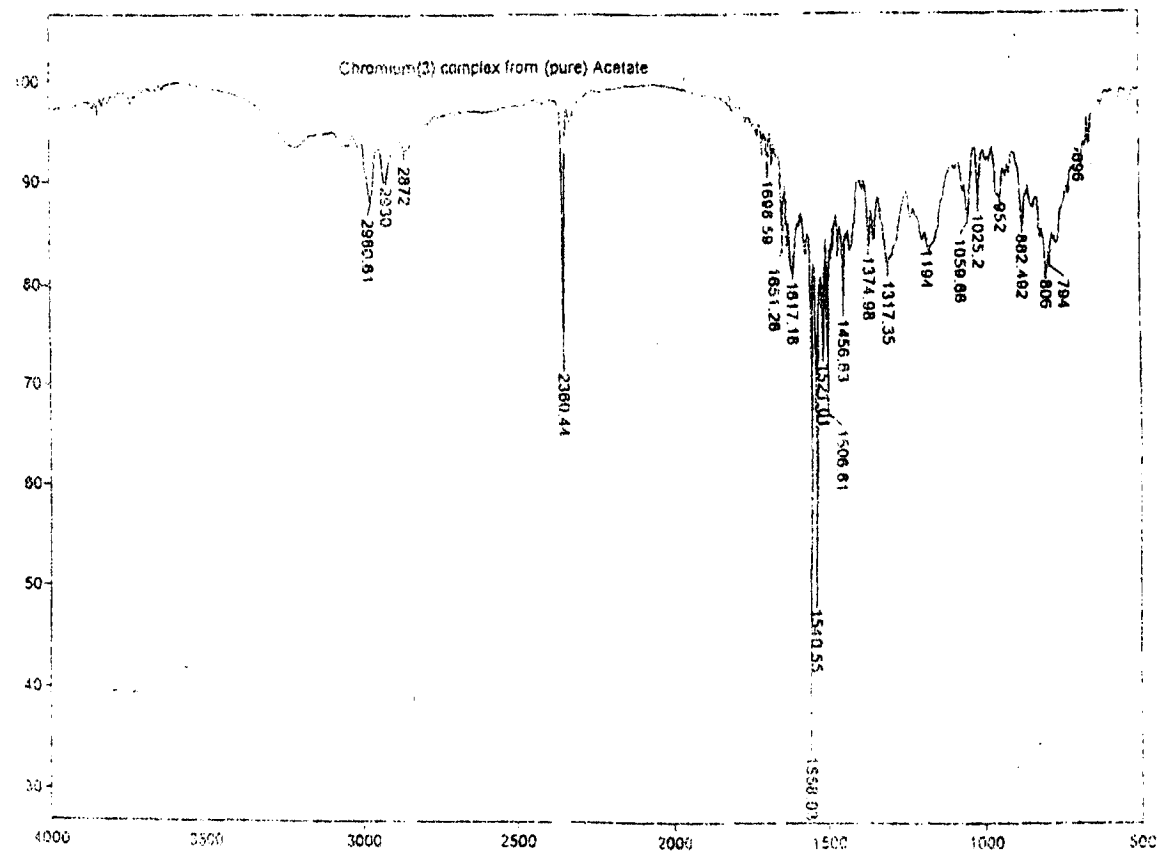

10.0. Fourier Tranform Infrared absorption spectrum of CrL_3 complex.

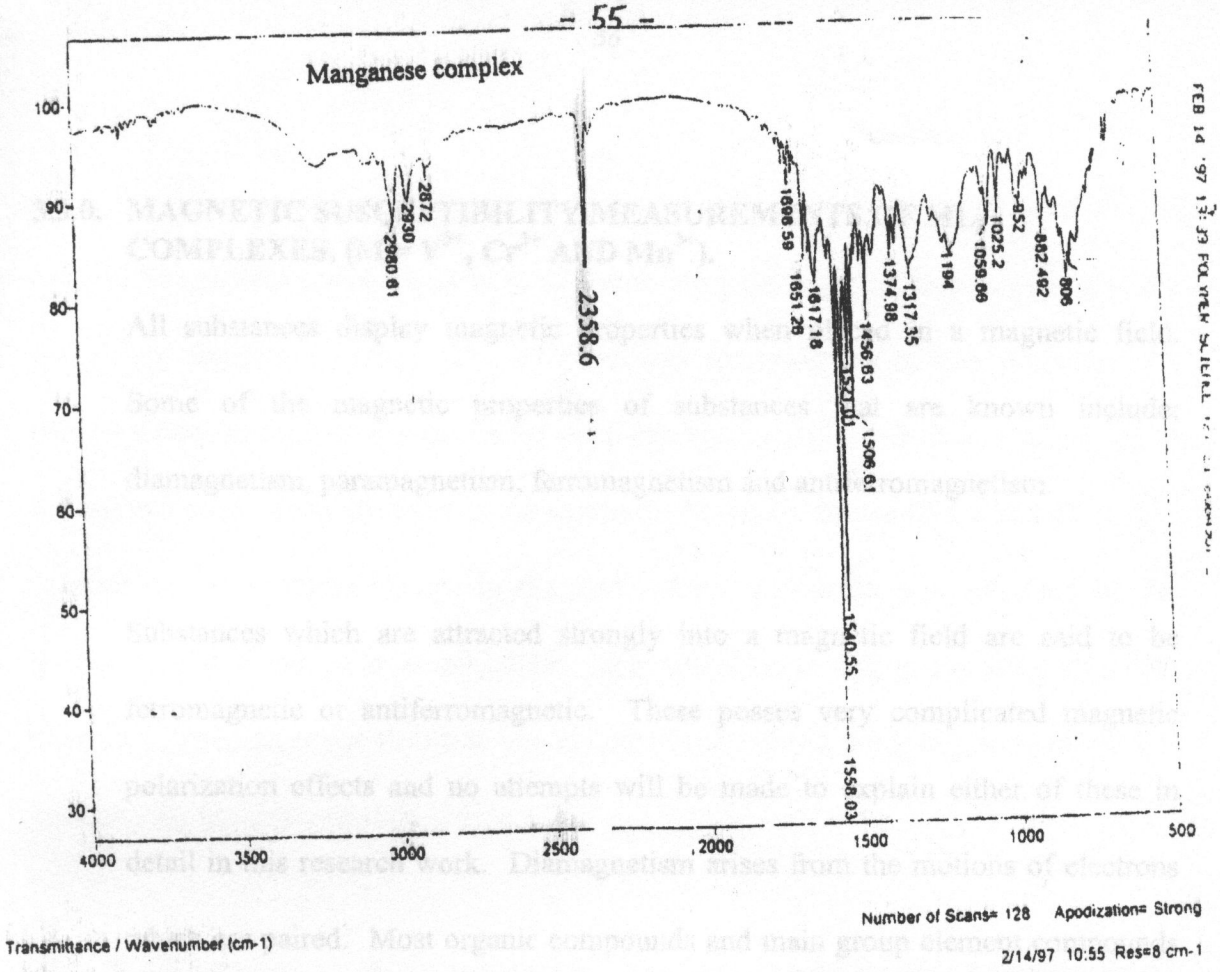

File # 4: ALBRT 03

Manganese complex

Figure 11 : Fourier Transform Infrared absorption spectrum of MnL_3 complex.

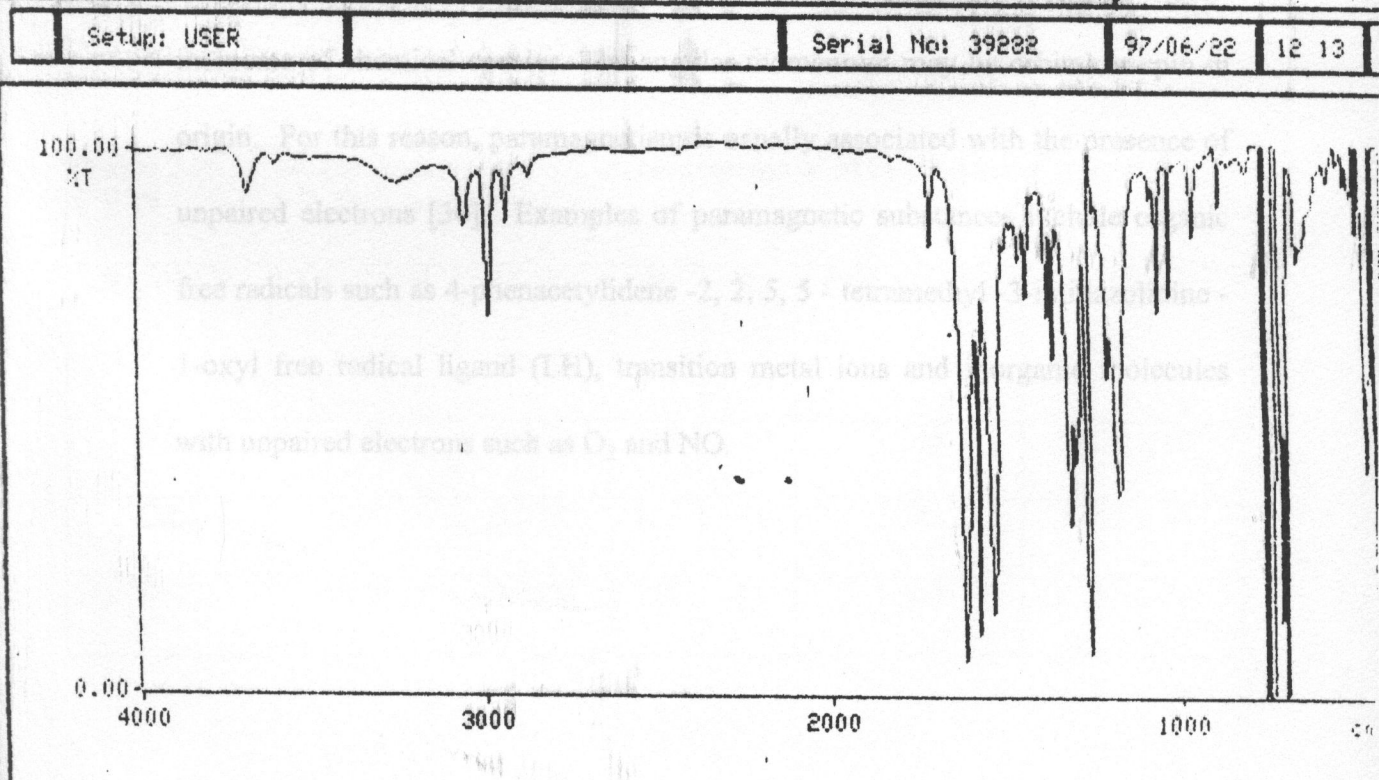

12.0. Fourier Transform Infrared absorption Spectrum of the pure ligand (LH).

3.3.0. MAGNETIC SUSCEPTIBILITY MEASUREMENTS OF ML_3 COMPLEXES, (M = V^{3+}, Cr^{3+} AND Mn^{3+}).

All substances display magnetic properties when placed in a magnetic field. Some of the magnetic properties of substances that are known include; diamagnetism, paramagnetism, ferromagnetism and antiferromagnetism.

Substances which are attracted strongly into a magnetic field are said to be ferromagnetic or antiferromagnetic. These posses very complicated magnetic polarization effects and no attempts will be made to explain either of these in detail in this research work. Diamagnetism arises from the motions of electrons which are paired. Most organic compounds and main group element compounds have their electrons paired and as such are diamagnetic and have very small magnetic moments. On the other hand, paramagnetism arises from the angular momenta of chemical species. The angular momentum may be orbital or spin in origin. For this reason, paramagnetism is usually associated with the presence of unpaired electrons [30]. Examples of paramagnetic substances include organic free radicals such as 4-phenacetylidene -2, 2, 5, 5 - tetramethyl -3-imidazolidine - 1-oxyl free radical ligand (LH), transition metal ions and inorganic molecules with unpaired electrons such as O_2 and NO.

Since the ML_3 complexes synthesized are composed of transition metal ions and an organic free radical ligand (LH) both of which are paramagnetic, this implies that the complexes are paramagnetic. The simplest way to make use of this property in a paramagnetic sample is to measure the magnetic susceptibility which can be related to the number of unpaired electrons in the complex. Magnetic susceptibility is defined as a measure of the apparent change in the mass of the sample as it is attracted by the magnetic field to which it is subjected. The attraction is due to the magnetic field generated by the unpaired electrons in a paramagnetic sample. Magnetic susceptibility is measured by the Gouy method [30].

With this in mind the magnetic susceptibility measurements of the ML_3 complexes were determined with a Gouy balance (MSB-MK1), using powdered specimens at 292°K. The results of the measurements are given in table 6.0 below.

Table 7.0: Magnetic susceptibility measurements of ML_3 complexes (where M = V^{3+}, Cr^{3+}, and Mn^{3+}).

SAMPLE	LENGTH (cm)	MASS (gms)	R	R_o	CONSTANT	Chi
VL_3	2.00	0.0751	113	-29	1.343	5.079×10^{-6}
CrL_3	1.90	0.0780	125	-28	1.343	5.005×10^{-6}
MnL_3	1.70	0.0696	116	-29	1.343	4.756×10^{-6}

The number of unpaired electrons on a given metal ion or an organic free radical ligand in a metal complex, determines the magnetic moments in Bohr magnetoms (B.M) affecting it, both by virtue of their spin or orbital motions [25]. Magnetic moments are not measured directly. They are calculated from the magnetic susceptibility measurements using the procedure described below:

The experimental magnetic moment values of the above complexes were calculated from the magnetic susceptibility measurements given in table 7.0, using the mass magnetic susceptibility equation [25],

$$Xg = \frac{CL\,(R - R_o)}{1 \times 10^9 . m} \qquad \text{(equ.1)}$$

Where L = sample length in centimeters

m = sample mass in grams

C = balance calibration constant

R = reading from the digital display when the sample is in place in the balance

R_o = reading from the digital display when the empty sample tube is in place in the balance.

After the mass susceptibility of the complexes were determined they were converted to the molar susceptibility (X_m) values using the equation [25],

$$X_M = Xg \times \text{molecular weight in } g.mol^{-1}. \qquad \text{(equ. 2).}$$

The molar susceptibility values were then used to calculate the effective magnetic moment (μ_{eff}) in Bohr magnetons (B.M), using the equation,

$$\mu_{eff} = 2.84\ (X_M \times T)^{1/2} \qquad \text{(equ. 3).}$$

Where T is the temperature at which measurements were taken, in Kelvin. For example the procedure for the calculation of magnetic moment from the experimentally determined magnetic susceptibility measurements was as follows:

For VL_3 complex

$$Xg = \frac{CL\ (R - R_o)}{1 \times 10^9 . m}$$

$$= \frac{1.343 \times 2.00\ [113 - (-29)]}{1.0 \times 10^9 \times 0.0751}$$

$$= \underline{5.079 \times 10^{-6}}$$

The Xg values for the three complexes are given in table 7.0 under Chi column.

$$X_M = Xg \times \text{Molecular weight in g.mol.}$$

$$= 5.079 \times 10^{-6} \times 826\ g.mol^{-1}.$$

$$= \underline{4\ .\ 1953 \times 10^{-3}}$$

$$\therefore \mu_{eff} = 2.84 \sqrt{(X_M . T)}$$

$$= 2.84 \sqrt{(4.1953 \times 10^{-3} \times 292)}$$

$$= 2.84 \sqrt{1.225}$$

$$= 2.84 \times 1.1068$$

$$= \underline{3.14\ B.M.}$$

The same procedure was used to calculate the effective magnetic moments for the other two complexes. The results for the three complexes are given in table 8.

After determining the effective magnetic moment values for the complexes from equation 1, 2 and 3, the values were compared with the theoretically calculated magnetic moments. The theoretical magnetic moments were calculated using a slight modification of the well known equation [31], $\mu_{AB} = [n\mu^2_A + m\mu^2_B]^{1/2}$ for a complex of the general formula A_nB_m where both A and B are paramagnetic. The equation is applicable to a cluster of different paramagnetic centres which includes the contribution of the metal ion to the magnetic moment by taking into account the L-component, where the theoretical magnetic moment for the metal is calculated using Van Vleck's equation [23],

$$\mu_M = g[J(J+1)]^{1/2} \qquad \text{(equ.4)},$$

where J = Russell Saunders coupling term and the g - value is calculated from the equation,

$$g = 1 + \frac{S(S+1) - L(L+1) + J(J+1)}{2J(J+1)} \qquad \text{(equ.5)}$$

Since, the transition metal complexes synthesized in this research work contain both a paramagnetic cation and anion, it was found necessary to calculate the overall magnetic moment for each complex, using the formula utilized by Ashley and Mitchell [33].

$$\text{i.e. } \mu_{ML_n} = [\mu^2_M + n\mu^2_L]^{1/2} \qquad \text{(equ.6)}$$

Where both M and L are paramagnetic and **n** is the number of ligands (L) coordinated to the central metal ion (M). Therefore the calculation of the overall magnetic moment

(μ_{ML_n}) was done, using equation (4) and the calculation of μ_L was done, using the equation given below.

$$\mu_L = [Z\,(Z + 2)]^{1/2} \qquad \text{(equ.7)}$$

Where Z = number of unpaired electrons in the ligand.

As an illustration , the steps of the calculation of the theoretical overall magnetic moment for VL_3 complex are outlined below.

(i). Calculation of magnetic moment for the central metal cation (M),

$$\mu_M = g\,[J\,(J + 1)]^{1/2}$$

for V^{3+} ($3d^2$), Ground state R S term = $^3F_2$, L =3, S = 1, and J-value = 2. The g-value was found to be 0.7 from equation (5).

$$\therefore \mu_M = g\,[\,J(J + 1)]^{1/2}$$

$$= 0.7\,[2\,(2 + 1)]^{1/2}$$

$$= \underline{1.72\ B.M}$$

(ii). Calculation of magnetic moment of the paramagnetic ligand (L),

$$\mu_L = [\,Z(Z+2)]^{1/2}, Z = 1$$

$$= [1\,(\,1+2)]^{1/2}$$

$$= \sqrt{3}$$

$$= \underline{1.73\ B.M}$$

(iii). Calculation of the overall magnetic moment ($\mu_{ML_n} = [\mu^2_M + n\,\mu^2_L]^{1/2}$, $n = 3$.

$= [(1.72)^2 + 3\,(1.73)^2]^{1/2}$

$= [\,2.96 + 8.9787]^{1/2}$

$= \underline{3.46\ B.M}$

The same procedure was followed for the calculation of the theoretical magnetic moments for CrL_3 and MnL_3. The experimental magnetic moment values, calculated from the magnetic susceptibility measurements and the theoretically calculated values for the three complexes are presented in table 8.0 below.

TABLE 8.0: The experimental and theoretical magnetic moment values for Vanadium, Chromium and Manganese complexes.

COMPOUND	μ_{eff}, Bohr magnetons (B.M)	
	Found	Calculated
VL_3	3.14	3.46
CrL_3	3.12	3.09
MnL_3	3.05	3.00

The experimental values of the μ_{eff} for the complexes show good agreement with the calculated values, after taking into account the L-component due to the spin-orbital contribution of the metal ion to the magnetic moment. The results of the measurements of the magnetic susceptibility (table 7.0) for the three complexes show that the

paramagnetic centres of the ligands are preserved during complex formation and that the metal ion is not coordinated to $\rangle$ N⟝ O groups. Surprisingly, these complexes, like the complexes of the second and third row transition metals, have shown magnetic properties which reflect not only the spin properties of the electron but also those associated with the orbital motion of the electron.

3.3.1. ELECTRON SPIN RESONANCE (ESR) SPECTRA RESULTS FOR ML_3 COMPLEXES, (M = V^{3+}, Cr^{3+} AND Mn^{3+}).

Electron spin resonance (ESR) is a branch of spectroscopy in which radiation of microwave frequency is absorbed by molecules, ions or atoms possessing electrons with unpaired spins.

The principle of ESR spectroscopy is similar to that of magnetic susceptibility measurements in that both are applicable to substances which posses unpaired electrons (i.e. paramagnetic substances). The only difference is on what is measured in each case. In magnetic susceptibility measurements, it is the apparent change in mass of the sample as it is attracted by the magnetic field to which it is subjected which is measured. But in ESR spectroscopy, the unpaired electron in a paramagnetic substance which has a spin quantum number of one-half will have two energy levels that differ slightly in energy under the influence of a strong magnetic field. The lower energy level corresponds to m_s = -1/2 and the higher to m_s = +1/2. It is the difference between these two energy levels which is measured. Therefore, when a magnetic field (H) of appropriate

frequency is applied to the electron spin functions α and β corresponding to m_s = +1/2. and -1/2, respectively, energy is absorbed. With fixed frequency operation variation of the magnetic field through the resonance condition set by

$$gB_NH = h\nu$$

leads to the observation of a resonance signal arising from the transition from the -1/2 state as shown in the diagram below [41].

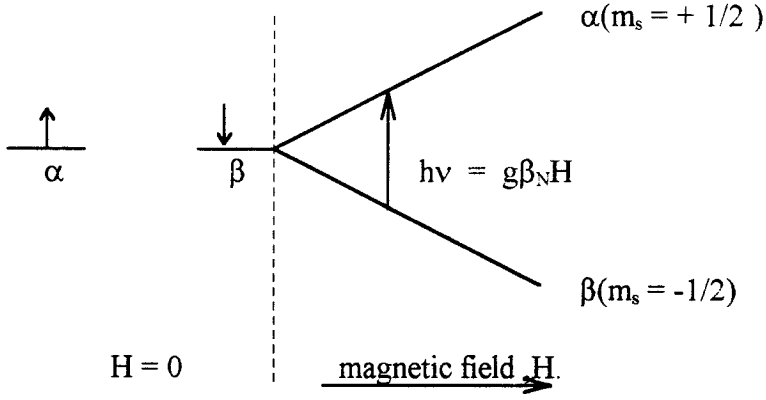

figure 13.0: The splitting of a state with m_s = 1/2 by a magnetic field, showing the resonance signal for the absorption of electromagnetic radiation.

Therefore, substances with unpaired electrons such as organic free radicals transition metal ions, ferro-and antiferromagnetic materials, and inorganic molecules with unpaired electrons such as oxygen and nitrogen oxide are amenable for study by ESR [34].

The ESR spectra of the ML_3 complexes, both on solid samples and in solutions of chloroform were recorded. The ESR spectra for the complexes were measured at two frequencies for samples in solid state [i.e. at 3358 ± 250G (a) and 3358 ± 50G (b)], and the samples dissolved in chloroform solution were measured at a frequency of 3373 ± 50G, labelled (c). The ESR signals recorded for each complex are shown in figures 14(a), (b), (c) and (d); 15(a), (b) and (c); 16(a), (b) ,(c).

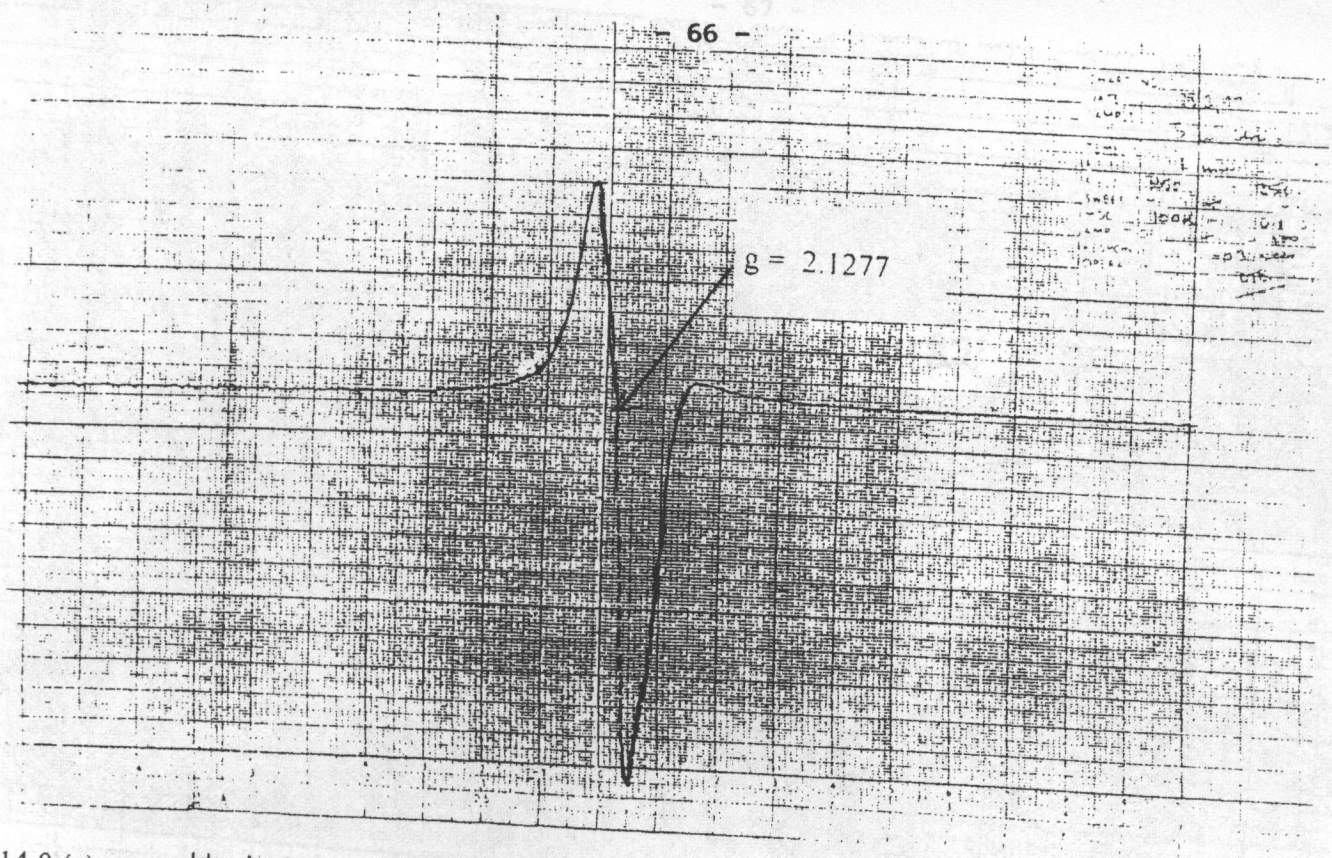

14.0.(a). The ESR spectrum of VL_3 complex in solid state taken at an applied field of 3358 ± 250 G.

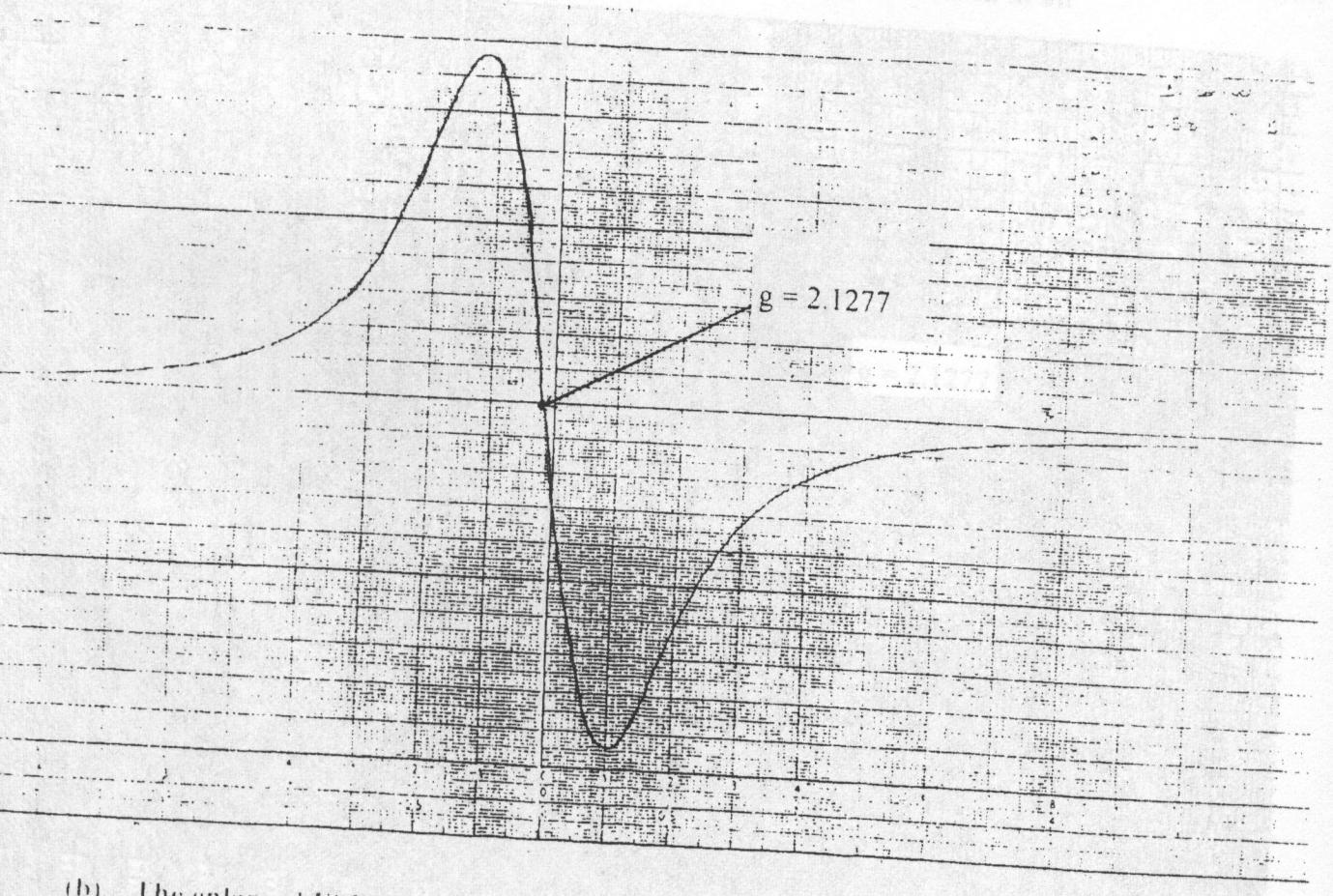

(b). The enlarged ESR spectrum of VL_3 complex in solid state taken at an applied field of 3358 ± 50 G.

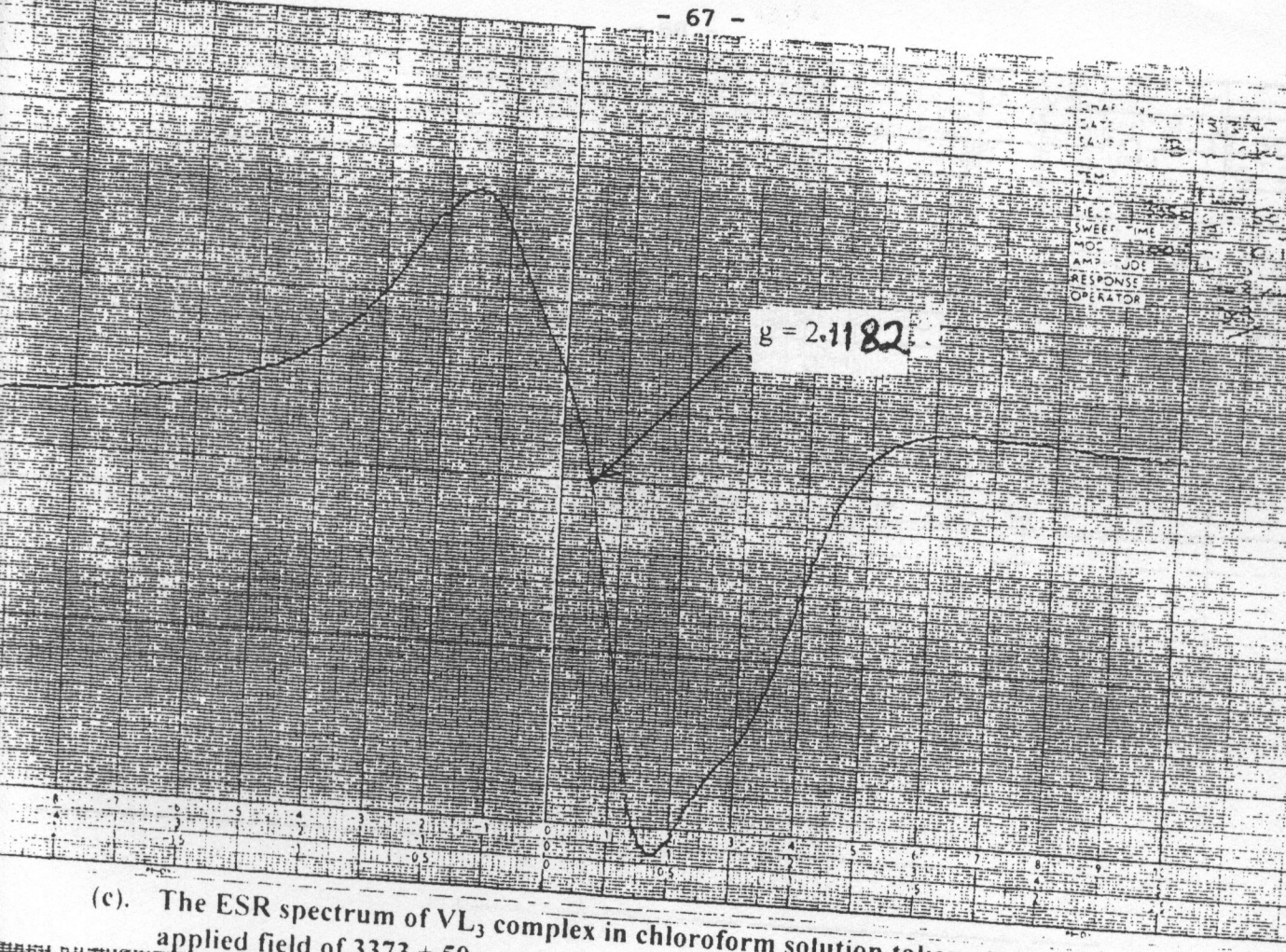

(c). The ESR spectrum of VL_3 complex in chloroform solution taken at an applied field of 3373 ± 50.

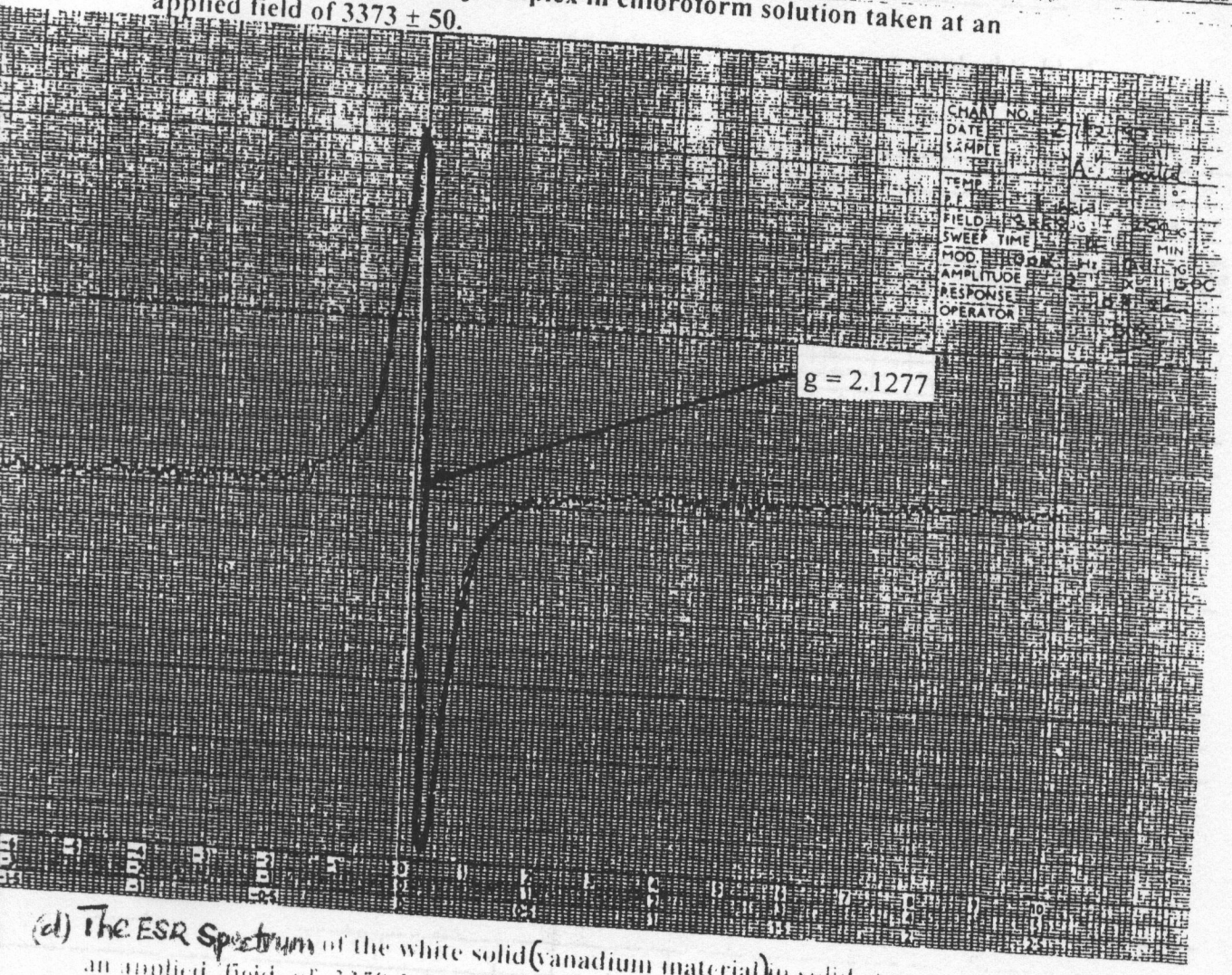

(d) The ESR Spectrum of the white solid (vanadium material) in solid state taken at an applied field of 3358 ± 250 G.

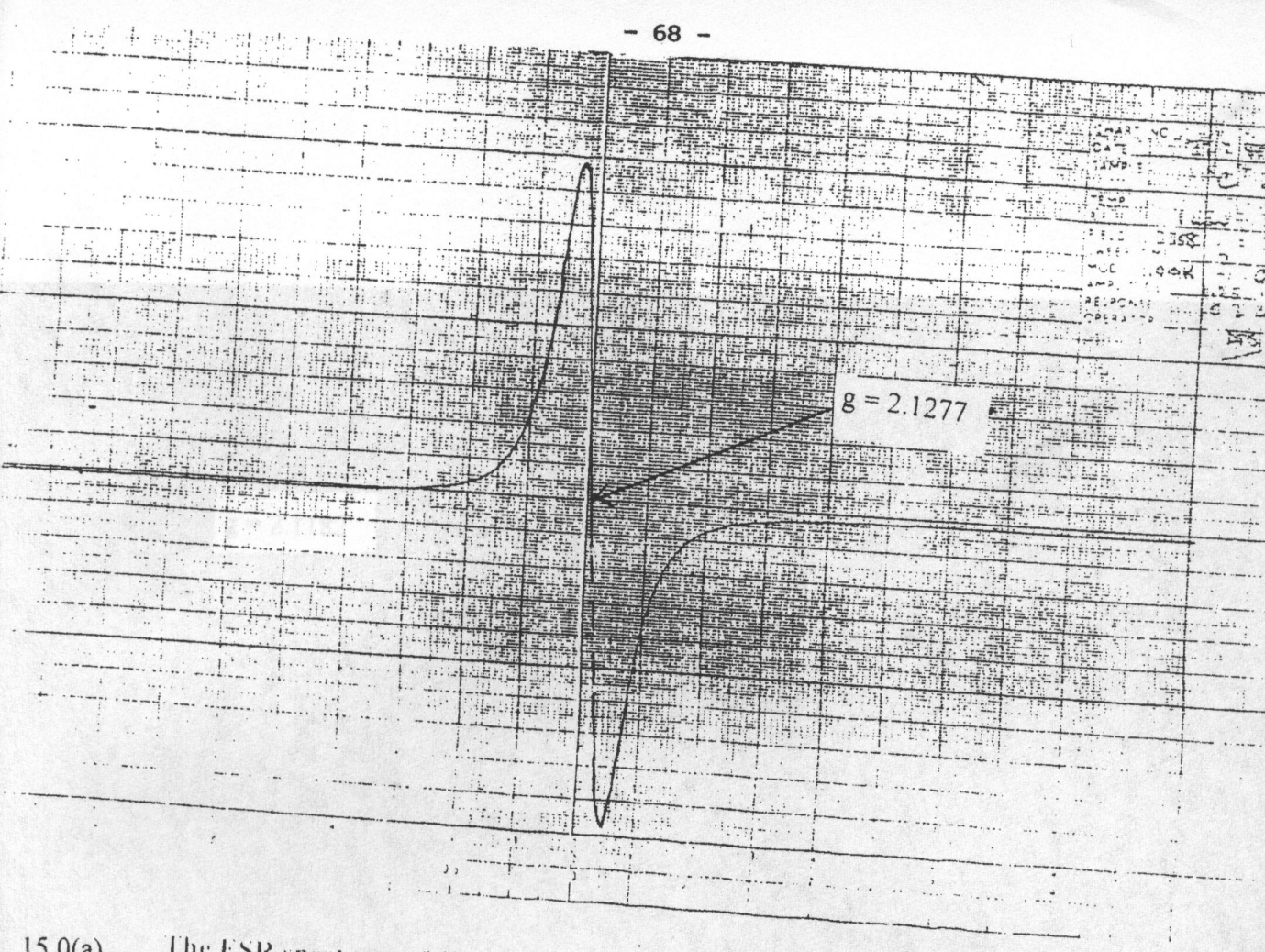

15.0(a). The ESR spectrum of CrL_3 complex in solid state taken at an applied field of 3358 (±) 250 G.

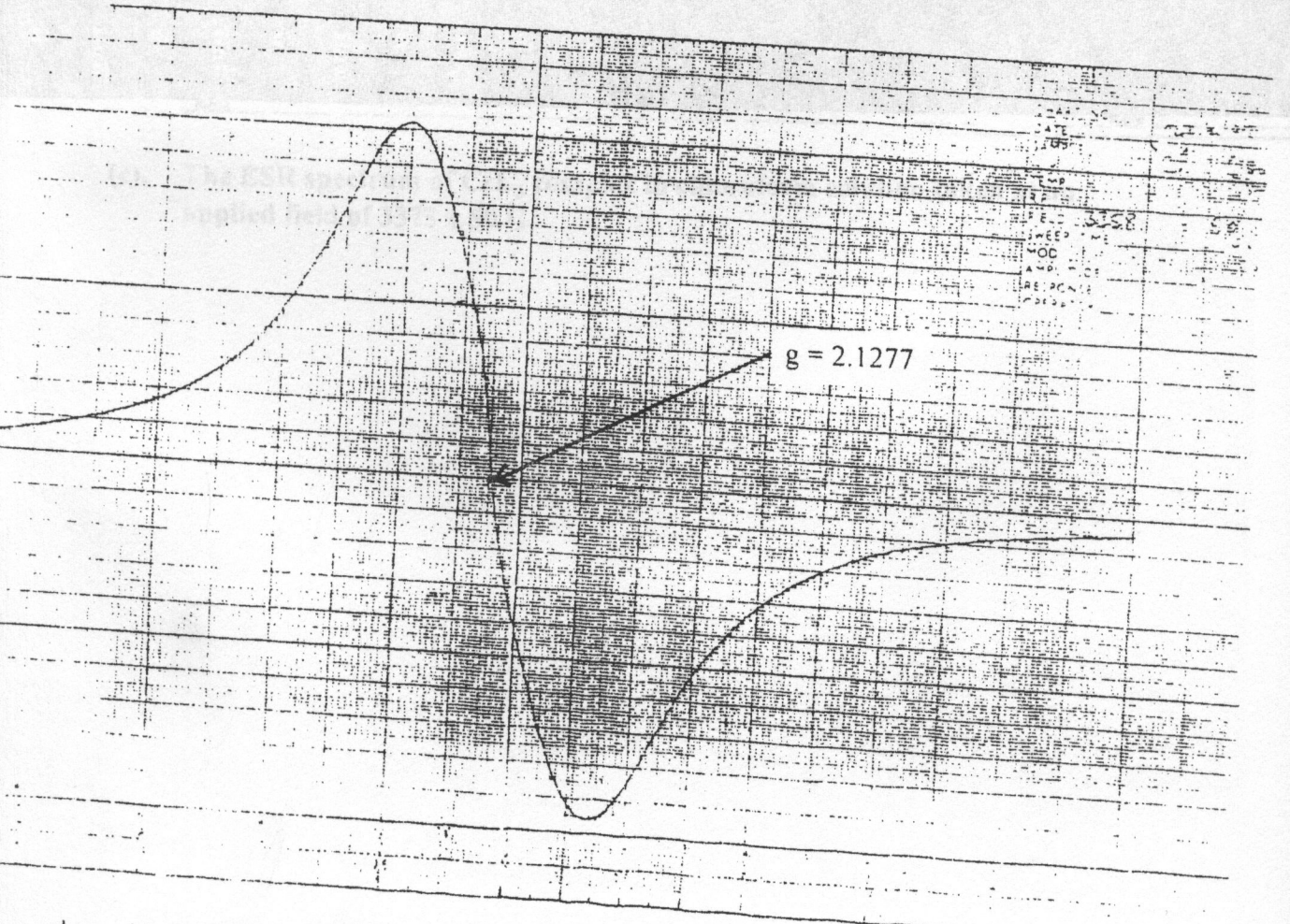

(b). The enlarged ESR spectrum of CrL_3

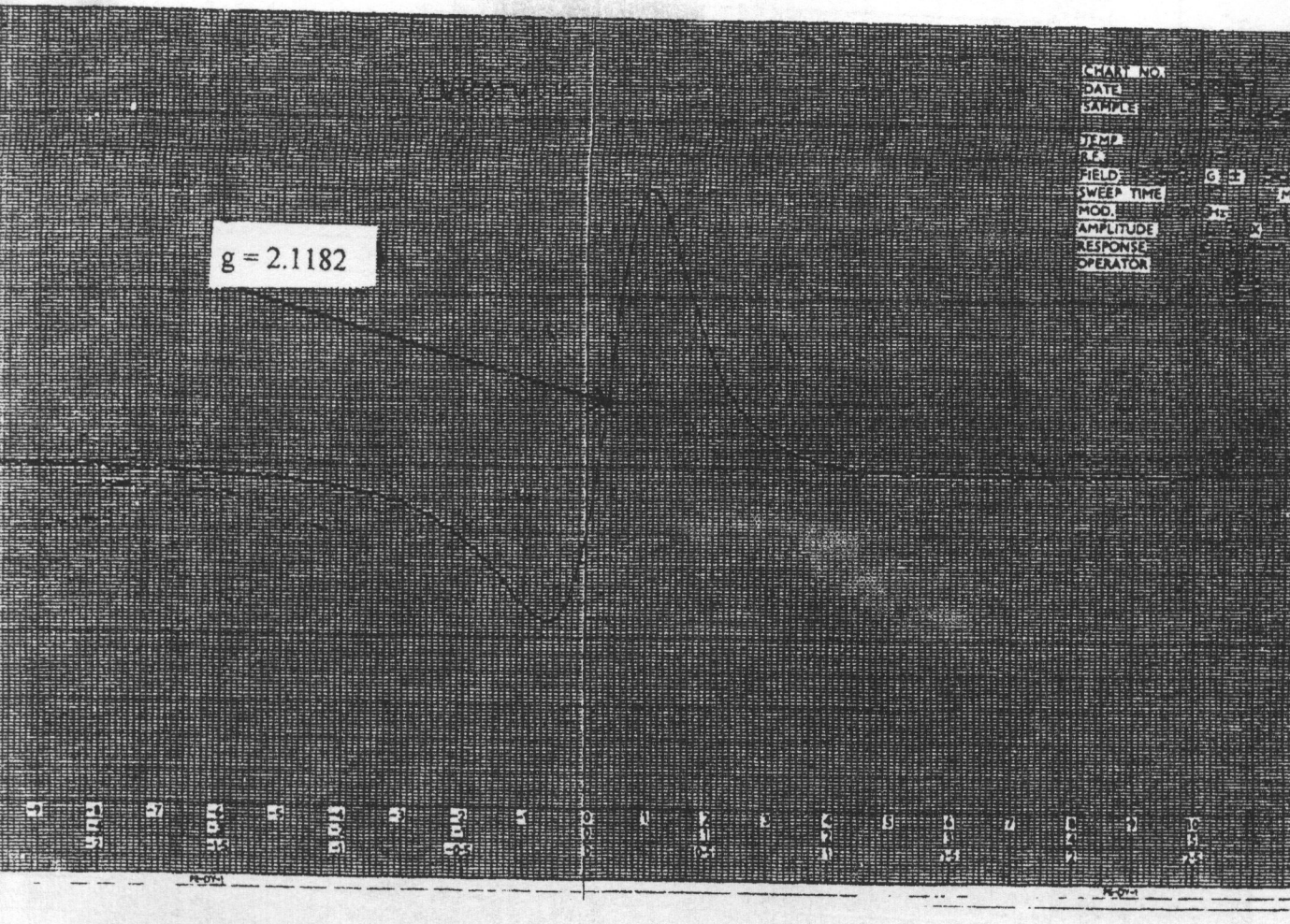

(c). The ESR spectrum of CrL_3 complex in chloroform solution taken at an applied field of 3373 ± 50 G.

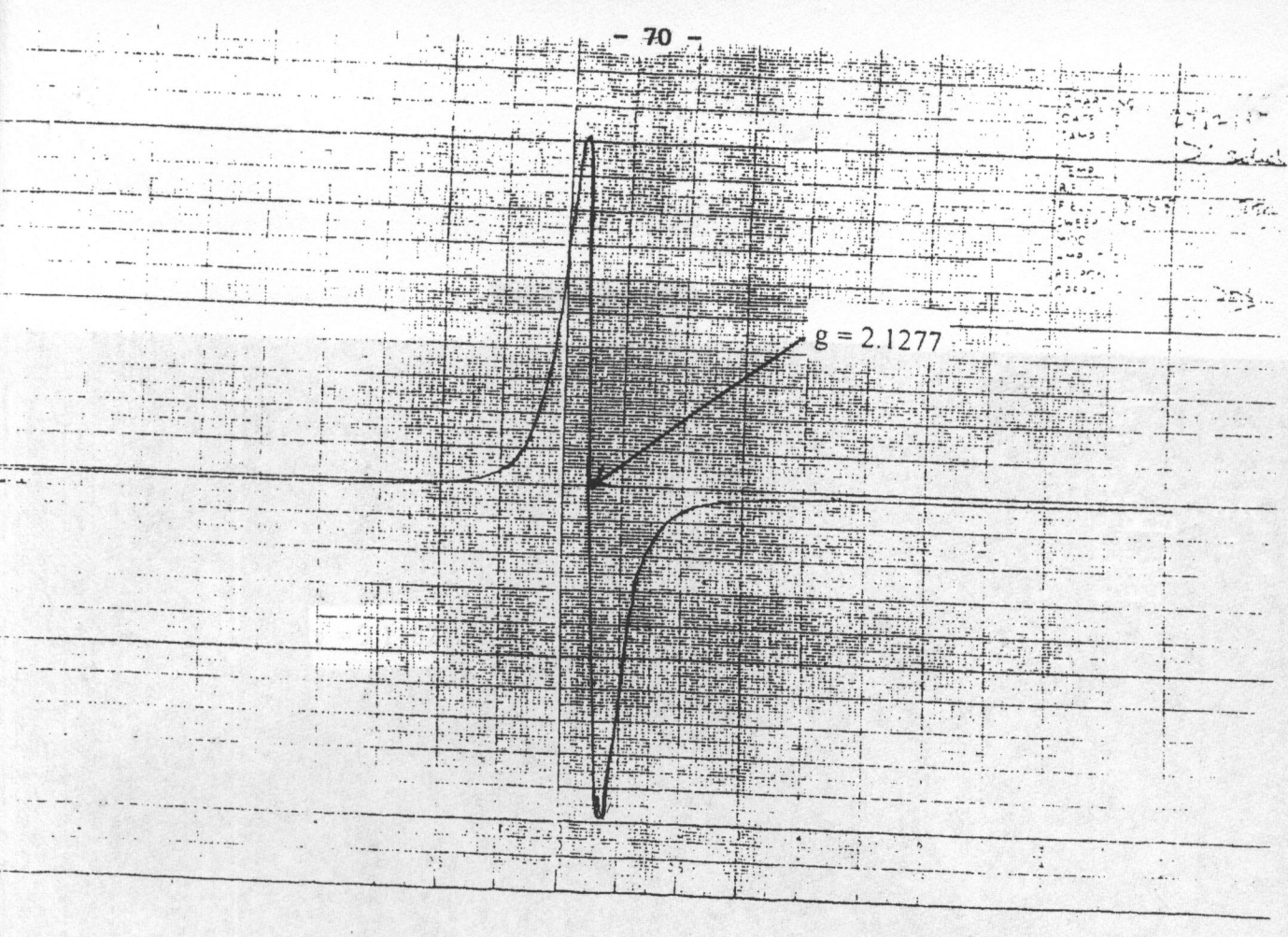

16.0. (a). The ESR spectrum of MnL_3 complex in solid state taken at an applied field of 3358 ± 250 G.

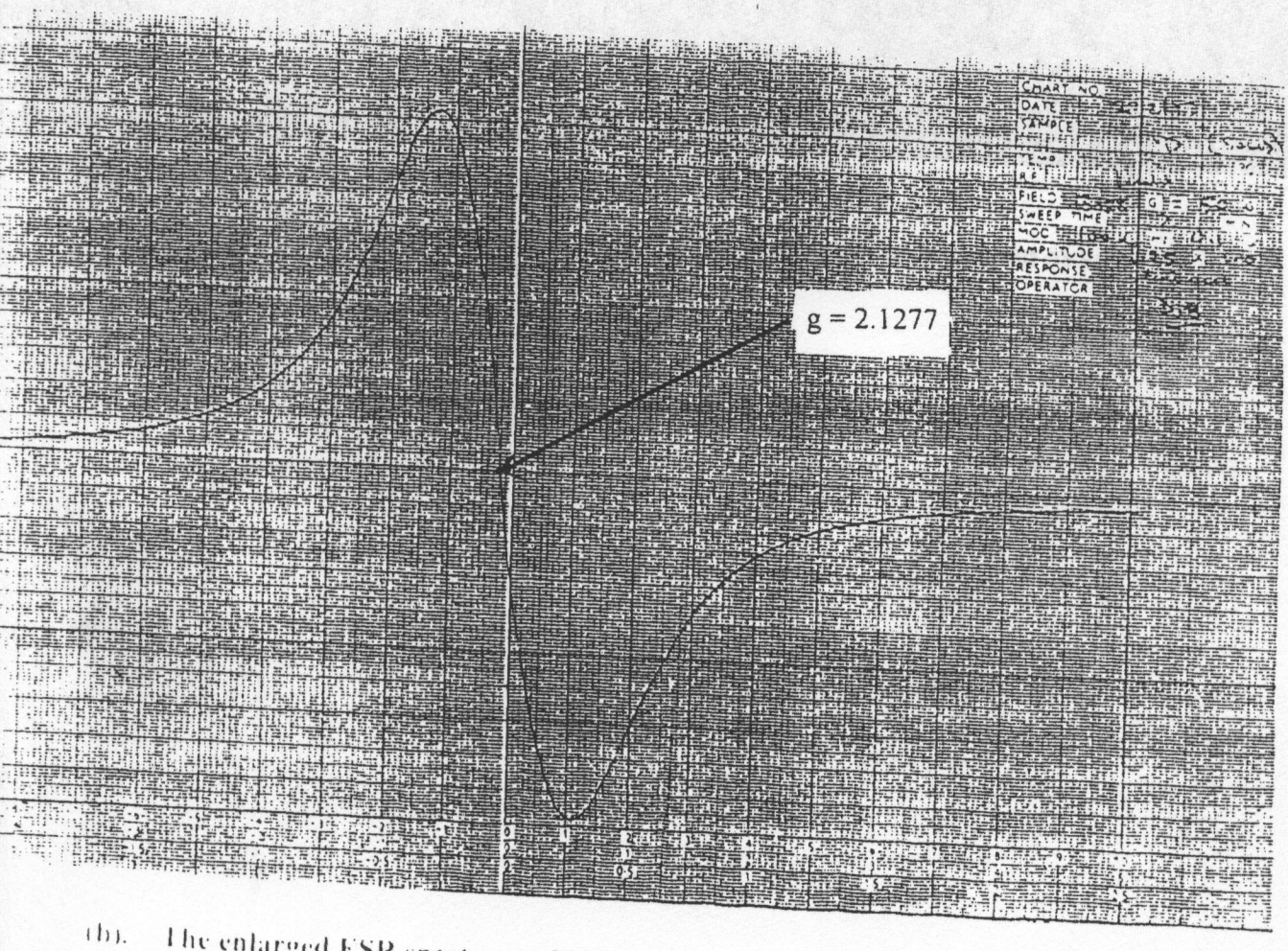

(b). The enlarged ESR spectrum of MnL_3 complex in solid state

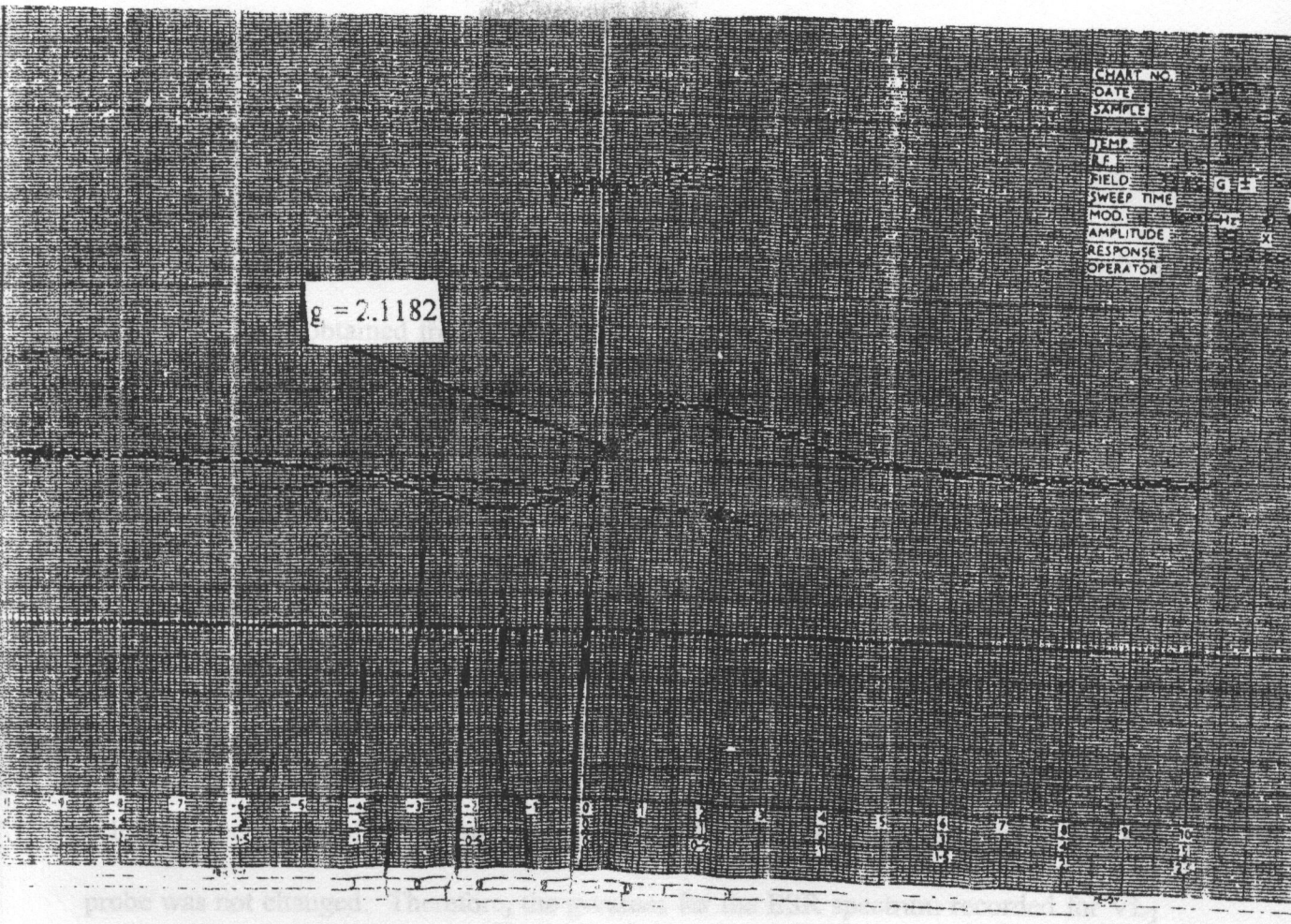

(c). The ESR spectrum of MnL_2 complex in chroloform solution taken at an applied field of 3373 ± 50 G.

It is observed that only one ESR signal was recorded in the spectrum of each complex . From the ESR spectrum of each complex the g-value was calculated using the equation 8 [35],

$$g = \frac{h\nu}{B_N H} \qquad \text{(equ.8)}$$

where ν is the fixed frequency of the probe and H (the applied field strength which is being swept) was obtained from the spectrum of each complex. B_N is the electron Bohr magneton which has the value 9.274096×10^{-21} erg. G^{-1} or 9.274096×10^{-24} JG^{-1} and h is plank's constant and has the value 6.6262×10^{-27} ergs or 6.6262×10^{-34} JS.

For the three complexes, the ESR spectra were taken with the applied field strength (H) at 3358 G for samples in solid state and the fixed frequency (ν) of the probe was at 1×10^{14} HZ. But, when the ESR spectra of the complexes were measured in chloroform solutions, the applied field strength used was 3373G and the fixed frequency (ν) of the probe was not changed. Therefore, the g-values for the ESR spectrum recorded for VL_3 complex, both in solid state and chloroform solution, were calculated using equation (8) as outlined below.

(i). Calculation of the g-value for VL_3 complex in solid state. For solid samples, H was fixed ata 3358G and ν was fixed at 1×10^{14}HZ.

$$\therefore g = \frac{h\nu}{B_N H}$$

$$= \frac{(6.6262 \times 10^{-34}\ JS) \times (1 \times 10^{14}\ HZ)}{(9.274096 \times 10^{-24}\ JG^{-1}) \times (3358G)}$$

$$= \underline{2.1277}$$

(ii). Calculation of the g-value for VL_3 complex in chloroform solution. In chloroform solutions, H was fixed at 3373G and ν was not changed.

$$\therefore g = \frac{h\nu}{B_N H}$$

$$= \frac{(6.6262 \times 10^{-34}\ JS) \times (1 \times 10^{14}\ HZ)}{(9.274096 \times 10^{-24}\ JG^{-1}) \times (3358G)}$$

$$= \underline{2.1182}$$

The same procedure was followed to calculate the g-values for CrL_3 and MnL_3 complexes. The g-values calculated from the ESR signals of the samples measured in solid state and chloroform solutions are given in table 9.0.

TABLE 9.0: ESR spectra data (g-values) for Vanadium, Chromium and Manganese complexes in solid state and chloroform solutions.

COMPLEX	ESR DATA (g-values)	
	SOLID STATE	CHLOROFORM SOLUTION
VL_3	2.1277	2.1182
CrL_3	2.1277	2.1182
MnL_3	2.1277	2.1182

In the ESR spectra of the three complexes in solid state, one symmetrical line with g = 2.1277 is observed.

Since each of the ML_3 complexes has 3 unpaired electrons (from magnetic moment results), it was expected that three ESR signals would be observed for each sample. However, only one signal was observed at the applied field of 3358G and a fixed frequency of 1.0×10^{14} HZ. This implies that three unpaired electrons in each complex are in the same environment and hence required the same transitional energy (hv), thus giving only one signal.

Since $h\nu = gB_NH$, and $g = \frac{h\nu}{B_NH}$, where h and B_N are constants. The using the same applied field (H) and frequency (ν) for each of the three complexes would as expected from the formular (Equ.8), give the same values of g (see table 9).

The g-values of the signals of the ML_3 complexes changed when measurements of chloroform solutions were taken (table 9.0). Besides, the shapes of the signals were broadened and this was in the increasing order of VL_3 [figure 14(c)) < CrL_3 (figure 15(c)) < MnL_3 (figure 16(c)].

In case of MnL_3, the signal in chloroform solution was almost flat. The reason for this is not clear. The change in ESR signals when a paramagnetic sample is in solution may be attributed mainly to electron spin exchange processes [14] which favour better signal resolutions in dilute solutions. In general, the ESR signals observed for the complexes are characteristic of the presence of the free radical entity ($\rangle N\!-\!\dot{O}$) [36].

3.3.2. ELECTROCHEMICAL STUDIES ON ML_3 COMPLEXES, (M = V^{3+}, Cr^{3+} AND Mn^{3+}).

The magnetic susceptibility and ESR spectra results for the complexes mentioned above, revealed that these complexes were paramagnetic. The complexes posses unpaired electrons on the free radical ($\rangle N-\dot{O}$) group attached to each ligand and the metal ion. Although the electrochemical properties of a large number of transition metal complexes have been done [37,38], none has been done so far on the ML_3 complexes. Such studies are quite appealing particularly due the presence of the free radical ligands on the ML_3 complexes.

Hence, voltammetric studies of the free radical ligand and the synthesized ML_3 complexes were carried out. Voltammetric (or electrochemical) studies are concerned with electrode reactions at the indicator or micro-electrode, i.e., with reactions involving a transfer of electrons between the electrode and the components of the solution. These components are called oxidants when they can accept electrons, and reductants when they can lose electrons [39].

Cyclic voltammetry (also called linear sweep voltammetry), consists of cycling the potential of a stationary electrode immersed in a quiescent solution and measuring the resultant current. The potential is scanned at a maximum (or minimum) electromotive force where the scan direction is reversed and the potential is returned at the same scan rate to the initial potential. The initial direction of potential scan can be either negative or

often used is the hanging mercury drop electrode (HMDE). During the forward portion of the scan, the electroactive species react at the electrode surface. The reaction product is a reduced species if the initial potential scan is towards more negative potentials or an oxidized species if the initial scan is towards more positive potentials:

$$OX + ne \rightarrow Red. \qquad \text{(Equ. 10)}$$

where OX = oxidized species,

Red = Reduced species and

n = number of electrons transferred during the electrode reaction.

If the reaction product is also electroactive, i.e, if the initial electrochemical reaction is reversible, the product can react during the reverse scan to yield the original electroactive species:

$$Red \rightarrow OX + n\,e \qquad \text{(Equ. 11)}$$

Equation (11) is the reverse of equation (10) [40].

As a consequence, a current flows through the cell in the opposite direction to that of the current flow which yielded the original peak. For a reversible reaction, the peak observed during the reverse scan is the same size as the peak observed during the forward scan, and this permits the display of a complete voltammogram with cathodic (reduction) and anodic (oxidation) wave forms one above the other, as shown in figure 17.

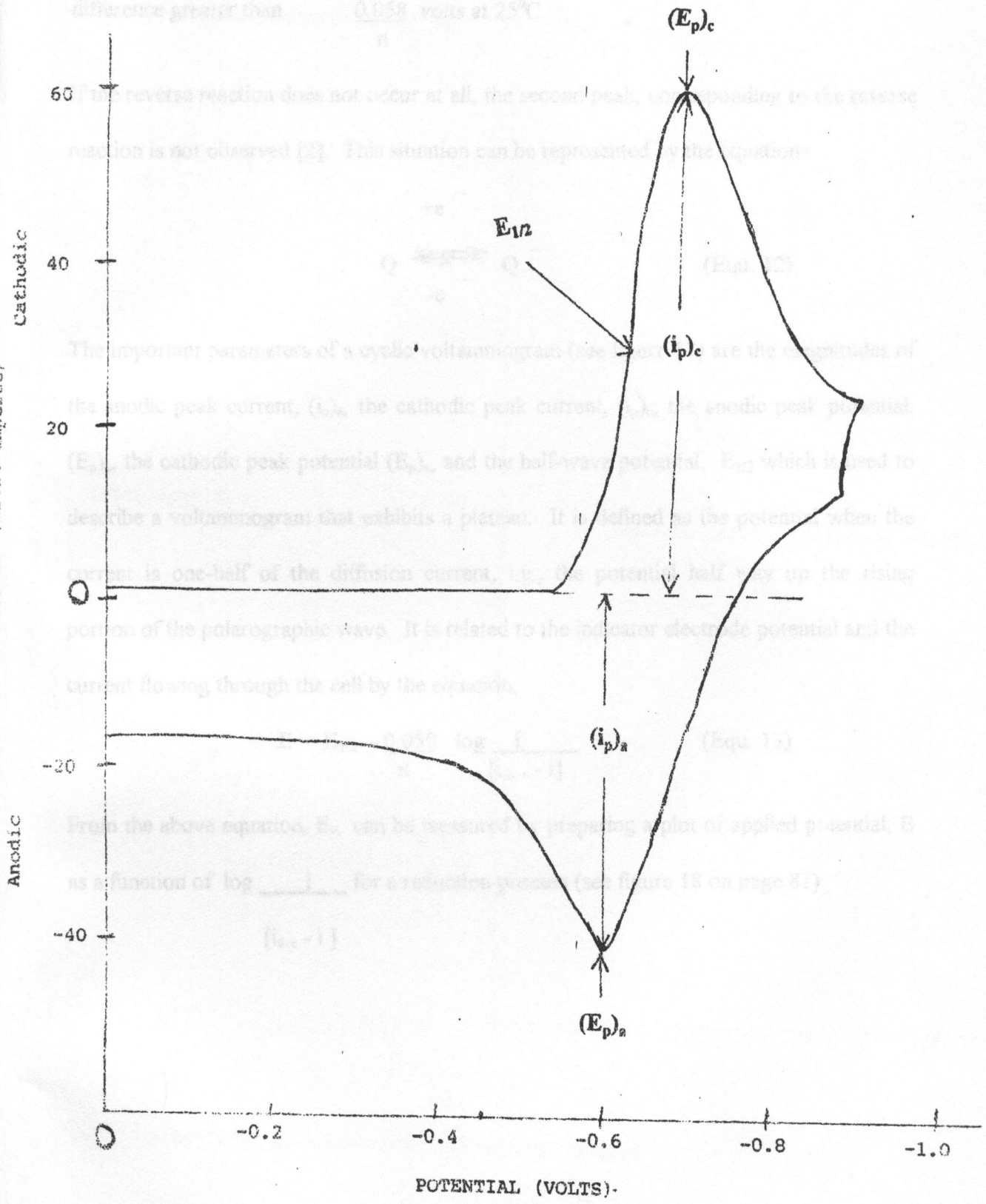

17.0. **Cyclic voltammogram showing important parameters.**

If the electrochemical reaction is not reversible, the two peaks are separated by a potential difference greater than $\frac{0.058}{n}$ volts at 25°C.

If the reverse reaction does not occur at all, the second peak, corresponding to the reverse reaction is not observed [2]. This situation can be represented by the equation:

$$Q \underset{-e^-}{\overset{+e^-}{\rightleftharpoons}} Q^- \qquad \text{(Equ. 12)}$$

The important parameters of a cyclic voltammogram (see figure 17) are the magnitudes of the anodic peak current, $(i_p)_a$, the cathodic peak current, $(i_p)_c$, the anodic peak potential, $(E_p)_a$, the cathodic peak potential $(E_p)_c$, and the half-wave potential, $E_{1/2}$ which is used to describe a voltammogram that exhibits a plateau. It is defined as the potential when the current is one-half of the diffusion current, i.e., the potential half way up the rising portion of the polarographic wave. It is related to the indicator electrode potential and the current flowing through the cell by the equation,

$$E = E_{1/2} - \frac{0.059}{n} \log \frac{i}{[i_{d,c} - i]} \qquad \text{(Equ. 13)}$$

From the above equation, $E_{\frac{1}{2}}$ can be measured by preparing a plot of applied potential, E as a function of $\log \frac{i}{[i_{d,c} - i]}$ for a reduction process (see figure 18 on page 81).

GRAPH OF APPLIED POTENTIAL (E) Vs $\text{Log}\frac{i}{[i_{d,c} - i]}$

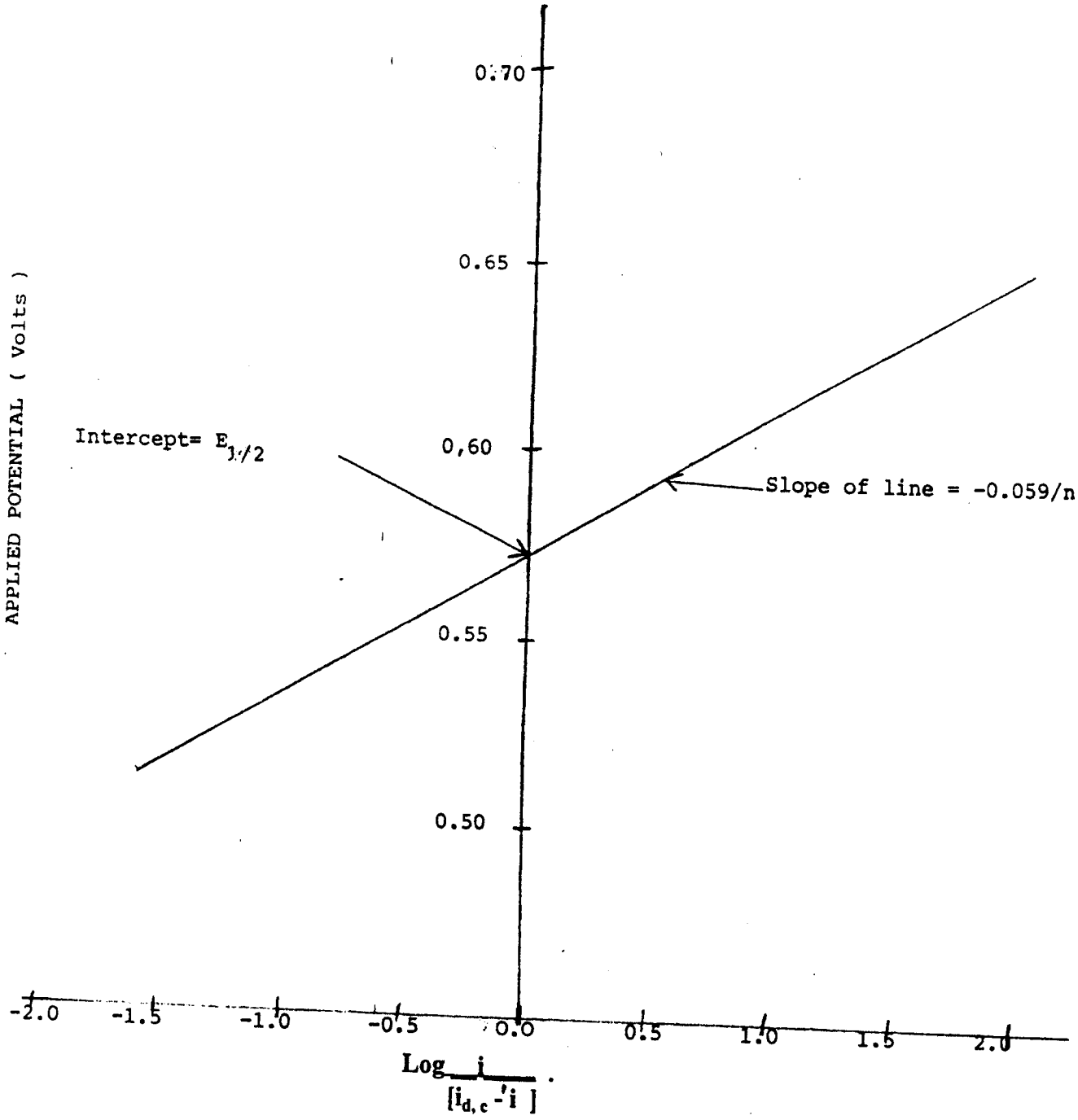

18.0. **Influence of applied potential on measured current.**

The linear plot intercepts the potential axis at the half-wave potential, and the straight line obtained from the above plot yields a slope of $\frac{0.059}{n}$

from which (number of electrons transferred during the electrode reaction) can be determined. The number of electrons transferred in the electrode reaction for a reversible couple can also be determined from the separation between the peak potentials:

$$(E_p)_a - (E_p)_c = \frac{0.057}{n}, \text{(volts)} \qquad \text{(Equ. 14)}$$

which is valid when the switching potential is at least 100/n(mV) past the cathodic peak potential [41].

The electrode behaviour of solutions of the free radical ligand (LH), VL_3, CrL_3 and MnL_3 complexes were investigated by cyclic voltammetry as described below. A PAR 174A potentiostat was used for cyclic, linear sweep voltammetry and controlled potential electrolysis. The working electrode was a hanging mercury electrode. A platinum wire was the counter electrode and the reference electrode was a Ag/AgCl connected to the cell solution via a salt bridge containing the electrolyte solution. A fresh drop was introduced following extrusion of the aged mercury drop. A fresh mercury drop or freshly cleaned electrodes were placed in a cell containing acetonitrile-water (1:1), 0.1M tetramethyl ethyl ammonium bromide (TEAB) and the free radical ligand or metal complex for each experiment. The linear sweep voltammetry was done at scan rates in the range of 5mV/sec - 500mV/sec. The concentration used for each analyte were; $[VL_3] = 2.50 \times 10^{-3}$M, $[CrL_3] = 2.67 \times 10^{-3}$M, $[MnL_3] = 1.43 \times 10^{-3}$M, and $[LH] = 4.0 \times 10^{-3}$M.

Attempts to carry out oxidation processes on the free radical ligand and the ML_3 complexes did not yield meaningful results. However, the reduction process on solutions of the compounds gave reversible voltammograms and hence, attention was directed to this process. The voltammograms at the mercury electrode for the reduction process for the three complexes recorded are shown in figures 19, 20, 21 and 22.

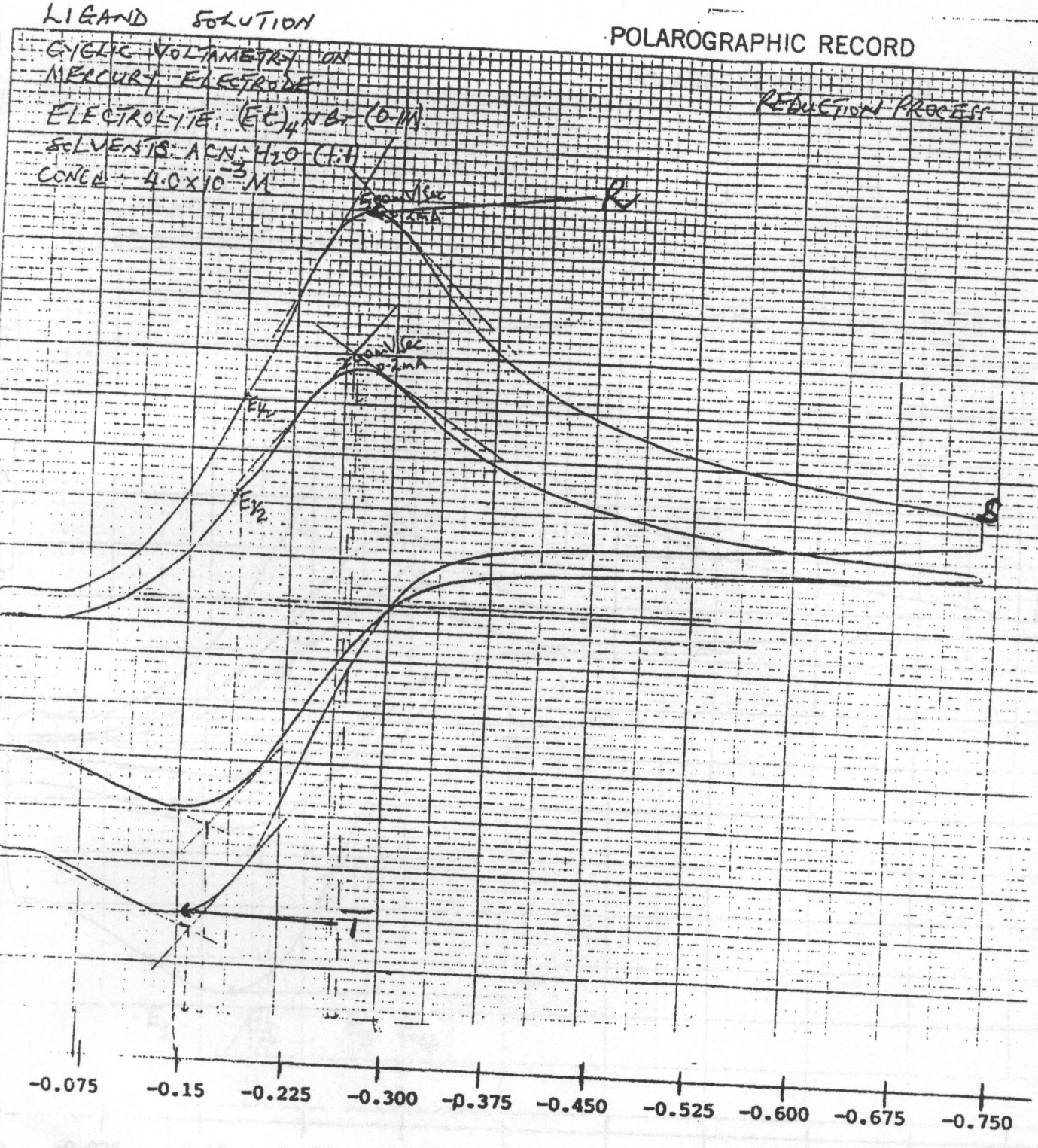

19.0: Cathodic scan cyclic voltammograms of the Ligand (LH) (Ca 4.0×10^{-3}M) in acetonitrile - water (1: 1)solution containing 0.1M TEAB at a mercury disk electrode(23± 2°C) and scan rate of 0.5 vs^{-1}.

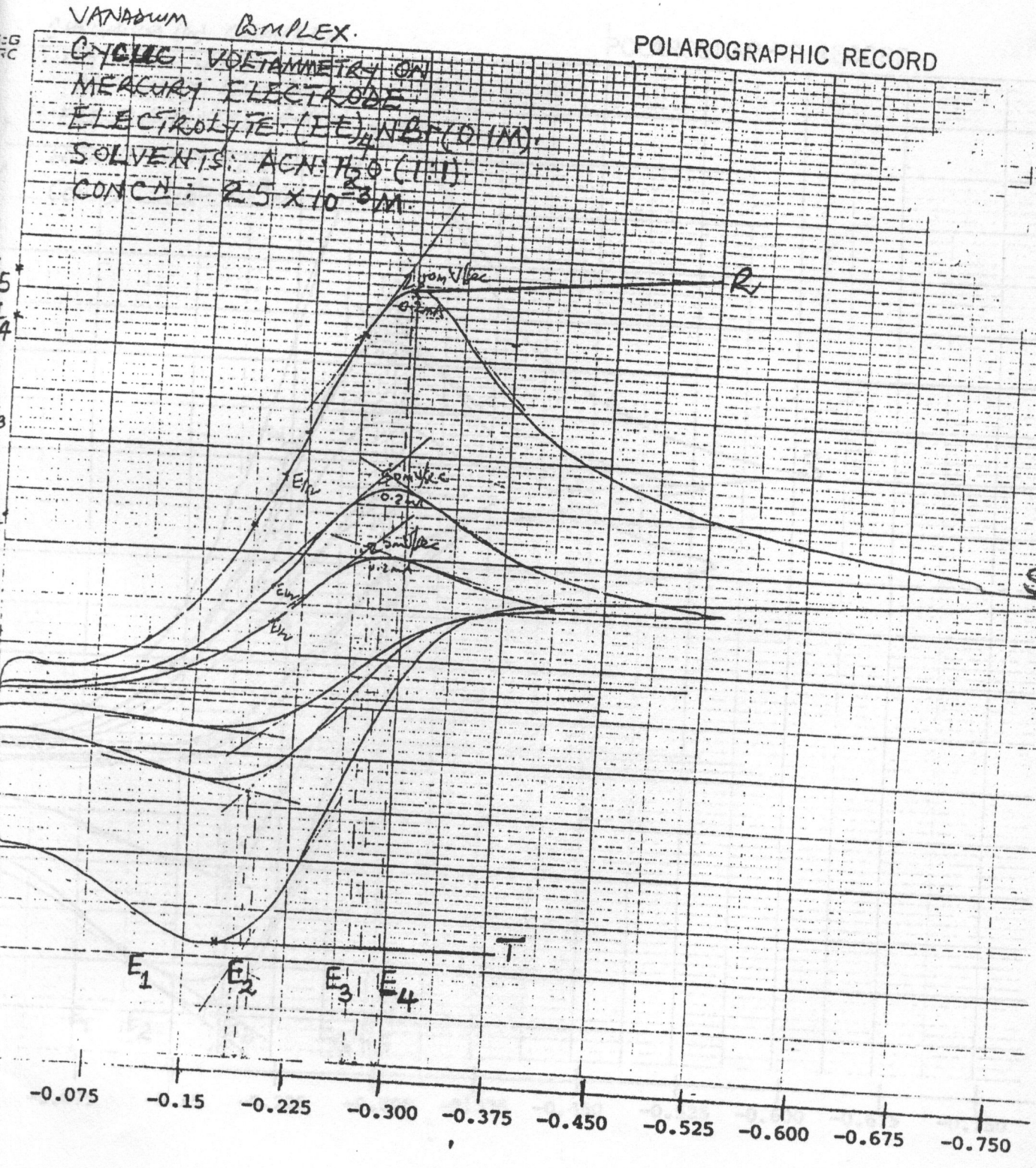

20.0: Cathodic scan cyclic voltammograms of 2.5×10^{-3} M of VL_3 complex in acetonitrile -water (1:1) solution containing 0.1M TEAB at a mercury disk electrode (at 23±2°C) and scan rate of $0.5 vs^{-1}$.

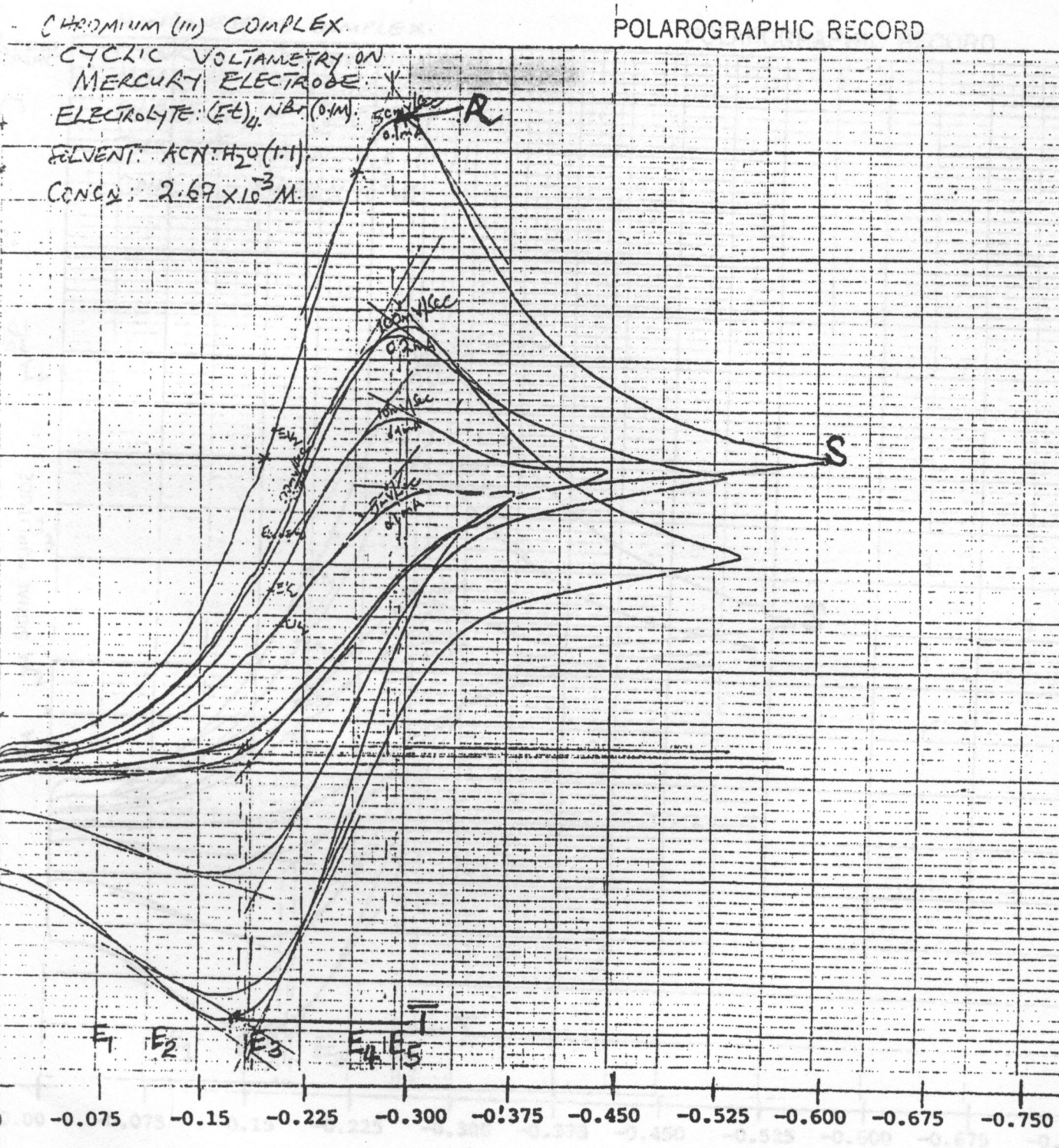

21.0 **Cathodic scan cyclic voltammograms of 2.67 x 10^{-3}M CrL_3 complex in acetonitrile -water (1:1)solution containing 0.1M TEAB at a mercury disk electrode (at 23±2°C) and scan rate of 0.5 vs^{-1}.**

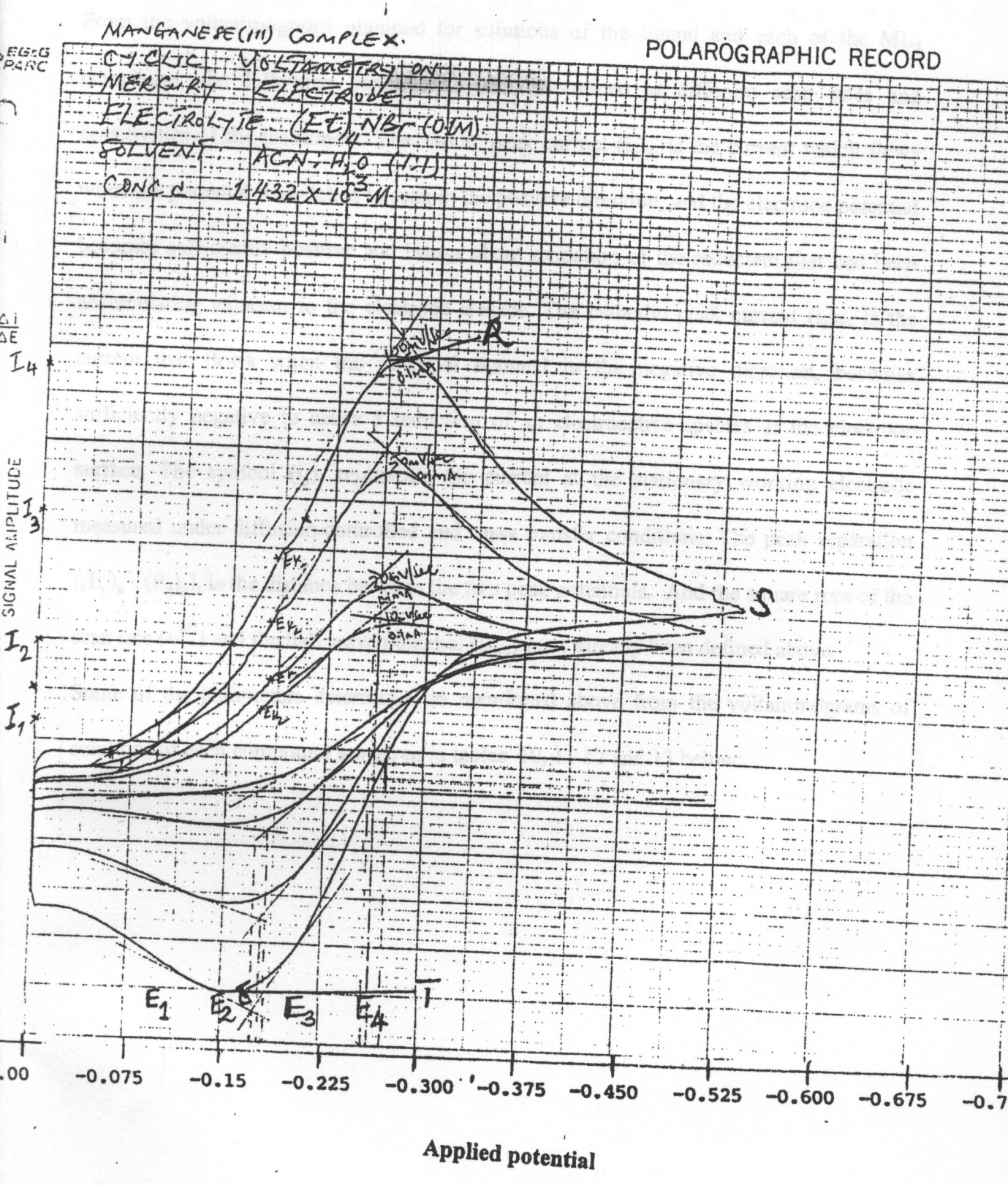

22.0 Cathodic scan cyclic voltammograms of 1.43×10^{-3}M MnL_3 complex in acetonitrile - water (1:1) solution containing 0.1M TEAB at a mercury disk electrode (at 23±2°C) and scan rate of $0.5vs^{-1}$.

From the voltammograms obtained for solutions of the ligand and each of the ML_3 complexes, the following parameters were determined at different scan rates and sensitivities of the instrument. The anodic peak current $(i_p)_a$, is the current which flows when the potential is switched to scan in the positive direction, and the electrode potential becomes sufficiently positive and brings about oxidation of the reductant that had been accumulating adjacent to the electrode surface. The cathodic peak current $(i_p)c$, is the current that flows when the potential scanned in the negative direction, becomes sufficiently negative to cause a reduction of an electroactive species at the electrode surface. The symbol (i_p), represents the current at the stationary working electrode measured under diffusion-controlled and mass transfer conditions. The peak separation $[(E_p)_a - (E_p)_c]$, is the distance between the two peak potentials. And the square root of the scan rate $(\nu^{1/2})$ and the half wave potential $(E_{1/2})$ have already been defined above.

Some of the parameters determined as mentioned above from the voltammograms of solutions of each compound are given in tables 10, 11 12 and 13 below:

TABLE 10.0: The diffusion current (i_p), peak separation ($|E_{pa} - E_{pc}|$), square root of scan rate ($\nu^{1/2}$), half-wave potential ($E_{1/2}$) and $\log \frac{i}{[i_{d,c} - i]}$ determined from the voltammogram of the ligand.

Scan Rate (mV/Sec)	Sensitivity (mA)	i_p μA	E_{pa}-E_{pc} (V)	√scan rate	$E_{1/2}$ (V)	i (μA)	E (volts)	$\log \frac{i}{[i_{d,c} - i]}$
10.0	0.10	16	0.090	3.162	0.188			
						6.0	0.1275	-0.6917
20.0	0.10	18.4	0.083	4.472	0.179			
						11.0	0.1575	-0.3478
50.0	0.10	27.2	0.079	7.071	0.181			
						21.0	0.2025	0.1609
100.0	0.10	35.5	0.101	10.000	0.184			
						28.0	0.225	0.5721
200.0	0.20	51.0	0.095	14.142	0.176			
						35.0	0.2625	1.8451
500.0	0.20	79.0	0.113	22.360	0.192			

TABLE 11.0: The diffusion current (i_p), peak separation ($| E_{pa} - E_{pc} |$), square root of scan rate ($\nu^{1/2}$, half-wave potential ($E_{1/2}$) and $\log \frac{i}{[i_{d,c} - i]}$ determined from the voltammogram of the VL_3 complex.

Scan Rate (mV/Sec)	Sensitivity (mA)	i_p μA	E_{pa}-E_{pc} (V)	√scan rate	$E_{1/2}$ (V)	i (μA)	E (volts)	$\log \frac{i}{[i_{d,c} - i]}$
5.0	0.10	17.5	0.089	2.236	0.203			
						6.0	1.125	-1.0670
10.0	0.10	20.0	0.088	3.162	0.203			
						29.0	1.875	-0.2188
20.0	0.20	28.0	0.082	4.472	0.203			
						48.0	2.625	0.2189
50.0	0.20	40.0	0.089	7.071	0.203			
						68.0	2.925	0.8783
100.0	0.20	53.0	0.097	10.00	0.199			
200.0	0.20	78.0	0.110	14.142	0.210			
500.0	0.50	110.0	0.131	22.360	0.199			

TABLE 12.0: The diffusion current (i_p), peak separation ($|E_{pa} - E_{pc}|$), square root of scan rate ($\nu^{1/2}$), half-wave potential ($E_{1/2}$) and $\log \frac{i}{[i_{d,c} - i]}$ determined from the voltammogram of the CrL_3 complex.

Scan Rate (mV/Sec)	Sensitivity (mA)	i_p μA	E_{pa}-E_{pc} (V)	√scan rate	$E_{1/2}$ (V)	i (μA)	E (volts)	$\log \frac{i}{[i_{d,c} - i]}$
5.0	0.10	26.0	0.1020	2.236	0.207			
						2.5	0.075	-1.3665
10.0	0.10	33.0	0.975	3.162	0.201			
						7.5	1.200	-0.8477
20.0	0.10	40.0	0.0968	4.472	0.203			
						27.5	1.950	-0.0794
50.0	0.10	60.5	0.0968	7.071	0.203			
						56.5	2.625	1.1500
100.0	0.20	82.4	0.1175	10.00	0.209			
						59.5	2.925	1.7745
200.0	0.20	97.0	0.1313	14.142	0.214			
500.0	0.50	170.0	0.1425	22.360	0.218			

TABLE 13.0: The diffusion current (i_p), peak separation ($|E_{pa} - E_{pc}|$), square root of scan rate ($\nu^{1/2}$), half-wave potential ($E_{1/2}$) and log $\frac{i}{[i_{d,c} - i]}$ determined from the voltammogram of the MnL_3 complex.

Scan Rate (mV/Sec)	Sensitivity (mA)	i_p μA	E_{pa}-E_{pc} (V)	√scan rate	$E_{1/2}$ (V)	i (μA)	E (volts)	log $\frac{i}{[i_{d,c} - i]}$
10.0	0.10	18.0	0.0863	3.162	0.1763			
						3.0	0.0975	-1.097
20.0	0.10	20.0	0.0788	4.472	0.1838			
						11.0	1.500	-0.428
50.0	0.10	31.0	0.0825	7.071	0.8100			
						24.0	2.025	0.163
100.0	0.10	40.5	0.1013	10.00	0.1838			
						39.0	2.550	1.415
200.0	0.10	56.8	0.1155	14.142	0.1875			
500.0	0.20	86.0	0.1155	22.360	0.1883			

Note that there is no data for the last two rows of the last three columns in table 10, 12 and 13. The reason being that the (id,c) for the ligand (LH), VL_3, CrL_3 and MnL_3 complexes determined from the voltammograms were 35.5 μA, 68.5μA, 60.5μA and 40.5μA respectively. Hence, values of i(μA) above the id,c calculated from each voltammogram gave negative numbers from the formula $\frac{i}{[id,c-i]}$ making it impossible to calcualte the values for log $\frac{i}{[id,c-i]}$ and use them to complete the tables. However, the first four data points determined for i and log $\frac{i}{[id,c-i]}$ w ere adequate for drawing the. required graphs.

In the voltammograms shown in figure 19, 20 21 and 22 for solutions of the ligand and the ML_3 complexes, the initial potential applied was 0.0V. This was chosen to avoid any electrolysis of electroactive species in the samples when the experiments were started. Then the potential was scanned in the negative direction and when the potential became sufficiently negative to cause a reduction of the electroactive species in each compound at the electrode surface, cathodic current began to flow. The cathodic current increased

rapidly until the surface concetration of oxidant at the electrode surface approached zero, as shown by the current wave, now diffusion controlled, with a maximum peak at **R** (figure 19,20 21 and 22). The current then decays with $t^{-1/2}$ according to the Cottrell equation,

$$i_p = n^{3/2} F^{3/2} (Jc\nu D_{ox}/RT)^{1/2} Ac_{ox} \chi(\sigma t) \qquad \text{(equ.15)},$$

where $\chi(\sigma t)$ has a value of 0.446 for a simple, diffusion - controlled electron transfer reaction, R is in JK^{-1} mol^{-1} and **T** is in Kelvin, **A** in cm^2, **D** in cm^2/sec, **C** in mol/cm^3, and ν in V/sec, as the solution surrounding the electrode is depleted of the oxidant due to its electrochemical conversion to the reduced state. The slight final rise at point **S** (fig.19, 20, 21 and 22) is caused by the discharge of the supporting electrolyte. At this point, the switching potential was switched to scan in the positive direction. However, the potential was sufficiently negative to continue the reduction of the oxidant and so a cathodic current continued for a brief period. Finally the electrode potential became sufficiently positive to bring about oxidation of the reductant that had accumulated adjacent to the

electrode surface. At this point , an anodic current began to flow and to counteract the cathodic current. The anodic current increased rapidly until the surface concentration of the accumulated reductant approached zero, at which point the anodic current shows a peak at point **T** (figure 19 ,20, 21 and 22). The anodic current then decays as the solution surrounding the electrode is depleted of the reductant formed during the forward scan, giving a shape of the voltammogram as shown in each of the four figures. The shapes of the cyclic voltammograms for each compound show that the reduction process was reversible and therefore, the processes that were taking place to give such wave forms as observed can be represented by an equation for a reversible process given below.

$$ML_3 \underset{-e^-}{\overset{+e^-}{\rightleftharpoons}} ML_3^-$$

The reversibility of the reduction process for solutions of the compounds mentioned above was confirmed by considering the situations described below. The average E_p for each voltammogram for each solution of the compounds dealt with was found to be about 94.8mV and was independent of the scan rate (table 10, 11, 12 and 13). Since for a reversible wave, E_p is independent of the scan rate [39], therefore, this is in agreement with the findings on the reduction process of the solutions of the compounds mentioned in this section. To further ascertain the reversibility for the reaction of the solutions of the compounds, the (i_p) values were plotted against the values of the square root of scan rate for each compound. The graphs obtained for each compound are shown in figures 23, 24,25 and 26.

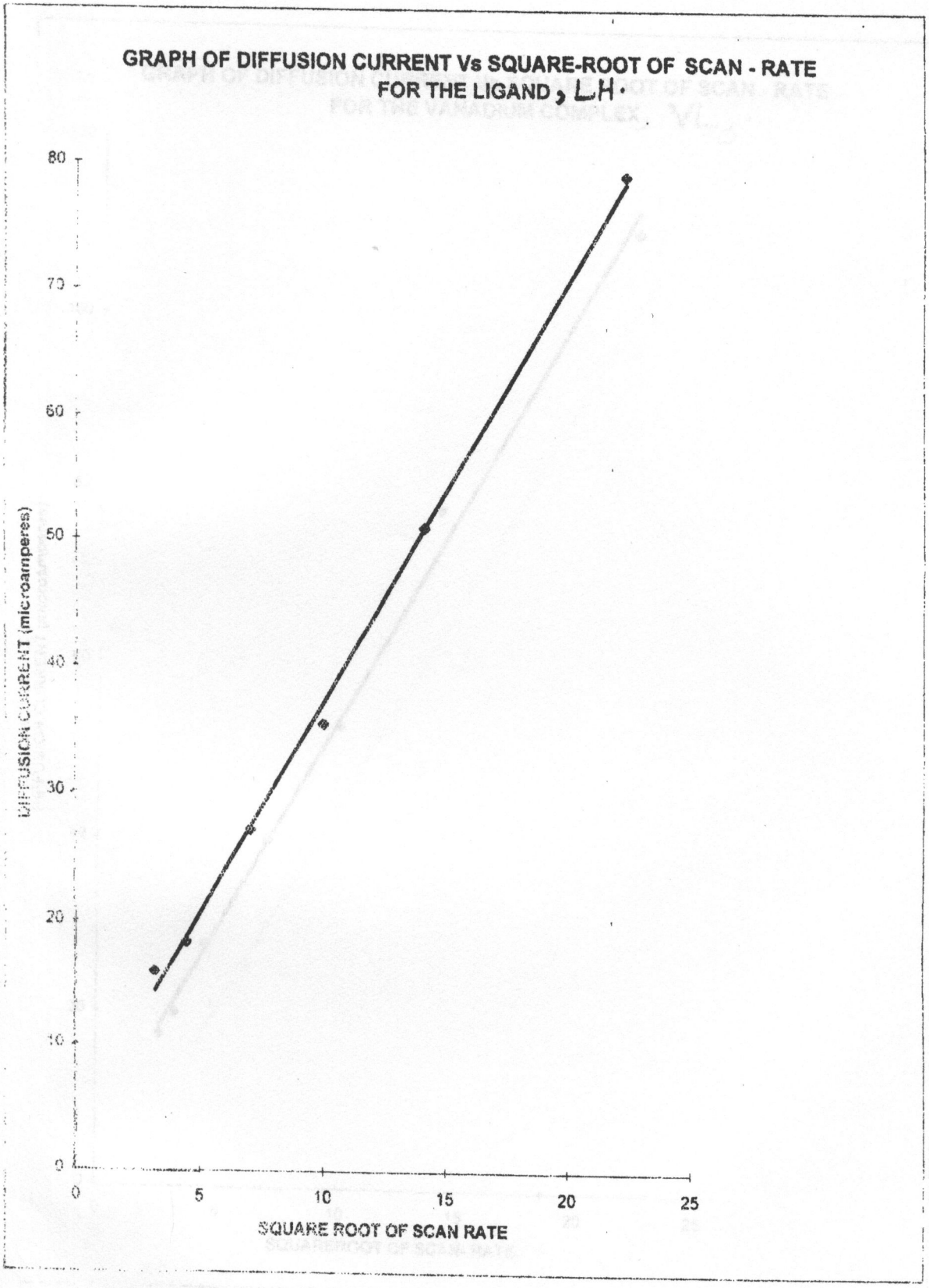

23.0. **Dependence of cathodic peak currents $(i_p)c$ on the scan rate in solutions of acetonitrile-water (1:1) containing LH and 0.1M TEAB.**

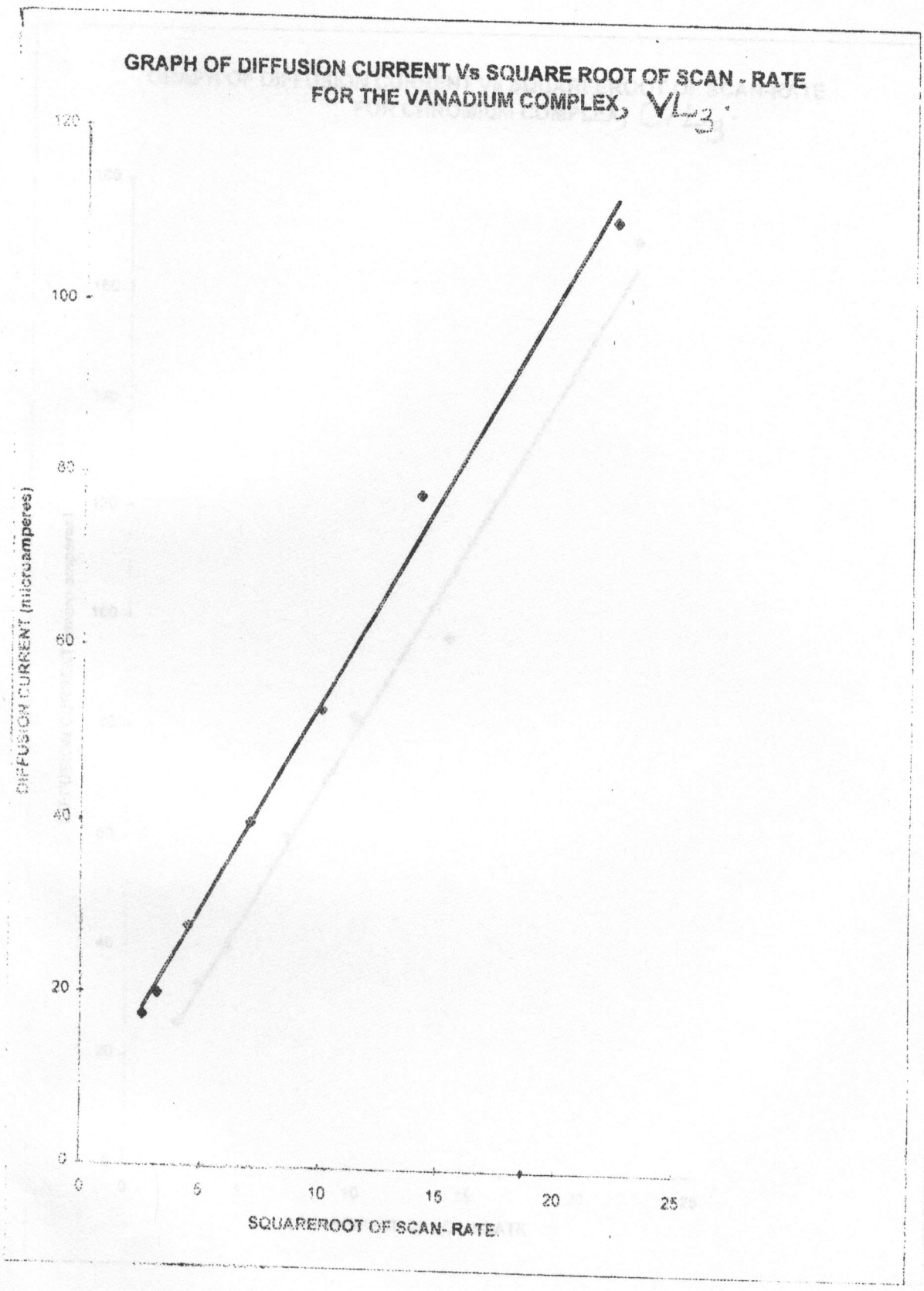

24.0. **Dependence of cathodic peak currents (i_p) c on the scan rate in solutions of acetonitrile - water (1:1) containing VL_3 complex and 0.1M TEAB.**

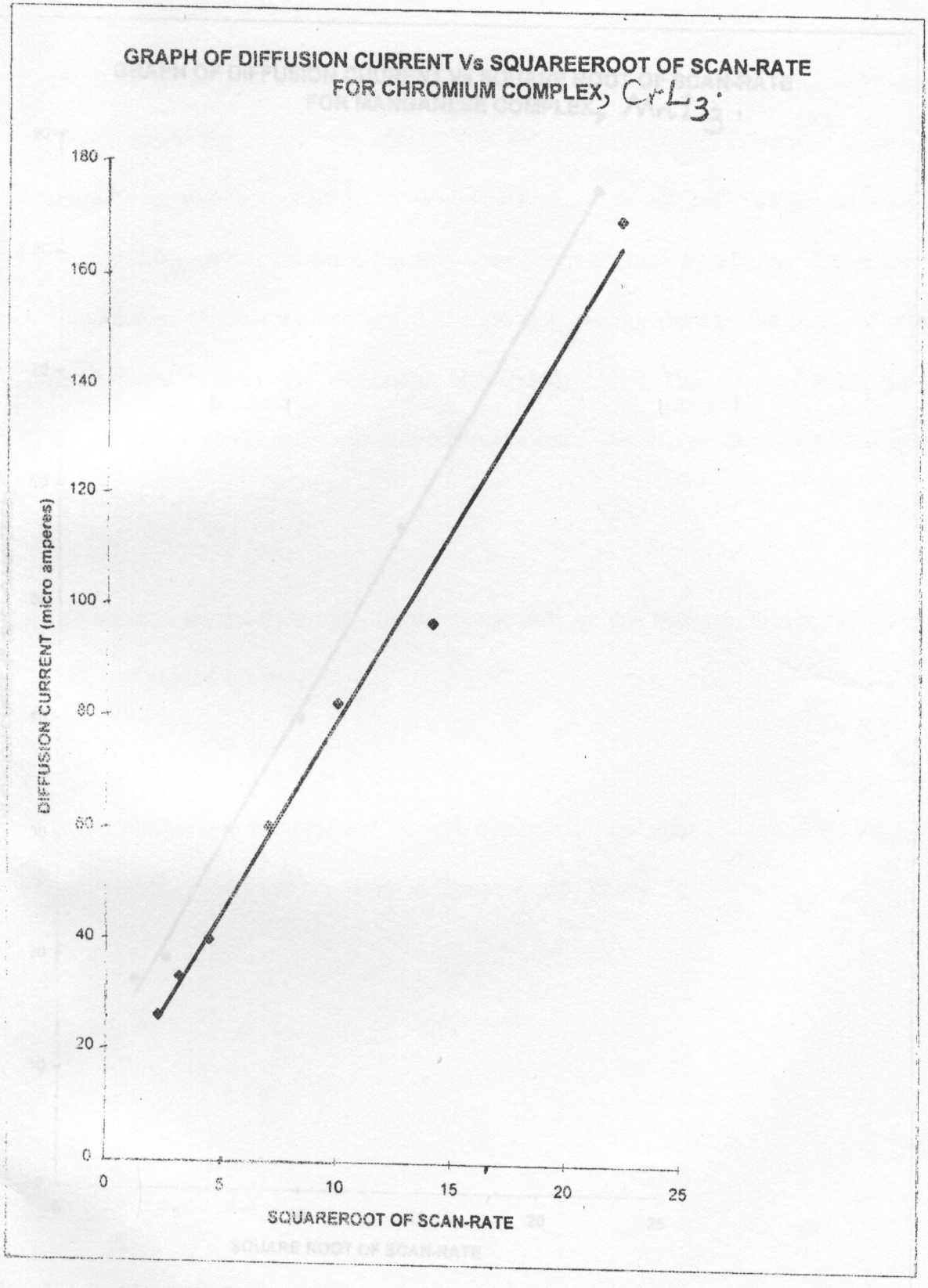

25.0. **Dependence of cathodic peak current (i_p) c on the scan rate in solutions of acetonitrile - water (1:1) containing CrL_3 complex and 0.1M TEAB.**

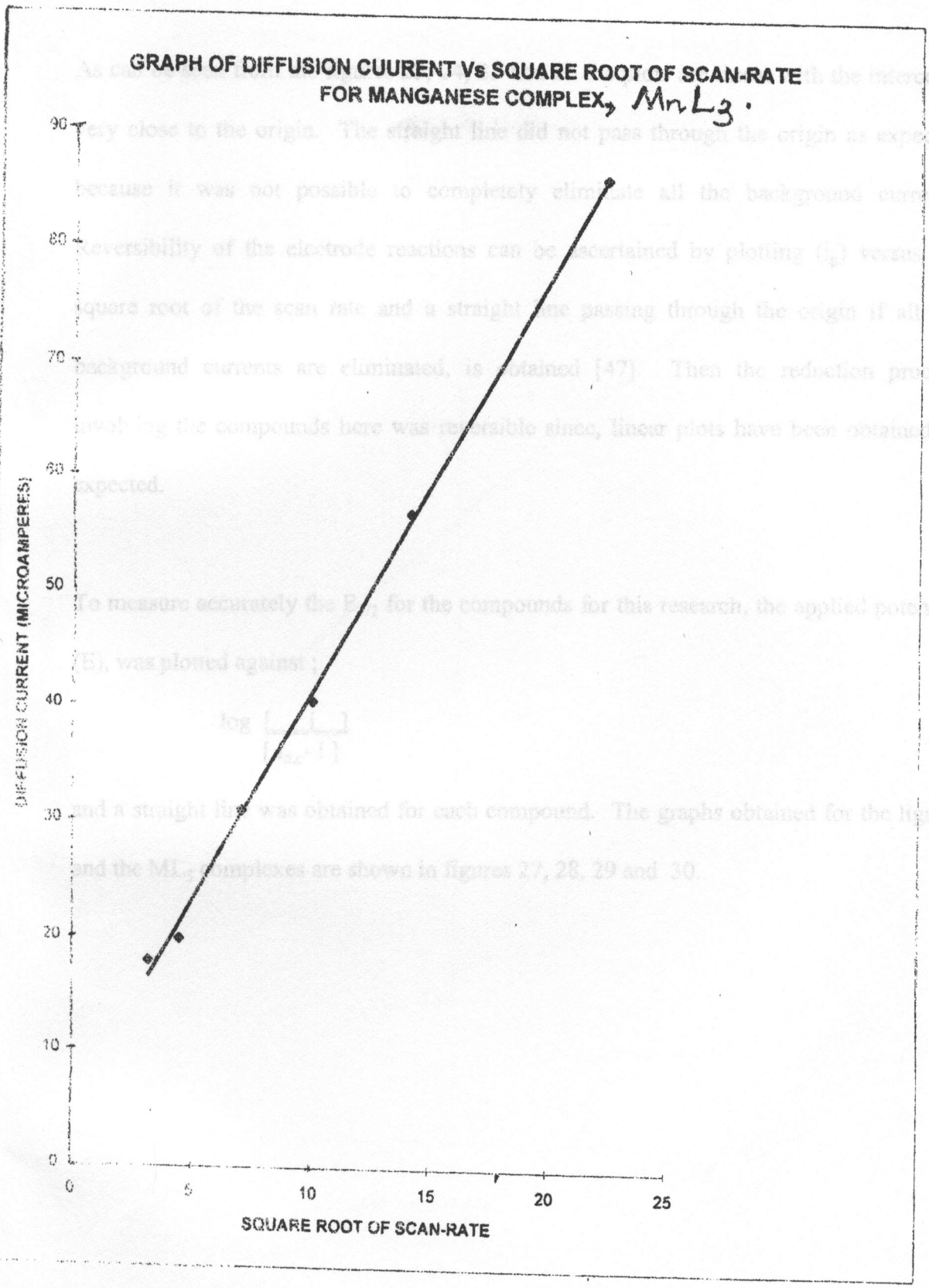

26.0. **Dependence of cathodic peak current $(i_p)_c$ on the scan rate in solutions of acetonitrile-water (1:1) containing MnL_3 complex and 0.1M TEAB.**

As can be seen from the figures 23, 24, 25 and 26 the plots are linear with the intercepts very close to the origin. The straight line did not pass through the origin as expected because it was not possible to completely eliminate all the background currents. Reversibility of the electrode reactions can be ascertained by plotting (i_p) versus the square root of the scan rate and a straight line passing through the origin if all the background currents are eliminated, is obtained [47]. Then the reduction process involving the compounds here was reversible since, linear plots have been obtained as expected.

To measure accurately the $E_{1/2}$ for the compounds for this research, the applied potential (E), was plotted against ;

$$\log \left[\frac{i}{i_{d,c} - i} \right]$$

and a straight line was obtained for each compound. The graphs obtained for the ligand and the ML_3 complexes are shown in figures 27, 28, 29 and 30.

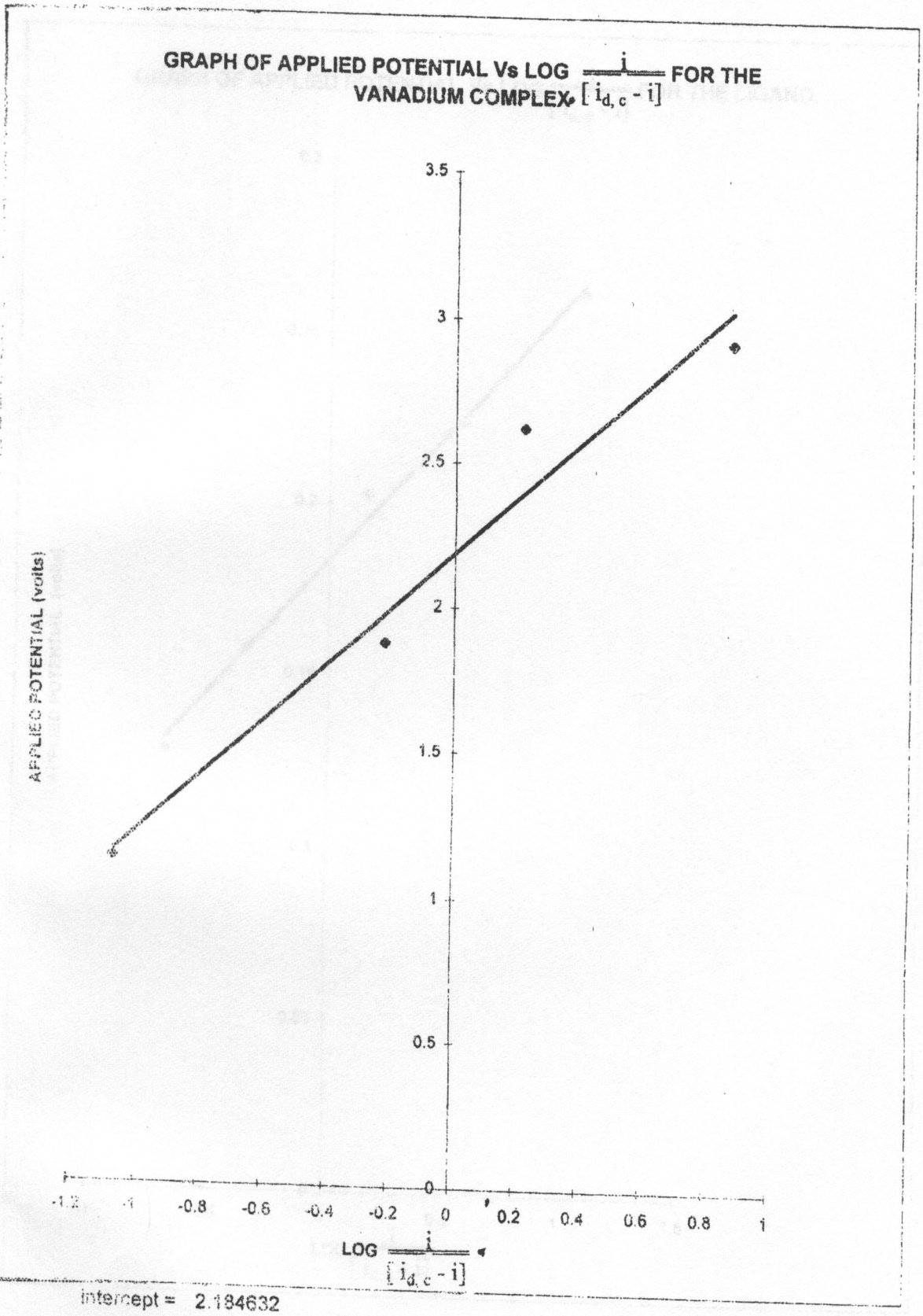

28.0. **Influence of applied potential on measured current in solutions of acetonitrile containing VL_3 complex and 0.1M TEAB.**

GRAPH OF APPLIED POTENTIAL Vs LOG $\frac{i}{[i_{d,c} - i]}$ FOR THE LIGAND.

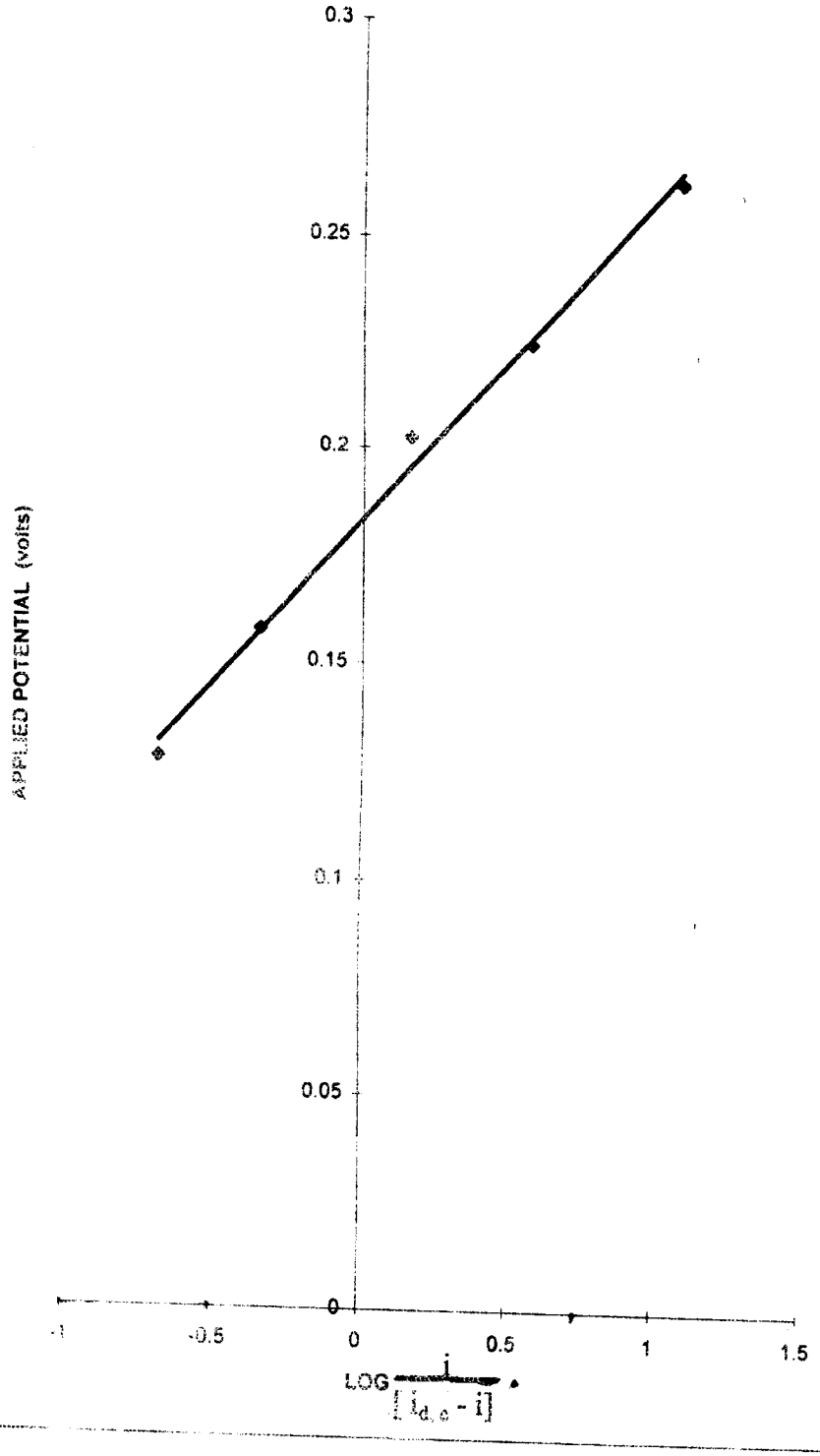

intercept = 0.183273

27.0. **Influence of applied potential on measured current in solutions of acetonitrile containing LH and 0.1M TEAB.**

GRAPH OF THE APPLIED POTENTIAL Vs $\text{Log}\frac{i}{(i_{d,c} - i)}$ FOR THE CHROMIUM COMPLEX.

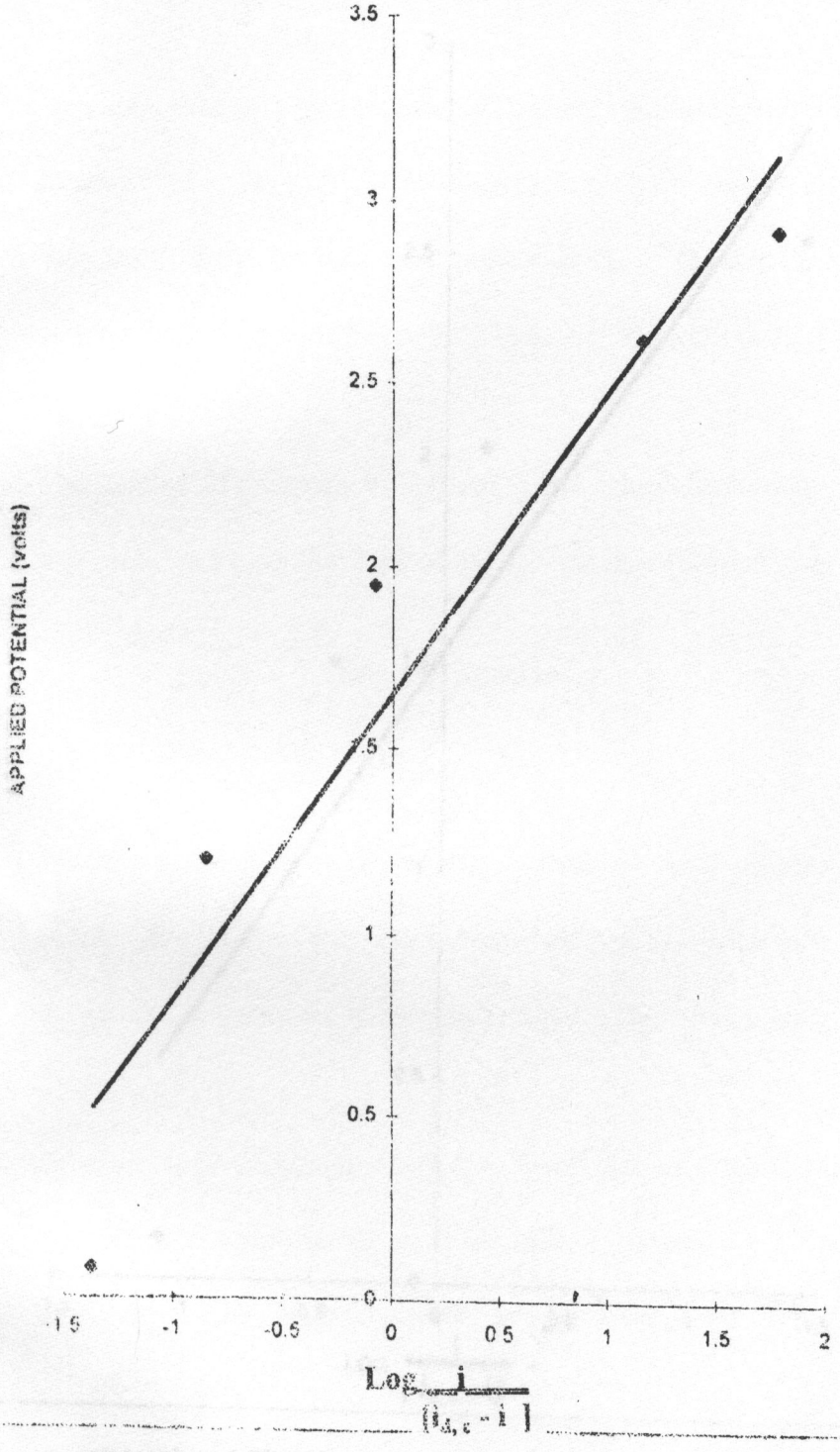

intercept 1.649716

29.0. **Influence of applied potential on measured current in solutions of acetonitrile containing CrL_3 complex and 0.1M TEAB.**

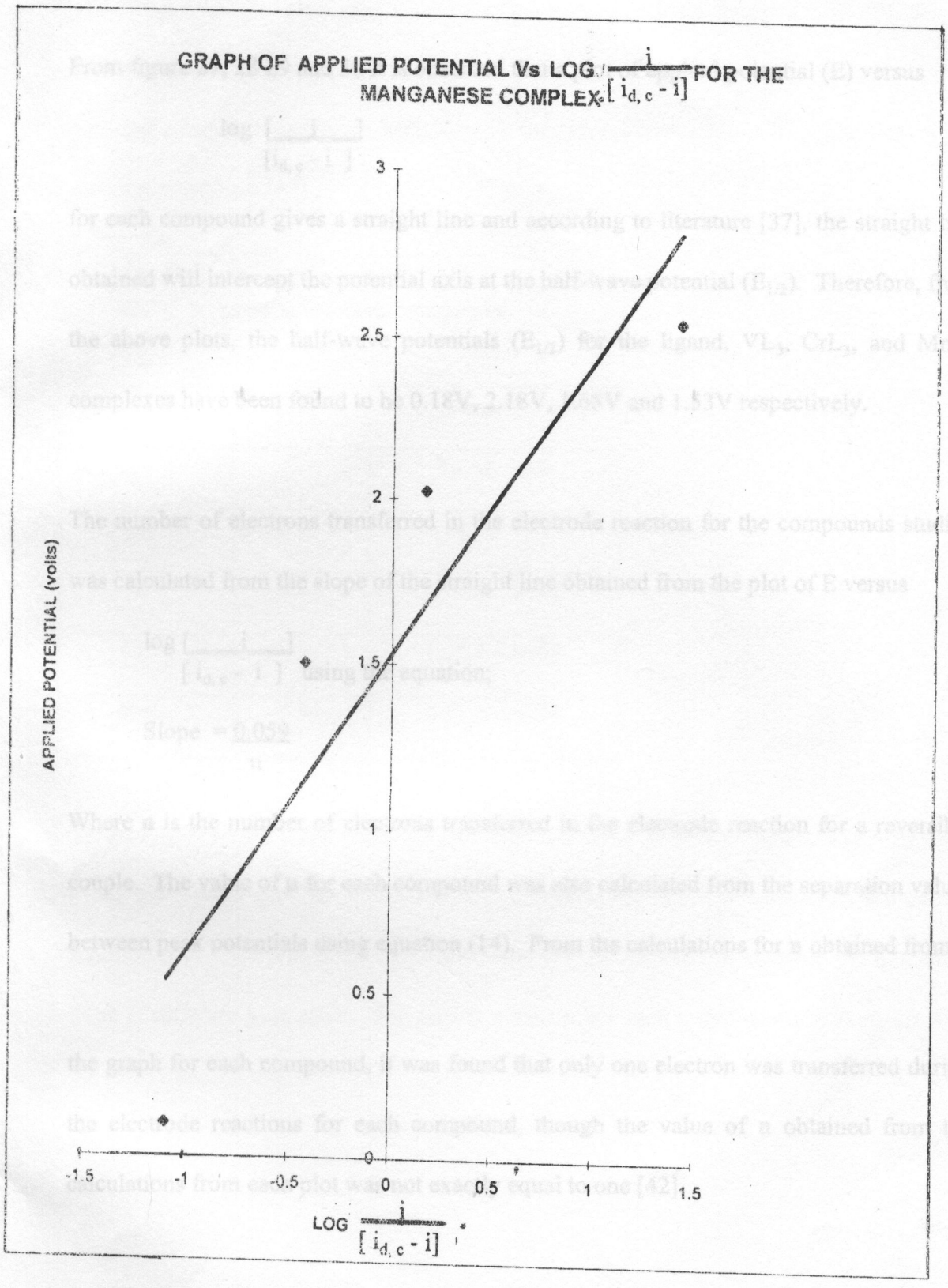

30.0. **Influence of applied potential on measured current in solutions of acetonitrile containing MnL_3 complex and 0.1M TEAB.**

From figure 27, 28 29 and 30 it is observed that a plot of applied potential (E) versus

$$\log \left[\frac{i}{i_{d,c} - i}\right]$$

for each compound gives a straight line and according to literature [37], the straight line obtained will intercept the potential axis at the half-wave potential ($E_{1/2}$). Therefore, from the above plots, the half-wave potentials ($E_{1/2}$) for the ligand, VL_3, CrL_3, and MnL_3 complexes have been found to be 0.18V, 2.18V, 1.65V and 1.53V respectively.

The number of electrons transferred in the electrode reaction for the compounds studied was calculated from the slope of the straight line obtained from the plot of E versus

$\log \left[\frac{i}{i_{d,c} - i}\right]$ using the equation;

$$\text{Slope} = \frac{0.059}{n}$$

Where **n** is the number of electrons transferred in the electrode reaction for a reversible couple. The value of **n** for each compound was also calculated from the separation values between peak potentials using equation (14). From the calculations for **n** obtained from

the graph for each compound, it was found that only one electron was transferred during the electrode reactions for each compound, though the value of **n** obtained from the calculations from each plot was not exactly equal to one [42].

The values of **n** and half-wave potentials ($E_{1/2}$) obtained from figure 27, 28, 29 and 30 for each compound, are given in table 14.0 below. The deviations in the values of **n** obtained from 1 could have been due to the unexpected complicated kinetics in the electrode reactions [43].

TABLE 14.0: The half-wave potentials ($E_{1/2}$) and n-values calculated from the graphs for each compound.

SOLUTION	n	$E_{1/2}$, Red
		V, Ag/Agcl
Ligand (LH)	1.10	0.18 ± 0.0044
VL_3	0.67	2.18 ± 0.0032
CrL_3	0.92	1.65 ± 0.0054
MnL_3	0.95	1.53 ± 0.0031

To determine whether the electrode reactions for solutions of the ligand, VL_3, CrL_3 and MnL_3 complexes were simple diffusion controlled reactions, calculations of the current function ($i_p/\nu^{1/2}$ C), which depends on $\mathbf{n}^{3/2}$ and $D^{1/2}$ [in the Cottrell equation (15)], were done at different scan rates. The results obtained for each compound are given in table 15, 16, 17 and 18 below.

TABLE 15.0: Variation of current function ($i_p / \nu^{1/2}C$) with scan rates for ligand.

SCAN RATE (mV/sec)	i_p (μA)	√SCAN RATE (mV)	$i_p/\nu^{1/2}.C$ μA(mMmV)$^{-1}$
10.0	16.0	3.162	1.30
20.0	18.4	4.472	1.03
50.0	27.2	7.071	0.96
100.0	35.5	10.000	0.89
200.0	51.0	14.142	0.90
500.0	79.0	22.360	0.89

The average value for the current function ($i_p/\nu^{1/2}.C$) = 0.995 μA (mMmV)$^{-1}$.

(mMmV)$^{-1}$ = per millimole.millvolt.

TABLE 16.0: Variation of current function ($i_p/v^{1/2}C$) with scan rates for VL_3 complex.

SCAN RATE (mV/sec)	i_p (μA)	√SCAN RATE (mV)	$ip/v^{1/2}.C$ $(mMmV)^{-1}$
5.0	17.5	2.236	3.10
10.0	20.0	3.162	2.53
20.0	28.0	4.472	2.50
50.0	40.0	7.071	2.30
100.0	53.0	10.000	2.12
200.0	78.0	14.142	2.21
500.0	110.0	22.360	1.97

The average value for the current function ($i_p/v^{1/2}.C$) = 2.40 μA $(mMmV)^{-1}$.

TABLE 17.0: Variation of current function ($i_p/v^{1/2}C$) with scan rates for CrL_3 complex

SCAN RATE (mV/sec)	i_p (μA)	√SCAN RATE (mV)	$i_p/v^{1/2}.C$ $(mMmV)^{-1}$
5.0	26.0	2.236	4.40
10.0	33.0	3.162	3.91
20.0	40.0	4.472	3.35
50.0	60.5	7.071	3.20
100.0	82.4	10.000	3.10
200.0	97.0	14.142	2.57
500.0	170.0	22.360	2.85

The average value for the current function ($i_p/v^{1/2}.C$) = 3.34 μA $(mMmV)^{-1}$.

TABLE 18.0: Variation of current function ($i_p/v^{1/2}C$) with scan rates for MnL_3 complex

SCAN RATE (mV/sec)	i_p (μA)	√SCAN RATE (mV)	$i_p/v^{1/2}.C$ $(mMmV)^{-1}$
10.0	18.0	3.162	3.98
20.0	20.0	4.472	3.13
50.0	31.0	7.071	3.10
100.0	40.5	10.000	2.83
200.0	56.8	14.142	2.81
500.0	86.0	22.360	2.69

The average value for the current function $(i_p/v^{1/2}.C) = 3.10\ \mu A\ (mMmV)^{-1}$.

The current function $(i_p/v^{1/2}.C)$ values obtained for solutions of the compounds dealt with (table 15, 16, 17 and 18) were almost constant for each compound and indepedent of the scan rate. A constant current function independent of scan rate [42] is a proof that the electrode reactions for the free radical ligand and the ML_3 complexes were diffusion-controlled.

Therefore, in general, the study has revealed that only one electron is transferred in the electrode reactions for these reversible processes for the compounds and that the reactions were mainly diffusion-controlled [40-46]. However, more work needs to be done in order to confirm these findings and also to find out whether the electron transferred during the reduction process for the complexes goes to the ligand or the metal ion. It is probable that the electron is transferred to the free radical entity (N—O·) attached to the ligand rather than the metal ion.

CONCLUSION

The complexes of Vanadium, Chromium and Manganese ions with 4-phenacetylidene -2, 2, 5, 5 - tetramethyl - 3- imidazolidine -1- oxyl free radical ligand have been synthesized. From elemental analysis, mass spectra (FAB), ESR spectra data and magnetic susceptibility measurements, the complexes have the formulation, ML_3 (where M = V^{3+}, Cr^{3+} and Mn^{3+}). Besides, the ESR spectra data and magnetic susceptibility measurements have indicated that the complexes are all paramagnetic. On the other hand, the cyclic voltammetric studies on the complexes, have revealed that they can undergo reversible reduction reactions at the working electrode.

BIBLIOGRAPHY

1. Volodarskii L.B., Grigor`ev L. A., and Sagdeev R. Z., Biological Magnetic Resonance, 2, 169 (1980).
2. Larionov S. V., Ovacherenko V. I., Kirichenko V.N., Mokhosoeva V. K., and Volodarskii L. B., Izvest. Akad. Nank SSSR, Seriya Khim., 1982.
3. Larionov S. V., Patrina L. A., Dolgorusk S. N. and Durasov V. B., Koord. Khim., 15, 7, 949-954 (1987).
4. Durarant P. J. and Durrant B., Introduction to Adavanced Inorganic Chemistry, Longman, 1st ed. London, 1962.
5. Rawcliffe C. T. and Rawson D. H, Principles of Inorganic and Theoretical Chemistry, Heinemann, 2nd ed. London, 1974.
6. Mackay K. M. and Mackay R. A, Modern Inorganic Chemistry, International Textbook Company Ltd, 3rd Ed., Great Britain, 1981.
7. Mackay K. M and Mackay R. A, Modern Inorganic Chemistry, International Textbook company ltd, 3rd ed., Great Britain, p. 76 (1981).
8. Cotton F. A and Wilkinson G, Advanced Inorganic Chemistry, John Wiley & Sons, 3rd ed., London, 1972.
9. Durrant P. J. and Durrant B, Introduction to Advanced Inorganic Chemistry, John Wiley & Sons, 2nd Ed. p. 90 - 104 and 940 - 955 (1966).
10. John Keana F. W, Chemical Review, 78, 37 - 50 (1978).

23.Indrichan K. M, Larionov S. V, Gerbe`len N. V and Ovcharenko V. I, Izvest, Akad. Nauk SSSR, Seriya, Khim, 7, 1664, 1985.

24.Morat C and Rassat A, Tetrahedron, 28, 735 (1972) and ref. 11, p.199 .

25.Zviszafram ronald M. Pike and Singh M, "Microscale Inorganic Chemistry", © 1991.

26.Geoffrey P and Haydn S., "Practical Inorganic Chemistry", Preparations, Reactions and Instrumental Methods, 1st Ed., Willmer Brother Ltd, Great Britain, p. 51 (1968).

27.Donald L Pavia, Gary M. Lampmann and George S Kriz Jr., " Introduction to Spectroscopy", Saunders series, 1976.

28.G`eb`el`eu N. V and Indrichan K. M, "The mass spectroscopy of Coordination compounds", Izd. Shtiintsa, Kishinev, (1984).

29.Douglas A Skoog, "Principles of Instrumental Analysis", Saunders College, 3rd ed. New York, 1985.

30.Figgs B. N, Lewis T, "The Magnetic Properties of Transition metal complexes", in progress in Inorganic Chemistry, New York, 1964.

31.Chester A. W and Schweizer A. E, "Inorg. Nuclear Chem., Letters", 7, 451 (1971).

32.Drago R. S., "Physical methods in Chemistry", Saunders College, 2nd Ed. p. 421, 1977.

33.Ashley J. H. and Mitchell P.C. H, J. Chem. Soc., A, 2821 (1968).

34.Douglas A. Skoog, "Principles of Instrumental Analysis", Ed., Sauanders College, New York, p. 448, 1985.

35.Drago R. S, "Physical Methods in Chemistry", 2nd Ed, W. B Saunders Co. Philadelpia, p. 324, 1977.

36.Drago R. S., "Physical Methods in Chemistry", 2nd Ed., W. B. Saunders Co. Philadelphia p. 348, 1977.

37.Claude P. Andrieux, Phillipe Happiot and Jean - Mechel Saveant, Chemical Review, 90, p. 723 - 738, 1990.

38.Dennis H. Evans, Chemical Review, 90, p. 739-751, 1990.

39.Arthur I. Vogel, "Longman, p. 1000 - 1008, 1961.

40.Robert D. Braun, "Introduction to Instrumental Analysis", McGraw-Hill, USA, p. 790-793, 1987.

41.Lynne L Merrit, Jr., John A Dean, and Frank. A. Settle Jr., " Instrumental Methods of Analysis", 7th Ed., Wadsworth, inc., U.S.A., p. 713 - 714, 1988.

42.Nicholsion R. S., Analytical Chemistry, 37, p. 135 (1965).

43.Nicholsion R. S., and Shain I, Analytical Chemistry, 36, p. 706 (1964).

44.Figgs B. N., "Introduction to Ligand Field", John Wiley & Son, New York, p. 293, 1967.

45.Bard A. J and Faulkner L. R., "Electrochemical Methods, Fundamentals and Applications", John Wiley, New York, p. 229, 1980.

46.Kaiyuan yang, Simon G. Bott, and Michael G Richmond", Organometallics", 14, p. 2387 - 2394 (1995).

47. Rozantsev E.G. 1970, Free Nitroxyl Radicals, Plenum Press, New York.